EXPERIMENTAL STUDY OF THERMALLY STRATIFIED CO-AXIAL JETS WITH TRIP RING EXCITATION

By

SUKANTA BHATTACHARJEE

A THESIS

SUBMITTED TO THE DEPARTMENT OF MECHANICAL ENGINEERING IN

PARTIAL FULFUILLMENT OF THE REQUIREMENTS FOR THE DEGREE

OF

MASTER OF SCIENCE IN MECHANICAL ENGINEERING

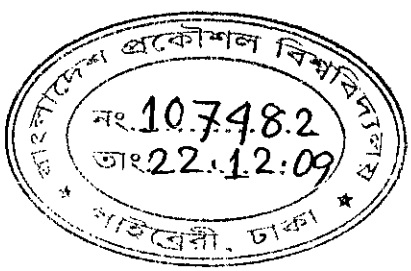

DEPARTMENT OF MECHANICAL ENGINEERING

BANGLADESH UNIVERSITY OF ENGINEERING AND TECHNOLOGY

DHAKA-1000, BANGLADESH

December 2009

RECOMMENDATION OF THE BOARD OF EXAMINERS

The board of examiners hereby recommends to the Department of Mechanical Engineering, BUET, Dhaka, the acceptance of this thesis titled **"EXPERIMENTAL STUDY OF THERMALLY STRATIFIED CO-AXIAL JETS WITH TRIP RING EXCITATION"** submitted by **Sukanta Bhattacharjee,** Student No: **040810041,** Session: **April 2008,** as satisfactory in partial fulfillment of the requirements for the degree of masters of science in Mechanical Engineering on **December 13. 2009.**

Chairman (Supervisor)

Dr. M. A. Taher Ali
Professor
Department of Mechanical Engineering
BUET, Dhaka, Bangladesh.

Member (Ex-officio):

Dr. Abu Rayhan Md. Ali
Professor & Head
Department of Mechanical Engineering
BUET, Dhaka, Bangladesh.

Member:

Dr. Md. Quamrul Islam
Professor
Department of Mechanical Engineering
BUET, Dhaka, Bangladesh.

Member:

Dr. Mohammad Mamun
Associate Professor
Department of Mechanical Engineering
BUET, Dhaka, Bangladesh.

Member (External):

Md. Abdus Salam
Head
Department of Aeronautical Engineering
MIST, Dhaka, Bangladesh.

CERTIFICATE OF RESEARCH

This is to certify that the work presented in this thesis is carried out by the author under the supervision of Dr. M. A. Taher Ali, Professor of Department of Mechanical Engineering, Bangladesh University of Engineering and Technology, Dhaka.

M A Taher Ali

Dr. M. A. Taher Ali

Sukanta Bhattacharjee

Sukanta Bhattacharjee

DECLARATION

No portion of the work contained in this thesis has been submitted in support of an application for another degree or qualification of this or any other University or Institution of learning.

Sukanta Bhattacharjee

Sukanta Bhattacharjee

Author

Dedicated to my parents

ACKNOWLEDGEMENT

The author wishes to convey his sincere gratitude and indebtness to Dr. M. A. Taher Ali, Professor, Department of Mechanical Engineering, Bangladesh University of Engineering and Technology (BUET) for his kind guidance, supervision and moral support throughout the entire period of the research work. His initiatives, encouragement, patience and invaluable suggestions are gratefully acknowledged.

The author is also deeply indebted to the committee members, Md. Abdus Salam, Head, Department of Aeronautical Engineering, MIST, Professor Dr. Md. Quamrul Islam, Department of Mechanical Engineering, BUET, Professor Dr. Abu Rayhan Md. Ali, Head, Department of Mechanical Engineering, BUET and Dr. Mohammad Mamun, Associate Professor, Department of Mechanical Engineering, BUET. Their comments, suggestions and approvals have certainly improved the quality of the work.

The author also extends his appreciation to the staffs of Fluid Mechanics Laboratory, Machine shop, Sheet metal shop and Carpentry shop for their continuous co-operation at different stages of the work.

Special thanks are offered to my friends who have helped me accomplishing my thesis. Finally, I am grateful to my parents for their constant encouragement and support

ABSTRACT

Experimental investigation of the mean flow characteristics in the velocity field as well as the thermal field of thermally stratified free and trip ring excited co-axial jets have been carried out for different flow conditions. Isothermal as well as thermally stratified or non-isothermal co-axial jet flows are developed by issuing two jets with different unidirectional velocities from a concentric compound nozzle. The hot central jet comes out from a central nozzle while the annular ambient jet is emitted through the annular space between the outer and the central nozzle. Four outer to inner jet velocity ratios have been considered in the experiment. The temperature of the central jet is varied to establish different temperature gradient between the central jet and the annular jet by varying the supply voltage to the heater placed upstream of the central nozzle. Three different values of temperature ratios have been considered. The excitation is made by two trip rings, one placed inside the central nozzle called inner trip ring and the other placed outside the central nozzle called outer trip ring. Measurements of mean velocity and mean temperature are made in the mixing zone of these two jets with the help of a pitot static tube with embedded thermocouple in it.

For the nozzle configurations used in the present study, mixing as well as momentum exchange in co-axial jets occur more readily at lower velocity ratio than those of the higher one. Thermal diffusion from the hot central jet is also found to occur more rapidly at lower velocity ratio. In case of inner or outer trip ring excited co-axial jets, a negative pressure zone is created due to the presence of the wake. This wake facilitates better mixing between two jets. Amongst the inner and outer trip ring excited and unexcited configurations of this experiment inner trip ring is found the most efficient one in mixing different jets both dynamically and thermally.

NOMENCLATURE

Symbol	Definition
C_g	Geometric virtual origin
C_k	Kinematic virtual origin
D_i, d	Diameter of the inner nozzle
D_o, D_2	Diameter of the outer nozzle
h	Manometric height
K_c	Decay rate
K_s	Spread rate
M	Mach number
n	Power index
P_s	Mean static pressure
P_a	Atmospheric pressure
P_t	Total pressure
Re	Reynolds number
Fr	Froude number
T	Local mean temperature
T_1	Mean temperature of inner jet
T_2	Mean temperature of outer jet/ ambient
T_c	Centerline temperature
U	Mean axial velocity
V	Transverse velocity
U_1	Central mean jet velocity
U_2	Annular mean jet velocity
U'	Mean axial velocity with respect to annular jet velocity
U_m	Maximum velocity on jet axis
U_m'	Maximum velocity on je axis with respect to annular jet velocity

U_c	Centerline velocity
$A_1 = (\pi d^2/4)$	Area of inner nozzle
$A_2 = (\pi (Do^2-d^2)/4)$	Area of annular/ outer nozzle
L_p	Length of potential core
L_{tp}	Length of thermal potential core
x	x co-ordinate
y	y co-ordinate
z	z co-ordinate
r	Radial co-ordinate

Greek Symbols

γ	Specific weight
θ	Non-dimensional temperature
η	Self-preservation variable for velocity
η_t	Self-preservation variable for temperature
μ	Absolute viscosity
ν	Kinematic viscosity
ρ	Density
τ	Shear Stress
α	Thermal Diffusivity

Subscript

a	air
c	centerline
co	centerline at origin
g	geometric
k	kinematic
p	potential core

CONTENTS

List of Figures

Chapter 1
INTRODUCTION

1.1 An Overview

Fluid flow cases are the most common phenomena both in nature and in engineering fields and there are innumerable types of flow situations like boundary layer flows, free shear layer flows, wake flows, flow through pipes and ducts, flow through turbo machines, flow through reducers and diffusers, flow through orifices and nozzles, jet flows and many others. Again, each of the flow types may occur in varieties of the boundary conditions. Because of the diversity and vastness of the fluid flow situations, there is enough scope to know the flow behavior of a particular flow situation. Jet flow is one of such flow, which is generally found in nature in different forms and boundary conditions and is used extensively in engineering installations, such as burners of combustion chambers, rocket engines, fluid injectors and many others.

1.2 Jet flow

Jets and plumes constitute omnipresent phenomena in nature. Some of these phenomena are obvious to even the most casual observer – like the jets, which exit from one's mouth when exhaling in a cold morning, while others may require extraordinary efforts to be seen – like astrophysical jets at distance of light years away visible only through telescope. The jet technology dominate our lives from propelling the aircrafts which move us across the continents to a simple air hose of the machine shop, from the stacks which spew the waste products of the industry to the diffuser array which disperse effluent into our streams and rivers.

A jet is formed when a fluid is discharged through an opening or nozzle from a container under high pressure into a region of low pressure. The ambient fluid surrounding the jet

may itself be in motion or at rest. Depending on the surrounding in which the jet is discharged, it can be classified into three major categories:

i. Free jet
ii. Confined or Bounded jet
iii. Wall jet

Any combination of these basic jets ultimately lead to the formation of another type of jets and may be termed as compound jet and co-axial jet is one of its kind.

i. Free jet: It is the very basic and simple form of jet flows. It is formed when the jet flows in an infinite fluid reservoir having no influence of solid surface as shown in figure 1.2.1. The exhaust from an engine is expelled into the atmosphere in the form of free jet.

ii. Confined or Bounded jet: In this type of jet, the fluid is discharged into a confined region bounded by solid surface as shown in figure 1.2.2. This kind of jet is encountered in the design of water jet pumps, furnace and steam-jet ejector of air conditioning system.

iii. Wall jet: In case of wall jet, the fluid is made to impinge on a rigid wall as shown in figure 1.2.3. After impingement, the fluid flows over the wall along its length. The wall may be straight and parallel to or at some angle with the flow or it may be curved. This type of jet is frequently employed for rapid cooling of hot body known as jet impingement quenching or jet cooling. In the manufacturing world, jet cooling is used in processes like extrusion, casting, forging, annealing and galvanizing. The fluid flow in the pelton wheel presents a very common example of wall jet.

The co-axial turbulent free jet is produced when two miscible streams of fluid are emitted from two concentric nozzles forming the compound nozzle with different unidirectional speed. These fluid streams mix up into a region of fluid with which each fluid stream is completely miscible [figure 1.2.4]. It is a simple way by which two fluid streams get

mixed. Co-axial jets are an integral part of many engineering system where mixing of different fluid streams is required. They are used to provide the mixing between fuel and oxidizer in combustors of propulsion systems and power producing gas turbine systems as well as waste combustion and incineration systems. In the combustor, the flow comes out as co-axial jet with fuel flow as the inner jet and air flowing as annular one. The process by which the liquid fuel is atomized by high-speed annular gas jet is known as "air-blast atomization".

1.3 Jet flow Field

Figure 1.3.1 represents a typical velocity field distribution of a circular jet. The time averaged jet velocity profile at the exit of the nozzle is uniform and forming the hat top shape. As a result, of the velocity gradient that exists between the jet and ambient fluid, a thin unstable shear layer is created at that region. This shear layer is subjected to flow instability that eventually leads to the formation of strong interaction zone resulting in turbulent fluctuations and continuous growth of shear layer in the downstream direction. This highly turbulent shear flow entrains ambient fluid into the jet and enhances the mixing. Consequently, the shear layer and the jet spread along the direction perpendicular to the main jet flow. Near the nozzle exit and along the central portion of jet, there is a region with an almost uniform mean velocity and low turbulence level called the potential core. Because of the propagation of shear layer, the potential core decreases and ultimately disappears when shear layer from all sides merges at the center. The entrainment and mixing process continues beyond the potential core region and eventually the velocity distribution relates to an asymptotic bell shaped velocity profile.

1.4 Flow structure of free jet

Based on experimental observations of the mean turbulent velocity field, the whole flow structure of a free jet can be divided into three distinct regions in the direction of flow related to centerline velocity decay. These are initial region, transition region and developed region as shown in the figure 1.4.1. The first region just after the nozzle exit is known as the initial region. As the jet boundary penetrates towards the axis or centerline

of the jet creating a wedge shape region of constant jet exit velocity. This wedge shaped region of the jet is known as potential core, which is surrounded by a mixing layer. The initial region of the jet extends until the potential core is disappeared by the penetration of the shear layer from all sides. For an axisymmetric jet, it is well documented that the length of potential core as about four times the diameter of the nozzle.

The second region of the flow structure of free jet is known as transition region, which starts after the initial region and dependent on Reynolds number. The higher the Reynolds number, the smaller the transition length. In this region the velocity starts to decrease often approximated as proportional to $x^{0.5}$ where x is the axial distance from the nozzle exit [48].

The combined initial and transition regions is known as developing region where the entrainment of ambient fluid creates a continuous transfer of momentum and energy from the jet to its surroundings and generates instability due to intensive shearing of the ambient fluid forming the shear layer. The thickness of shear layer increases as the jet travels downward from the jet exit.

Further, downstream there exists a developed region where the flow variables (i.e. mean velocity, turbulent intensity, Reynolds shear stress) become approximately self-preserving. In this region, the turbulence parameters extend up to the axis and as a result, the potential core disappears. Here the transverse distribution of the mean velocity (U) in the x-direction i.e. the variation of U with y at different axial locations has the same geometrical shape. At every section, the velocity decreases continuously from a maximum value on the jet axis to a zero value far away in the radial direction and the velocity decay is assumed potential to x^{-1} [48].

1.5 Flow structure of co-axial free jet

As represented in figure 1.4.1, the initial region of a co-axial jet consists of two potential cores separated by an annular mixing region. In the stream wise direction the central jet interacts only with the annular jet but the later interacts with both the central inner jet and

the ambient room air at the boundary. Thus, near the exit of a co-axial jet two distinct potential cores exists, one at the center and the other along the mean circumference of the annular jet forming a wedge shaped ring. Of the two mixing regions, one is between the central and inner boundary of the annular jet and the other is between the ambient room air and the outer boundary of the annular jet. As the flow proceeds the width of each core decreases approximately linearly with distance along the downstream direction and the cores terminate when these two (inner and outer) annular mixing regions meet together. As the flow is developing, it is in a state of intense mixing and it becomes fully turbulent in its developed state. In the developing stage, the inner mixing layer spreads towards the outward direction more rapidly to meet the outer one and further in the downstream distance, the co-axial jet produces a velocity profile identical to that produced by a single axisymmetric one indicating the complete mixing and fully developed flow condition. The characteristics of flow properties in this region become self-preserving.

1.6 Motivation behind the present study

Jet flow is one of the basic flow configurations that are found both in nature and in industrial applications. Most of the jets encountered in our daily life are turbulent in nature. Simple flow cases are relatively easy to handle and solve theoretically but when it involves two or more turbulent fluid streams then the flow structure becomes too complicated to solve theoretically. Therefore, experimental investigation is the best option to know about the flow field of interacting jet flows.

The extensive use of turbulent jets in different engineering arena attracts the attention of the researchers from 1950's. Some of these research works have been done on co-axial jets considering both fluid streams at the same temperature. However, there are numerous engineering applications where two fluid streams of different temperatures having co-axial jet flow configurations mix together. For instance, the exhaust of an engine expelled to the atmosphere and the emission from a chimney present classic example of non-isothermal single jet. In the combustion chamber of a gas turbine, the flow of hot combustion products and secondary cooling air represents essentially a thermally stratified co-axial jet. This type of non-isothermal jet is also found in chemical process industries where two different fluid streams of different temperatures and also with

different densities and velocities mix up together in the form of co-axial jet to react chemically. In some effluent treatment plant, dozing is injected in the effluent in the form of jet with a temperature different from that of the effluent representing a flow structure of thermally stratified co-axial jet. In most of the cases an excitation is used for better mixing of different fluids like in gas turbine combustion chambers, fuel injectors in internal combustion engine or chemical mixing process.

Despite numerous applications of excited non-isothermal co-axial jets, the available research work on this topic is much less than that of isothermal co-axial jets or non-excited non-isothermal co-axial jets. For this reason, to get a better understanding of the interaction of thermally stratified co-axial jets with excitation, the present work has been selected for this research work.

1.7 Research Highlights

Begum [5] studied the flow field of isothermal co-axial jets of three different annular to central area ratios as 0.56, 1.25 and 2.61 with annular to central jet velocity ratio ranging from 0.0 to 0.90. Hasan [49] studied the effect of thermal stratification in the mixing process of co-axial jets. He also studied the thermal field of non-isothermal co-axial jet for different Reynolds number and different temperature ratio. In fact more research work is still required to explore the flow field of co-axial jets even at higher annular to central area ratios as well as the mutual interaction of the dynamical velocity field with the thermal field that results in case of non-isothermal jets in presence of different types of excitation encountered in real applications. Essentially more attention is paid to both these facts in the present study.

For the current investigation, two concentric circular jets have been used. A 29 mm diameter nozzle jet is placed at the center of 63 mm diameter nozzle set up, which has already been installed by previous researchers [5, 39]. In the heating chamber installed by Hasan there is a 1500-watt nicrome wire heater to make the hot central jet. The heat flux of the electric heater and thus the temperature of the central jet is controlled by using a voltage regulator attached to that heater. Two different annular to central temperature ratios (0.925 and 0.974) are used in present experiment. Excitation is made in either

central jet or in annular jet with different inner and outer trip ring. Nylon is used to manufacture this trip rings for better dimensioning and better gripping with the central nozzle wall in elevated temperature. To ascertain the extent and nature of the thermal field and the velocity field as well as their relative influence on each other, both the velocity and the temperature are measured along the transverse direction at different downstream locations from the nozzle exit for different initial and boundary conditions i.e. for different velocity ratios, temperature ratios and outer or inner trip ring.

1.8 Objectives of the Present Work

The main objectives of this experimental study are to introduce an excitation in the velocity field of thermally stratified co-axial jets by installing an outer or inner trip ring in the exit of the nozzles these rings create wakes, which enhance the mixing of the hot central jet with the cold annular jet. The objective of this research is to investigate the mean velocity and thermal characteristics in the near-field of the jets for different initial and boundary conditions and also to compare the results with those of isothermal and non excited counterparts. Investigation includes:

i. Measurement of mean velocity of isothermal co-axial jets for inner, outer and without trip ring excitation along the transverse direction at different downstream locations from the nozzle exit to find out
   a. The initial mixing zone
   b. Partial self preserving zone
   c. Fully developed zone

ii. Measurement of mean velocity and temperature of thermally stratified (non-isothermal) co-axial jets for inner, outer and without trip ring excitation along the transverse direction at different downstream locations from the nozzle exit.

iii. Study of centerline temperature decay of non-isothermal excited and non-excited co-axial jets to identify the thermal potential core.

iv. Analysis of the effect of velocity ratio, temperature ratio and excitation method on mean velocity and temperature profiles of isothermal and non-isothermal jets.

v. Study of the effect of velocity, temperature and excitation method on streamwise velocity and temperature characteristics of jets.

Chapter 2
LITERATURE REVIEW

Jet is one of the most common flow configurations that are encountered both in nature and in industrial applications frequently. Considering the significant use and occurrences of jets, many research works have been done in the past and still are going on at present on different types of jet configurations. The reviews of some of the earlier research works related to the present investigation are presented below in three categories:

1. Circular jet
2. Co-axial jet
3. Annular jet

2.1 Circular jet

Gamma [18] performed his experimental study on circular air jet in both acoustically excited and unexcited condition. He reported that the decay of the centerline velocity took place at a faster rate when the initial flow was turbulent as compared to initially laminar flows. The kinematic virtual origin was found to move further downstream with increasing Reynolds numbers. The centerline turbulent intensities were found to enhance at lower excitation frequencies but after reaching the maximum, they started to decrease with further increase in excitation frequency.

Islam [24] studied the flow characteristics of circular jet at different exit conditions. The exit conditions of the jet were obtained by changing the length of the nozzles (l/d = 1.5, 5 and 8), by attaching vertical flanges of different diameters (1.5d, 2d, 2.5d and 4d), by making wedges of different angle (60, 45 and 30 degree) at the exit section. He worked with Reynolds number ranging from $2X10^4$ to $1X10^5$. He found that the mean static pressure in the potential core was positive while that in the mixing region was negative.

The increase of exit length, Reynolds number and wedge angle caused the centerline mean velocity to decrease slightly with a corresponding rise in mean static pressure. But for vertical flanges, the centerline velocity near the nozzle exit increased sharply with a drop of centerline mean static pressure. The stream-wise velocity profiles were saddle shaped, which moved downstream and ultimately disappeared at the end of the potential core. The peak value of the saddle shaped profile was found to increase due to exit vertical flange while the increase of exit length, Reynolds number and wedge angle caused it to decrease. The spread of the potential core was found to rise with the increase of nozzle exit length, Reynolds number and attachment of vertical flanges.

Selim [39] studied the effect of displacement thickness and Reynolds number on the free shear layer of axisymmetric and asymmetric jets. According to his results, the thickness of initial boundary layer suppressed the peak value of turbulence intensities and increased the spread rate of jet. His results revealed that the self- preservation characteristics of the axisymmetric jet were independent of Reynolds number and initial boundary thickness. Asymmetry in the jet flow in one axis was found to have little effect on the mean velocity in the other axis but suppressed turbulent intensities in those axes.

Islam [23] carried on his experimental study of jets issued with triangular splines parallel to the flow. He measured the velocity and longitudinal turbulence intensity with the help of a pitot static tube and hot wire anemometer respectively. In his study the exit boundary layer mean velocity profiles were found to be very close to the Blasius profile and centerline mean velocity was b\observed to decelerate up to 1.5% within the potential core. The kinematic and the geometric virtual origins were found to exist in the downstream and upstream of the nozzle exit respectively. As a result of the presence of splines, the saddle shaped mean velocity profile was found to diminish with a reduction in the entrainment and spread rate of the jet as compared to other nozzles studied.

Wignanski and Fiedler [47] made their experimental study on axisymmetic isothermal turbulent jet issued from a 2.6 cm. diameter round nozzle at a Reynolds number of $1X10^5$ with an exit turbulent intensity of 0.1%. The mean velocity profile of the concerned jet was found to become self-preserving at 20 diameters downstream from the nozzle exit. The location of kinematic virtual origin was found to be at 3 diameters downstream from

the nozzle exit when measurement considered up to 50 diameter and that at 7 diameters downstream when measurements considered up to 100 diameters.

Husain and Zedan [22] measured the mean velocity and determined the jet boundaries for different boundary layer thickness. From their experimental results, they found that the mean velocity was self-preserving at a distance from the nozzle exit, which varied with the initial turbulence level and boundary layer thickness. According to their study, for turbulent boundary layer, the geometric virtual origin was found close to the physical origin at the nozzle exit.

Bradshaw [8] investigated the effect of initial conditions on the development of free shear layer produced by a circular nozzle having exit diameter of 5.08 cm. at a Reynolds number of $3X10^5$. The initial boundary layer thickness was changed by using parallel circular sections of different lengths that were screwed at the end of the nozzle. Tripped concentric rings changed the state of the initial boundary layer thickness. According to his study, the shear layer became fully developed at $x = 7X(\gamma/U_e)X10^5$ from the nozzle exit for any boundary layer thickness. A significant change in the geometrical virtual origin was observed with the change of boundary layer thickness in his study.

Lighthill [31] through his study showed how the shearing motions in a turbulent jet could shed some of the energy in the form of sound radiation. He found out that the r.m.s. turbulent velocity was the only parameter that affected the total acoustic power generation and which was also dependent on jet velocity. In order to reduce the noise generation of jets, he made three suggestions as:

a. Reduction of jet speed.
b. Diminishing the relative velocity of the jet and the adjacent air to reduced the turbulent intensity and
c. Making use of multiple jet in place of single jet so that the peak noise generated from the cluster of nozzles would cancel out each other resulting in less noise.

Hossain [21] worked on swirling circular jets having four different swirl numbers. Swirling jets were produced by flowing air through circular straight nozzles having helical threads of different pitches. All measurements were taken at a Reynolds number

of $5.3X10^4$. The jet under investigation was found to be more like a twinjet formed by the interaction of two flow streams created at the two sides of thread boundary having interconnection between them at the center. These flows were of similar characteristics and interacted with each other. In the axial direction the velocity maxima was found to move away from the center due to the centrifugal force created by the swirl.

Billant, Chomaz and Huerre [6] made an experimental study to characterize the various breakdown states taking place in a swirling water jet. The experiments were conducted with two jets of different diameters for different swirl ratios and different Reynolds numbers ranging from 300 to 1200 for a pressure driven water jet discharging into a large tank. Breakdown was observed to take place after the swirl ratio reached a well-defined threshold value that was found to be independent of Reynolds number and the nozzle diameter.

Hibara [20] studied an axisymmetric jet with swirl issuing from a nozzle of 30mm diameter along a solid surface. The investigation was conducted for two different swirl intensities at a Reynolds number of $2.6X10^4$. He found out that axial velocity distribution of the flow changed gradually to that of the wall jet type in a vertical plane and of free jet type in horizontal plane as the flow progressed in the downstream direction. The flow was found to extend more broadly in a horizontal plane than in a vertical one, with an increase of initial swirl number. The wall pressure was found to take positive or negative maximum value in the regions where secondary flow impinged or it left away. The results also showed the effect of turbulent diffusion to be predominating in the upstream region which continued to decrease as the flow moved in the downstream direction.

2.2 Co-axial Jets

Begum [5J experimentally studied the mixing of circular co-axial free jets for different area ratios and velocity ratios. She made her study for four different velocity ratios ranging from 0.10 to 0.90 for each of the nozzle configurations having area ratio 0.56. 1.25 and 2,61. Measurements were taken with 1.6 mm OD pilot static tube for Reynolds numbers ranging from $1.04x10^4$ to $4x10^4$. In her investigation, the curvature effect of the nozzle was found to be prominent in reshaping the thickness of inner and outer boundary

layers of the exit velocity profile. The potential core length of co-axial jet was found to have elongated from that of the single jet but remained almost constant for all velocity ratios and increased with the increase of area ratio. She observed that mixing of co-axial jets took place earlier for lower values of velocity ratios and area ratios. Spread rate of co-axial jet was found to have decreased in comparison to that of a single jet. It was also found to decrease with the increase in area ratio.

Champagne and Wygnanski [11] conducted their experimental study to investigate the flow field generated by two co-axial jets by using hot wire anemometers. They provided mean velocity distribution, turbulence intensities and shear stresses for various area ratios of the external and internal nozzle as well as the ratios of the velocity of the jets issuing out from each of the nozzles. The experimental Reynolds number- was varied from 0 to 10^5 while the velocity ratio was varied from 0 to 10 and all measurements were taken for two nozzle configurations having area ratio 2.94 and 1.28. In this investigation they found out that, the initial flow close to the nozzle exit consisted of two potential cores separated by two mixing regions: one is the annular mixing region between the inner jet and outer jet and another is the outer mixing region between the outer jet and the ambient air. The length of external potential core was found to be independent of the initial velocity ratio and was equal to 8 times the width of the annular jet. But the length of the inner potential core appeared to be strongly dependent on the velocity ratio of the jets as well as the area ratio of the nozzles. The width of each core decreased approximately linearly with downstream distance and eventually they disappeared as the mixing cones joined together. The flow then became entirely turbulent and developed in the downstream direction until the jet became identical to the simple axisymmetric jet. They concluded that for a fixed area ratio, the velocity ratio of the outer to inner jet should be greater than one for enhance mixing between the fluid streams,

Morton [33] proposed a theoretical model for the co-axial turbulent jets produced when two miscible streams of fluid were emitted with two different unidirectional speeds from an inner and concentric outer nozzle in a region of fluid with which each of the streams were completely miscible. In his theoretical study, the mixing between the jets and between the annular jet and the surrounding ambient fluid were represented by assuming

constant entrainment rate. He derived the equations describing the velocities of the jets as well as the growth of the jet boundaries that were numerically integrated.

Rehab et al. [37] used hot wire anemometry to study the structure of turbulent coaxial jets for velocity ratios (r) higher than one. Two flow regimes were identified depending on whether the velocity ratio was larger or smaller than a critical value (r_c). When $r < r_c$, the fast annular jet periodically pinches the central one corresponding to the outer jet mode. When $r > r_c$ the inner potential core was found to be truncated and followed by an unsteady recirculation zone.

Buresti et al. [10] studied the mean and fluctuating flow field of a co-axial jet with ratios between the inner and outer diameters and velocities $D_1/D_2 = 0.485$ and $U_1/U_2 = 0.67$ respectively with turbulent exit boundary layers at high turbulence level by means of LDA and hot-wire anemometry. In their study, the profiles of mean axial velocity and that of axial and radial turbulence intensities and as well as shear stress distribution were described for the initial and intermediate zones of the jet near field. For lower values of Reynolds number and laminar boundary conditions, they found the length of the potential core to be in good agreement with available data obtained. They also suggested that the frequency of the flow fluctuations could better be recognized if the hot wire spectra of both the axial and radial velocities were analyzed. They observed significant radial differences in these frequencies in the initial and intermediate zone that became progressively more uniform with increasing distance from the nozzle exit. In the near-exit region of the inner mixing layer, they figure out the evidence of a probable alternate vortex shredding from the inner duct wall. This phenomenon was found to exist for $U_1/U_2 \geq 0.45$, with a constant Strouhal number ($S_t = 0.24$) based on the thickness of the wall and on the average velocity of the two streams.

Warda et al. [44] carried out an experimental study on the near field-region of the flow field of a co-axial jet by using Laser Doppler Anemometry. The jet under their consideration was made to issue from concentric round profiled nozzles and to discharge freely into still ambient air. The velocity ratio between the inner and outer streams of the jet (λ) was varied with an addition of wide interface between the fluid streams. The interface was found to affect the structure of shear layers between the two streams with a

significant effect on the velocity decay characteristics along the centerline. The obtained results showed that the inner potential core length of the coaxial jet was strongly dependent on velocity ratio (λ) while the outer potential core length having velocity ratios greater than unity seemed to be insensitive to the velocity ratio (λ). In their investigation the flow field did not show self-similarity up to x/d = 25. Jets with λ less than unity were found to develop faster than those with λ greater than unity. In addition, increasing the velocity ratio (λ) was found to accelerate the jet decay rate along the centerline.

Ahmed and Sharma [1] conducted an experimental investigation of turbulent mixing of two co-axial jets with low annular to core area ratio in a non-separating confinement. They measured the mean velocity and the streamwise and transverse turbulence intensities distributions at different streamwise locations by using Laser Doppler Velocimeter for seven velocity ratios ranging from 0.3 to 10.0. The experimental Reynolds number based on the mass averaged velocity and duct diameter was in the range of 4.2×10^5 to 7.0×10^5. From the results obtained they concluded that, mixing process in confined jets is not only dependent to the velocity ratio but also on the interactions between the boundary layers, mixing layers and the main flow particularly in case of lower area ratios.

Williams, Ali and Anderson [46] performed their experimental study on the noise, generated from cold subsonic co-axial jets issuing from concentric nozzles with external mixing. As the velocity of the annular jet was increased in relation to a given central jet velocity, an initial attenuation was observed. On further increasing the annular jet velocity until the velocities of the two streams were equal, the noise was found to be in excess of that of the central jet alone. This study of co-axial jet suggested a simple method of predicting the attenuation attained when a circular subsonic jet was surrounded by an annular jet of variable velocity.

Alpinieri [2] conducted his experimental work on the turbulent mixing process between co-axial jets of different density. In his investigation he used carbon dioxide and hydrogen as central jets, alternatively exhausting in to a moving concentric stream of air. The flow was isothermal and the velocities were in the low to high subsonic range. His

objectives were to investigate the nature of the turbulent diffusion when the velocity ratio as well as the mass flow rate per unit area between them approached to unity. From the radial and axial distribution of concentration and velocity, it was demonstrated that the product of local density and eddy kinematic viscosity coefficient could be assumed to be solely dependent on axial co-ordinate. Furthermore, no tendency towards the segregation of the streams was found when either the velocities or the mass flows of the streams were equal. He also showed that mass diffusion occurred more readily than momentum.

Au and Ko [4] experimentally studied the flow structure of co-axial jets for different velocity ratios of the inner to outer jet (U_1/U_2) ranging from 0.15 to 1.0. In their measurements of mean velocity, they observed that the initial region of co-axial jets could be divided into different regions as the initial merging zone, intermediate merging zone and fully merged zone. They also observed the presence of two trains of vortical structures in the mixing regions of co-axial jets. The vortices in the outer mixing zone were found to have the characteristics similar to a single jet and to be independent of velocity ratio. But the vortices in the inner zone was found to be dependent on velocity ratios and showed the characteristics similar to an annular jet at lower values of velocity ratios ($0.15< U_1/U_2 < 0.50$). From their analysis, they concluded that at lower velocity ratios the co-axial jets had an intermediate role between a single jet and co-axial jet.

The mixing of a subsonic confined air jet with a co-axial secondary air stream was investigated experimentally by Choi, Gessner and Oates [13]. In their study, they observed the effects of an improved adverse pressure gradient on the mixing characteristics in the initial mixing (potential core) and transition regions. The results indicated that, the presence of an adverse pressure gradient enhanced the rapid mixing and spreading of the shear layer in the initial mixing region as well as elevated turbulent normal stress and shear stress level in the outer portion of the mixing layer after the primary and secondary streams had merged. Significant radial static pressure variations occurred in both of the initial mixing regions and transition regions as a result of turbulent normal stress gradient and streamline curvature effect induced by the potential core entrainment.

Lima and Palma [32] studied the mixing of co-axial confined jets with large velocity ratio with the help of combined Laser Doppler Velocimetry/Laser Induced Fluorescence technique. They made the use of a fluorescent tracer in the inner jet for two velocity ratios between the mean axial velocity of the annular (U_2) and inner flow (U_1) equal to 3.2 and 6.5 for a Reynolds number of $3x10^4$, based on the bulk velocity and inner diameter of the outer tube. From the analysis of mean and instantaneous velocity and concentration fields, they concluded that the mixing was enhanced as the velocity ratio increase from 3.2 to 6.5, showing the dependence between mixing and intensity of shear layer between the two flows. It was also noticed that the topology of the mean velocity field was different between the two cases; for higher velocity ratio of 6.5 a recirculation region was found to develop at a distance of one inner diameter from the nozzle outlet with consequences on the jets near field.

Wicker and Eaton [45] conducted experimental study to determine the effect of an annular jet on the near field vortex structure and dynamics of an axisymmetric jet issuing into a quiescent ambient fluid. The effect of the velocity ratio between the two streams was investigated for a single nozzle exit area ratio, a single core Reynolds number and uniform density. In their study, the initial vortex development in the shear layer was found to develop independently but the core flow was found to be controlled by the large-scale structure in the outer layer. Axial excitation of the annular flow demonstrated a strong coupling between the large-scale structures in the outer layer and the evolution of the inner layer. Excitation of the core flow produced periodic structures in the inner layer but did not have any significant effect on the evolution of the outer layer.

Antonia and Bilger [3] carried out an experimental investigation of an axisymmetric air jet exhausting into a moving air stream for two values of the ratio of the jet velocity to external air velocity. The free stream air velocity (U_2) was kept constant at 30.5 m/s while two values of the jet velocity (U_1) were 91.3 m/s and 137 m/s resulting two nominal velocity ratios (U_1/U_2) of 3.0 and 4.5 respectively. Free stream turbulence level was maintained at 0.1%. The flow field was traversed by a pitot static tube while the pressure differentials were recorded with "Texas Precision Pressure Gauge". Their investigation showed that the mean velocity profiles remained insensitive to the flow development with fairly high levels of turbulent intensities. The magnitudes of those

levels were found to be compliant with the large entrainment rates but the values recorded were significantly different for the two values of the ratio of jet velocity to external air velocity. From the results obtained, they concluded that, assumption of turbulence similarity, whilst reasonable for two-dimensional jet-wake, was untenable for the axisymmetric case.

The flow field generated by the interaction of two unequal plane parallel air jets was investigated by Elbanna and Sabbagh [15]. They measured the mean static pressure and the mean and fluctuating velocities of the flow field for different velocity ratios ranging from 0.25 to 1.0. From axial and centerline distribution of mean velocity profiles, they figured out the confluence of the two jets. In their study, the confluence of ventilated jet was found to occur at a much larger distance from the nozzle exit than unventilated jets, i.e. air ventilation causes weaker interaction between the jets. They also found that the axis of the combined jet came closer to the power jet as the velocity of the weaker jet was decreased. Negative static pressure was observed in the upstream of the merging region while the highest pressure was found in the confluence region. Total momentum was found to remain constant at any section of the two jets, which is consistent with the principle of conservation of momentum.

Chigier and Beer [12] studied the flow field of a central round air jet surrounded by an annular air jet issuing into stagnant air surroundings. They measured the mean velocity and static pressure distributions in the region close to the exit of the nozzles and thereby examined the effect of the velocity ratio of the central the jet and the annular jet. The diameter of the central jet was 2.5 cm while the inner and outer diameters of the annular jet were 6.4 and 9.7 cm respectively. Measurements were taken for different ratios of the annular to central jet velocity as 2.35, 1.17, 0.235, 0.117 and 0.024. Their results showed that the annular jet had a nearly uniform distribution at the exit and as the jet moved downstream, the axis of the annular jet as determined by the position of velocity maxima, converged towards the central line. When the magnitude of the exit velocities in the central jet and annular jets were similar, the profile had the form of three separate distributions, which again merged to form an equivalent jet. When the central jet was dominant, the velocity profile was essentially determined by the decay of the central jet and the annular jet was found to have little influence at the outer edges of the profile. For

the dominant annular jet, all the streamlines of fluid issuing from the nozzle were found to converge towards the centerline and a large ring vortex was set up in the space separating the inner boundaries of the jet. The maximum reverse flow velocities were of the order of 15% of the mean axial velocity and the amount of fluid re-circulated in the vortex was about 6% of the mass leaving the nozzle. The streamlines produced in the concentric jets revealed that the central jet was completely absorbed by the annular jet after a relatively short distance from the boundary. In the space between the outer boundary of the central jet and the inner boundary of the annular jet, two counter rotating vortices were found to exist thus creating a region of separation in between the two jets. When the exit velocity of the central jet was increased each jet continued in its own path until the central jet became dominant in which case the annular jet was absorbed within the confines of the central jet after a short distance from the nozzle exit. The vortex center of the annular jet was found on the inner boundary of the annular jet and the point of maximum pressure was found to occur at the stagnation point where the converging streamlines impinged on the centerline and were then directed radially outward. In case of the dominant central jet the stagnation points were found to exist at the points of impingement of the converging annular and the diverging central streamlines.

The density field of co-axial jets with large velocity ratios and density differences was experimentally studied by Marinet and Schettini, [16]. The flow under consideration consisted of a low velocity-high density inner jet surrounded by a high velocity-low density annular jet. They made the use of thermo-anemometric method in association with an aspirating probe to determine the density field. In this investigation, the mixing was found to directly dependent upon the flow dynamics. They conclude that effects of density gradient on the mixing as well as on the flow dynamics could be well taken in to account by considering the specific outer to inner jet momentum flux ratio (M) not separately the density and velocity ratios. For a given value of momentum flux (M), a slight enhancement of mixing was found for density ratios much smaller than one ($\approx$ 0.14).

Chowdhury [14] made experimental study on swirling co-axial jets for different annular to central jet velocity ratios (U_2/U_1) ranging from 0.0 to 2.0. In her study, the swirl was imparted to the outer jet and the inner jet by spiral guide vanes attached on the outer or

inner surfaces of the central circular nozzle respectively. She carried out her experiment for two values of Reynolds number viz. $2.7x10^4$ and $4.01x10^4$ with guide vanes having helix angles of inclinations of 15° and 30° corresponding to swirl numbers of 0.27 and 0.58. For both of the swirling and non-swirling co-axial jets, she observed the identity of two jets up to three diameters of the inner nozzle for lower velocity ratios ($U_2/U_1 < 1.0$) while that was found up to five diameters of the inner nozzle for higher velocity ratios ($U_2/U_1 > 1.0$). The influence of the outer jet over central jet was found to increase as the velocity ratio and swirl angle increased. The addition of swirl in co-axial jets was found to result in better mixing and enhanced dispersion of the jets.

2.3 Annular Jet

Georgiou [19] numerically analyzed the flow of annular liquid jets at high Reynolds numbers by using finite element technique and the full-Newton iteration technique for different values of inner to outer diameter ratios and for non-zero surface tension. The simulation results revealed that at low Reynolds number, the annular film moved away from the axis whereas at high Reynolds numbers it moved towards the axis of symmetry and appeared to be very close to the axis far downstream thus forming a round jet.

Tagila et al. [41] performed an unsteady 3D numerical simulation as well as 3D LDA measurements of an annular jet with a blockage ratio of 0.89 at Reynolds number of $4.4x10^3$. The existence of an asymmetric flow inside the recirculation zone was found both in their simulation and measurements. The computed velocity fluctuations were in good agreement with the measurements. It was shown that the fluctuations in the recirculation zone mainly consisted of fluctuations of large-scale vortices implicitly proving the necessity of making simulations in unsteady manner. Fast Fourier frequency analysis based on the simulated velocity time series indicated the existence of large vortex structures oscillating at a frequency of 10 Hz, which was found to be in good agreement with previous measurements.

Ko and Chan [26] carried out an experimental study of the initial regions developed in three different annular jets having the following configurations:

1. A basic annular jet without any bullet at the center
2. An annular jet with a conical bullet at the center
3. An annular jet with an ellipsoidal bullet at the center

In the initial regions of the jets they identified three distinct zones- the initial merging zone, the intermediate merging zone and the fully merged zone. Within these zones, the mean velocity and turbulence intensity profiles were found to be similar to each other. The similarity curves also showed close resemblance to those of a single jet.

Later Ko and Chan [27] made further experiments on the detailed study of annular jets, measuring mean and fluctuating properties in the inner region. They referred to the annular jet without any bullet at the center as basic jet whereas those with conical or ellipsoidal bullets were termed as conical and ellipsoidal jet respectively. In case of conical jet, besides the jet vortices another train of vortices was found in the inner region because of the wake formation by the boundary layer on the surface of the conical bullet. The experiments in the inner region of basic annular jet showed a mean velocity profiles similar to those in the internal re-circulating region. They obtained a good correlation for the location of the minimum and maximum mean static pressure, vortex center and reattachment. It was also found that a train of wake vortices was generated in the internal re-circulating zone and a train of jet vortices was found to develop in the inner mixing region. Both types of vortices were found to decay rapidly within a distance of one outer diameter downstream. The disturbance associated with the wake vortices in the inner region was found to stimulate the outer mixing region resulting in another train of vortices in the outer shear layer.

The above bibliographical review shows that most of the research work done on jets has been made in isothermal conditions. Despite these, very few works on non-isothermal jets are found and their summaries are recapped below.

Saffir [38] determined the mean velocity field and temperature profiles of rectangular jets having different aspect ratios and nozzle configurations. In his experimental study the flow field for both velocity and temperature was found to be divided into three distinct regions referred to as potential core, the two dimensional region and axisymmetric regions. These three regions were not the same for the velocity and temperature distributions. The extent of each of these regions was found to be a strong function of nozzle aspect ratio and nozzle geometry. At large distance from the nozzle exit, both the velocity and temperature fields were found to behave in a manner similar to a circular jet of same area.

An experimental study of the mean velocity and temperature fields in round turbulent jets including the effect of entrainment on heat transfer was carried out by Obot et al [35] with various initial temperatures. For isothermal as well as non-isothermal jets they found that the rate of fluid entrainment was a strong function of nozzle design. They also observed that, for a given nozzle exit temperature and Reynolds number, the larger the mass flow rate of the ambient fluid entrained by a jet, the lower the jet temperature and enthalpy at locations downstream from the nozzle exit.

Kirra et al [29] simulated non-isothermal co-axial air jets with two different approaches: parabolic and elliptical approaches. They applied both the k-e model and the RSM model in their study. The numerical resolution of the equations governing the flow was carried out in parabolic approach by a "home-made" CFD code based on finite difference method while in elliptical approach, an industrial code (FLUENT) based on finite volume method was used to solve them. In forced convection mode ($Fr = \infty$), both the turbulence models were found to describe the mean flow acceptably. For outer to inner velocity ratio (r) less than 1, the results of the two approaches were found to be satisfactory for the velocity field. But for $r > 1$, significant difference between the results was noticed in their study. In mixed convection mode ($Fr \simeq 20$), the results for the temperature and turbulent sizes obtained from these two approaches were found to agree well with the correlations suggested by the experimenter only for $x/d \geq 55$.

2.4 Non-isothermal co-axial jets:

Hasan [49] investigated the effect of different Reynolds number and different area ratio and different velocity ratio on the spatio-temporal velocity field and on dynamical potential core, momentum diffusion and dynamical self-preservation characteristics of jets. He also conducted research on the effect of temperature difference between central and annular jets on the thermal potential core, thermal diffusion, dynamical and thermal self-preservation characteristics of non-isothermal co-axial jets. He concluded that the location of the virtual origin of co-axial jets depends on both annular to inner velocity ratio as well as area ratio of co-axial jets. According to his study, co-axial jet tended to lengthen the thermal potential core by 25% to 50%. The effect of temperature ratio on thermal potential core was found to be insignificant. Hasan showed that temperature decay took place more quickly at lower temperature ratio than at higher one in non-isothermal jets. The centerline temperature of non-isothermal co-axial jets was found to decrease faster at lower velocity ratio, which occured more rapidly than single jet. According to his findings dynamic self-preservation is attained within x/d = 2.0, in case of single jet. For co-axial jets, the degree of dynamic self-similarity in the near field was found to be poor for both values of experimental area ratios. The scenario eventually got worst at higher velocity ratios.

Chapter 3

THEORY

Co-axial jets are comprised of two concentric axisymmetric jets emitting from a compound nozzle at different unidirectional speeds in to a region of fluid with which each of the fluid streams is completely miscible. The outer jet is known as annular jet while the inner one referred to as the central jet. Depending on the thermal conditions of the annular jet and the central jet, the flow may be isothermal or thermally stratified (non-isothermal). An isothermal flow case presents both of the jets at same temperature while in case of non-isothermal flow, the central jet and annular jet are made to flow at different temperatures.

3.1 Governing Equations

Non isothermal turbulent jet flow is governed by the continuity equation, the Navier-Stokes equations and Energy equation. Exact analytical solutions of these equations are yet to obtain because of their non-linear forms. Hypothesis and empirical assumptions are to be introduced for obtaining a set of equations with time averaged dependent variables.

With the assumption of steady, incompressible flow with no boundary layer effect at the nozzle exit and boundary layer approximations with constant fluid properties, the general equations for mean motion and energy of turbulent jets can be given in simpler forms in accordance to the flow configuration and nomenclature as shown in figure 3.1.1, as follows:

The continuity equation:

$$\frac{d(Ur)}{dx} + \frac{d(Vr)}{dr} = 0$$

The momentum conservation equation:

$$U\frac{dU}{dx}+V\frac{dU}{dr}=\frac{1}{r}\frac{d}{dr}\left(r\frac{\tau}{\rho}\right)$$

The energy equation:

$$U\frac{dT}{dx}+V\frac{dT}{dr}=\frac{1}{r}\frac{d}{dr}\left(\alpha r\frac{dT}{dr}\right)$$

Where x is the shear stress, ρ is the fluid density and α is the thermal diffusivity; U and V are the mean velocities in x and r directions respectively and T is the mean temperature.

In case of a circular jet (A special case of co-axial jets with $U_2 = 0$, Fig. 3.1.2), further mathematical operation [36] leads the integral form of momentum equation as:

$$\frac{d}{dx}\int_0^\infty 2\pi r dr\rho U^2 = 0$$

The above equation tells that the rate of change of momentum flux in axial direction is zero; that is the momentum flux in axial direction is conserved. By performing similarity analysis, for circular jet, Rajaratnam [36] showed that in the developed zone of circular jet,

$$U_m \propto {}^1/_x$$

Where U_m is the jet velocity on the nozzle axis in the developed zone.

Like circular jet, similar mathematical operation results in the integral momentum equation of a compound jet [Fig. 3.1.1] as,

$$\frac{1}{2\pi}\frac{d}{dx}\int_0^\infty 2\pi r dr\rho U(U-U_2) = 0$$

The above equation says that excess momentum flux of the compound jet above that of the uniform jet is preserved in the axial direction. By rearranging, the above equation can be presented as:

$$\frac{d}{dx}\int_0^\infty rU(U-U_2)dr = 0$$

Thus the velocity distribution viewed with respect to the uniform flow is found to be similar, that is

$$\frac{U-U_2}{U_m-U_2} = \frac{U'}{U'_m} = f\left(\frac{r}{b}\right)$$

3.2 Empirical Relations

Frostall and Shapiro [17] made experiments with co-axial jet having flow configuration as shown in Fig. 3.2.1 and found that the velocity distribution in the fully developed region of the jet could be satisfactorily described by the cosine expression of Squire and Trouncer [40] as:

$$\frac{U'}{U'_m} = \frac{1}{2}\left(1+cos\frac{\pi}{2}\frac{r}{b}\right)$$

From the experimental results, Frostall and Shapiro [17] obtained empirical relations for the spread of jet as a function of the distance from the orifice and for the decrease in the jet velocity for different velocity ratios between the surrounding velocity (U_2) of the secondary flow and the axial velocity (U_1) of the jet.

The length of the potential core region x_c was determined mainly from the value of the ratio of U_2/U_1 and it was found to increase with velocity ratios. Frostall [17] proposed the following empirical formula:

$$\frac{x_c}{d} = 4 + \frac{U_2}{U_1}$$

This relation was valid for the range $U_2/U_1 \sim 0.2$ to 0.50. From the above equation the length of potential core for circular jet ($U_2/U_1 = 0.0$) is found to be 4d.

According to Frostall [17] measurements, the relative velocity of the jet at the axis decreased hyperbolically with increasing x.

$$\frac{U'_m}{U_1 - U_2} = \frac{x_c}{x}$$

For $x > x_c$

For the change in the jet half width ($y_{0.5}$) he obtained

$$\frac{2y_{0.5}}{d} = \left(\frac{x}{x_c}\right)^{1-\frac{U_2}{U_1}}$$

For $x > x_c$

The empirical hyperbolic equation 3.2.3 between the mean velocity and distance seems to apply even at large distances from the exit (For $U_2/U_1 = 0.50$, Frostall's measurements covers the range from x/d = 0 to x/d = 120). However, if the result were correct, one would expect a linear increase of the jet width with increasing x. But on the basis of the momentum integral equation, equation 3.2.4 does not agree with the equation 3.2.3; at any rate this is so if the velocity profiles in consecutive sections are similar. In addition, according to the Frostall's measurements, the profiles were practically similar i.e. at each section the velocities were expressed in terms of U_m and the radial distances in terms of the jet half-width.

According to the empirical equation 3.2.4, the increase in the jet width becomes zero if U_2/U_1 approaches to unity. This is logical provided that both the primary and secondary flows are free from turbulence.

Bradbury [7] also proposed another empirical relation for the developed region of a co-axial jet as follows:

$$\frac{U'_m}{\sqrt{U_1(U_1 - U_2)}} = \frac{6.3}{x/d}$$

3.3 Self-Preservation Variable

In study of jets it is common practice to plot velocity against self-preserving or similarity variables. The self-preserving independent variable was defined in different ways by different researchers to express the self-preserving condition of the jet. Actual self-preserving zone of a jet occurs when all of its mean and turbulent components are in equilibrium, which is in the fully developed region of a jet. Another self-preservation is also found within the potential region called partial selfpreservation region. The self-preserving independent variable was defined in different ways by different authors.

Islam [23] used $\eta = (y-y_{0.50})/x$ as the self-preserving variable for expressing the flow to be self-preserving in the developing region. Where,

- x is the axial distance
- y is the radial distance
- $y_{0.5}$ is the radial distance at which the local mean velocity is equal to half of
  the centerline velocity.

Rajaratnam [36] used $\eta = (y-y_{0.95})/(y_{0.50}-y_{0.95})$; where, $y_{0.95}$ is the radial distance at which the local mean velocity is equal to 95% of the centerline velocity.

Champagne and Wygnanski [11] considered $\eta = y/(x-x_h)$; where x_h is the distance of virtual origin from the nozzle exit plane.

Ko and Chan [26] used different self-preserving variables for different zones of a jet as follows:

$\eta = (y-y_{0.50})/ (y_{0.90}-y_{0.10})$	for initial merging zone
$\eta = (y-0.5D_e)/ x$	for intermediate and fully merged zone
$\eta = y/y_c$	for fully merged zone of annular jet zone

Where, y_c is the radial distance at which the local mean velocity is equal to half of U_m. U_m is the maximum mean velocity on the jet axis in the x-y plane and D_e is the equivalent diameter of the fully merged jet.

The flow structure of non-isothermal jets under current investigation also presents a thermal field in addition to the dynamical velocity field. To ascertain the self-preservation condition of this thermal field, a similarity variable of mean temperature is also defined as

$$\eta_t = (y-y_{t0.50})/x$$

Where, x and y are the axial and radial distance respectively and $y_{t0.5}$ is the radial distance at which the local mean temperature is equal to half of the centerline mean temperature at the corresponding axial location.

3.4 Virtual origin

The origin of the co-ordinate system of a jet has been taken as the geometric origin. However, practically it has been observed by many researchers that the jet seems to be discharged from either downstream or upstream of the lip of jet producing component. Thus, the virtual origin comes in defining jet characteristics instead of geometric origin and is classified as:

1. Kinematic virtual origin
2. Geometric virtual origin

The Kinematic virtual origin, C_k is determined from the decay of the centerline mean velocity, U_c. The non-dimensional inverse centerline velocity can be expressed by the following equation:

$$\left(\frac{U_{ce}}{U_c}\right)^2 = K_c\left(\frac{x}{d} - C_k\right)$$

Where K_c is the rate of the decay of centerline velocity.

The geometric virtual origin, C_g is determined from the growth of the jet half width $y_{0.50}$ as follows:

$$\left(\frac{y_{0.5}}{d}\right) = K_s\left(\frac{x}{d} - C_g\right)$$

Where, K_s is the spread rate of the jet half width ($y_{0.50}$).

Chapter 4
EXPERIMENTAL SET UP

This chapter provides a brief description of the experimental set up used for the current study along with the measurement systems used for velocity and temperature of the jet flow field. A short description of data analysis and calculation technique as well as that of the co-ordinate system is also included for better understanding of the overall experimental study and subsequent analysis of the results.

4.1 Jet flow Facility

The experimental study has been carried out by using the circular co-axial air jet facility as shown in the figures 4.1.1, 4.1.2 and 4.1.3. To make the flow of hot central jet to produce non isothermal single jet as well as thermally stratified co-axial jets, a series of heaters are installed in the flow path of the central jet prior to the experiments with some minor modifications of the existing circular co-axial jet flow facility.

The overall length of the flow facility [P. 1] is 8.1 m. It has axial flow fan unit, two settling chambers, two diffusers a silencer and a flow nozzle. The fan unit consists of three Woods Aerofoil fans (England) of the same series. A vibration isolator and a silencer are placed at the discharge of the fan unit. The fan unit generates both vibration and noise while generating the flow. The vibration isolator restricts the transmission of the vibration to the downstream side while the silencer reduces the noise. The fan unit receives air through the butterfly valve and discharges it into the silencer of the flow duct. Flow from the silencer passes on to the settling chamber through a diffuser. At the discharge, side of this chamber there is a flow straighter and wire screen of 12 meshes to straighten the flow and to breakdown large eddies present in the air stream. Air from this chamber then flows to the second settling chamber through a nozzle and second diffuser. The flow straighter and wire screens are used here to ensure a uniform axial flow free of

large eddies which may present in the upstream side of the flow. The flow from the second settling chamber then enters the 100 mm long and 80 mm diameter circular nozzle. At the farthest end the diameter of the flow facility is reduced from 475 mm to 80 mm where the experimental nozzle is fitted.

A centrifugal blower is placed below the main flow system to supply air to the central nozzle. A 100 mm discharge line of the blower is connected to the heating/settling chamber. A 62 mm PVC pipe is connected to delivery side of this chamber and enters radially into the 2nd settling chamber of the main flow system placed concentrically with the 475 mm diameter main flow set up by means of four pin centralizers in three different locations viz. 475 mm pipe flange [P. 2], 250 mm. pipe flange [P. 4] and 80 mm discharge flange [P. 5]. The distances between the three consecutives centralizers are 520 mm and 460 mm respectively. In between the centralizers, a 100 mm PVC pipe having length of 520 mm is placed and it is connected to the 62 mm radial pipe insertion through a 62 mm×100 mm diffuser. The outlet of the 100 mm PVC pipe is connected with a 29 mm steel pipe acting as the central nozzle via another diffuser. This 100 mm PVC pipe acts as a plenum chamber [P. 3] with two pairs of wire screens of 24×24 mesh inside it. These wire screens are placed at the entry and exit of this 100 mm PVC pipe to break the big eddies created in the upstream and thereby to produce smooth uniform flow with low levels of turbulent intensity. The heating system has a capacity of 3 kW and consisted of four 'different sections as divergent entry section, heater section, settling chamber and convergent exit section. Air from the centrifugal blower comes to the heater section through the divergent entry section. There are six heating elements in the heater section that are made of electric resistance wire and mica sheet and placed to ensure uniform heating to the flowing air throughout the section. After passing over the heaters, the hot air enters into the settling chamber where the temperature of the hot air attains more uniformity because of intermixing. The whole air heating system is insulated with asbestos cloth and glass wool to prevent the heat loss to the surrounding from the hot air. Finally, the hot jet is passed to the co-axial jet flow system through the exit section.

The flow through the central nozzle is regulated by controlling the supply frequency to the centrifugal blower whereas airflow through the annular nozzle is controlled by the butterfly valve and/or by regulating the speed of the fan units. The temperature of the

central jet is regulated by controlling the supply voltage to the heaters by means of a variac. The whole setup is mounted on rigid frames of M.S. pipes and plates and these frames are securely fixed with the ground so that any possible unwanted vibration of the system may be reduced to a minimum. To avoid the effect of ground shear, the set is installed at an elevation of 1.4 m from the ground.

For the present investigation, two outer nozzles of the same length (100 mm) but of different diameters such as 80 mm and 63 mm (figures 4.1.4.a and 4.1.4.b) are used. The diameter of the central nozzle jet is kept fixed at 29 mm with resulting two area ratios of 6.6 and 3.57 respectively.

4.2 Co-ordinate System

Throughout the whole experimental study, the nozzle exit center is taken as the origin. The centerline of the nozzle in the direction of the flow is denoted as positive x-axis and the radial distance pointing upwards is referred to as positive y-axis. The axis located at a position of 90° anti clockwise from the positive y-axis is taken as the positive z-axis as shown in figure 4.2.1.

4.3 Traversing Mechanism and Probe Setting

The pitot static tube is traversed in the air stream with the help of a Mitotoyo (Japan) co-ordinate measuring machine (Type- CS652) with ranges X co-ordinate 800 mm, Y co-ordinate 500 mm and Z co-ordinate 400 mm (P. 7). The probe is made to traverse by rotating the respective driving wheels of rack and pinion arrangement in each axes. A position can be fixed with the resolutions of 0.001 inch with the help of the wheel driving the rack and pinion mechanism and this can be read in the dial gauge.

To minimize the effect of any boundary layer in the jet flow, the nozzle centerline is set at 1400 mm above the ground and the traversing mechanism is placed on a hydraulically operated table designed for this purpose. To avoid any possible disturbance, the table is also placed 900 mm away from the nozzle axis. The table top can be moved up and down

hydraulically and is mounted on two 4500 mm long V-shaped rails and wheels. These rails are placed parallel to the nozzle axis. Thus the table with the traversing mechanism can move along the jet in axial direction through a distance of 4500 mm. The parallelism of the both the axes is secured with the help of plumb bob and cathetometer. The measuring probe is mounted on the z-arm of the traversing mechanism and can be placed in the centerline of the nozzle from the side by moving the z-arm. The probe could be moved in the x and y-axis direction by moving the z-arm in the x and y direction respectively. In case of further movement of the probe in the axial direction, the whole table could be moved on the rail by rotating the lead screw made for this purpose.

Great care is taken to set the probe as correctly as possible with respect to the flow direction and centerline of the nozzle. The base of the coordinate measuring machine is kept parallel to the centerline of the jet facility horizontally with the help of a high precision spirit level, plum bob and cathetometer. The alignment of coordinate measuring machine is necessary to ensure correct axial and cross movement of the probe.

4.4 Measurement of Velocity and Temperature

The mean velocity and temperature of the jet flow field for different initial and boundary conditions are measured by means of a pitot static tube of 3.0 mm outside diameter with an embedded T-type thermocouple (United Sensors, USA) at the tip along with a Furnace Control (U.K) pressure transducer (Model: FC014) and temperature display unit (figure 4.4.1, P. 8). The pressure signals of the pitot static tubes are transmitted to the pressure transducer through 1.4 mm flexible plastic tubes. The pressure corresponds to the velocity head of the pitot static tube. The velocity from the pitot static tube signal is expressed by $U^2 = 2(P_0-P_s)/p$, where p is the fluid density and P_0, P_s are the stagnation and static pressures respectively. The thermo-electric signal of the thermocouple embedded at the tip of the pitot static tube corresponding to local temperature (T) is transmitted to the temperature display unit by using extension cable. The temperature at the center of the exit plane of central jet is taken as its mean temperature T_1 while the ambient temperature T_2 is taken as that of the annular jet. The consistency of the central jet temperature (T_1) is monitored with the help of an additional thermocouple placed at

the delivery of the heating/settling chamber. Before starting the experiments, the pressure transducer has been calibrated for different ranges of scale with the help of an inclined manometer. Similar calibration is also made for thermocouples.

4.5 Data Analysis and Calculation Technique

All the measurement points are made non-dimensional by dividing the distances along the y-axis with the central nozzle exit diameter (d) and axial distance (x). The velocity (U) is made non dimensional by dividing them by the exit centerline velocity at the origin denoted by U_{co}. The local temperature of jet field T (K) is also made non-dimensional temperature variable (θ) according to the following relation

$$\theta = \frac{T - T_2}{T_1 - T_2}$$

Where, T (K) is the local temperature of jet flow field, T_1 (K) is the mean temperature of hot central jet and T_2 (K) is that of ambient annular jet or surroundings.

All measurements have been carried out for the central jet velocity of 20.56 m/s with corresponding Reynolds numbers of 3.72×10^4. Four different annular to central jet velocity ratios (U_2/U_1 = 0.0, 0.25, 0.50 and 0.75) have been taken into consideration for different thermal conditions of the jets. Based on absolute temperature scale, the ratio of the annular jet temperature (T_2) to that of the inner jet (T_1 is varied as T_2/T_1 = 1.0, 0.974 and 0.925. The computer program MS-Excel has been used to work out all the pertinent calculations and graphical calculations.

Chapter 5

RESULT AND DISCUSSION

5.1 General

Investigations of the dynamical and the thermal fields developed in trip ring excited non-isothermal co-axial jets are the main objectives of the current research. For this purpose, measurements of velocity and temperature of the flowing fluid have been made in the near field of co-axial jets for different initial and boundary conditions. In the present study, the co-axial jet is obtained by issuing flow from a concentric compound nozzle having an inner nozzle of 29 mm diameter. The diameter of the outer nozzle is 63 mm that result an annular to inner area ratio of the jet (A_2/A_1) as 3.57. The thermal condition of the flow is altered by changing the temperature of the inner jet T_1 (K) so that the ratio of the temperature of the annular jet T_2 (K) to that of the inner jet, T_2/T_1 is changed. Three different values of temperature ratios (T_2/T_1) are considered in the current study as 1.0, 0.974 and 0.925. The velocity of the inner jet (U_1) of co-axial flow is varied for different types of excitation while that of the annular jet (U_2) is changed to attain a velocity ratio (U_2/U_1) of 0.0, 0.25, 0.50 and 0.75 respectively. Moreover, the inner jet of co-axial flow is considered as the primary one while the annular as the secondary. So the Reynolds numbers are calculated considering the flow and geometric configurations of the inner jet.

A co-axial jets having velocity ratio (U_2/U_1) is equal to zero can be considered as a single jet. So this case of co-axial jets is often termed as single jet in the following discussion as a matter of simplicity.

5.2 Exit Velocity

A single jet is an extreme case of co-axial jets when the velocity of the annular jet becomes zero i.e. it is simply a co-axial jets having zero velocity ratio (U_2/U_1). Figures 5.2.1 present a comparative study between the exit velocity profiles of co-axial jets ($A_2/A_1 = 3.57$) with four different velocity ratios. Theoretically, the potential core at the

exit of the single and the co-axial jets should extend up to y/d = 0.50. But from the measurements it is fairly evident that due to the presence of boundary layers, the jet velocity starts to decrease earlier in each case. The existences of the boundary layers are also obvious in case of the annular potential core of the coaxial jets. Moreover, the boundary layer at the outer edge of the annular jet is found to be thicker than that of the inner boundary. This difference of thickness is due to the fact that the outer one is under the influence of concave surface which gives compressive action on the fluid thereby increasing the resistance to the flow and hence increases the thickness of the boundary layer. On the contrary the inner one has a convex surface giving the expanding action on the fluid which gives less resistance to the flow thereby decreasing the thickness of the boundary layer. As area ratio increases this effect also increases. The nose-shaped part in all the velocity profiles of co-axial jets indicates the presence of solid wall of the central nozzle. It will be noticed later in the subsequent figures that the magnitude of this shape increases with the increase of velocity ratio.

Effects of velocity ratios (U_2/U_1) at different types of excitation method are shown in figures 5.2.2 and 5.2.3. From these figures, it is quite clear that with the increase of velocity ratio, the nature of the central jet velocity profile changes from saddle shape to parabolic form. Therefore, near the central nozzle boundary, velocity decreases with the increase of velocity ratio. But in case of the annular jet, the velocity profile is changed from its symmetric nature to asymmetric shape i.e. as the velocity ratio increase, the velocity towards the outer wall increases relative to its inner wall. This is the consequence of the opposite curvature effect as described earlier.

From figure 5.2.4 to 5.2.6 the effect of different excitation for specific velocity ratio is shown. In figure for velocity ratio of 0.25 there is a negative pressure zone in the excited jets, created by both outer and inner rings. This creates the reverse flow or the circulation of fluids in the place between the central and annular jets. The reverse flow is creates some wakes which can not be measured by the current experimental setup. This negative pressure zone is indicated by the dotted line in the graphs. In case of outer ring excitation the region is form around 0.6 to 0.7 and in case of inner ring excitation the region is from around 0.4 to 0.5. The actual reason of this specific place is the placement of the rings and the width of the rings. There is also a slight increase of velocity before the inner ring

and after the outer ring, when the velocity ratio is 0.75. This acceleration of fluid may be caused by the sudden decrease of area due to the presence of rings.

5.3 Exit Temperature

Figure 5.3.1 illustrates the exit temperature profiles of a non-isothermal single jet with temperature ratio (T_2/T_1) 0.974 and 0.925 respectively at Re = 3.72×10^4. Theoretically the thermal potential core like dynamical core should extend from y/d = 0 to y/d = 0.50 at the exit. But it is observed that the temperature starts to decrease earlier near the boundary of the nozzle exit. This may be the consequence of heat transfer from the hot air to the surroundings during its journey from the heating chamber to the nozzle exit due to the prevailing temperature gradient. As a result, the thermal potential core at the nozzle exit decreases in size and becomes irregular. Moreover, heat transfer from the hot jet causes the temperature of the surrounding fluid to raise outside (y/d > 0.50) the jet boundary as shown in figure 5.3.1.

A comparative study of the exit temperature profiles between non-isothermal single jet and thermally stratified co-axial jets with different velocity ratios is shown in figures 5.3.2, 5.3.3 and 5.3.4. In case of co-axial jets, the temperature near the boundary of the central jet is found to decrease much rapidly than that of single jet. In other words, the size of the thermal potential core of co-axial jets at the nozzle exit is smaller than that of single jet. This is due to the fact that, the flow of the annular jet in case of co-axial jets takes away larger amount of heat from the hot central jet during its journey from the heater chamber to the nozzle exit. Thereby the size of the thermal potential core at the nozzle exit reduces in non-isothermal co-axial jets.

Figure 5.3.5 represents the effect of velocity ratio (U_2/U_1) on the exit temperature profile of non-isothermal co-axial jets. All the curves are more or less similar to each other and thereby no significant effect of velocity ratio on the exit temperature profile of co-axial jets is noted.

Fig 5.3.6 and 5.3.7 represents the effect of inner trip ring excitation on single jet for temperature ratio of 0.925 and 0.974. It is found that the thermal potential core is far shorter in the inner trip ring excited single jet then the unexcited single jet. This phenomenon can be explained by the enhanced mixing by the wakes created by the ring.

In figure 5.3.8 to 5.3.13 the effect of different types of excitation is shown. In each graphs it is clearly visible that the temperature gradient is more prominent in unexcited co-axial jets than the excited ones. This is due to the enhanced mixing by the wake produced by the excitation rings. Moreover in every case the thermal potential core for outer trip ring excited jets is longer than that of inner trip ring excited or unexcited jets. This is caused by the convex nature of the outer trip ring, which gives an expanding effect on the cooler outer jet and prevents the hot jet form the circular nozzle to mix with it. While in inner trip ring excited co-axial jets the inner ring tends to compress the jet due to its concave nature.

From figure 5.3.14 to 5.3.19 the effect of different velocity ratio for inner trip ring excited co-axial jets with specific temperature ratio is exhibited. It is observed that higher velocity ratio tends to decrease the thermal potential core and decrease the temperature more gradually than that of a single jet. It is caused by the heat transfer between the hot jet and cold jet, through the steel tube which carries hot central jet from the blower.

In comparison with the single unexcited jet, outer trip ring excited jet, for all velocity ratio and temperature ratios, have generally the same thermal potential core length but with a more gradual change in non dimensional thermal characteristics. This phenomena is shown in fig 5.3.20 to 5.3.25.

5.4 Centerline Velocity

The fundamental axis of any jet flow is its centerline. Different important aspects of flow field such as the potential core length, momentum transfer amongst fluid streams; virtual origin etc. can be identified from the flow characteristics along the centerline of a jet.

Figure 5.4.1 presents the centerline velocity profiles of a single jet (29 mm) and that of co-axial jets ($A_2/A_1 = 3.57$, $U_2/U_1 = 0.25$) at isothermal condition. In case of the single jet the centerline velocity remains constant up to some axial distance and then starts to decrease monotonically in the downstream direction. This portion of jet flow field with undiminished centerline velocity is known as potential core. The length of potential core (Lp) for single jet is found to be 4d and that of co-axial jet to be 6.5d. The length of the potential core of co-axial jet is greater than that of the single jet because of the fact that in case of single jet, the interaction between the jet and stationary surrounding causes the rapid growth of shear layer towards the central axis of the jet that results in rapid decay of the jet velocity along the downstream direction, but in the case of co-axial jets, the presence of annular jet enhances mixing process with much less interaction thereby with less energy dissipation which retards the growth of the shear layer towards the axis of the jets from the surroundings. From this figure it is also clear that the decay of centerline velocity occurs relatively at a faster rate in the single jet than that of the co-axial jets. This shows the augmented momentum transfer in the developed zone of the single jet as compared to the co-axial jets.

The effect of velocity ratio (U_2/U_1) on the centerline velocity decay of co-axial jets ($A_2/A_1 = 3.57$) are manifested in figure 5.4.2 for Reynolds number 3.72×10^4. The centerline velocity seems to be almost constant up to x/d = 6 for all velocity ratios. Afterwards, the centerline velocity starts to decrease monotonically in the downstream direction. However it is found that at lower velocity ratio, the centerline velocity of co-axial jets decrease at faster rate along the jet axis. This happens because lower velocity ratio presents larger velocity gradient between the central jet and adjacent annular jet creating more resistance to the flow of the central jet by the annular jet. As a result, the velocity along the axis of the central jet is found to decay faster rate at lower velocity ratio in the downstream direction.

Amazingly the length of the potential core is decreased to 3d in case of inner trip ring excitation, which is indicated by the figure 5.4.3 And the velocity is decreased in a more rapid rate than that of non excited or outer trip ring excited co-axial jets. Such behavior can be explained by the wakes created after installing the inner trip ring. These wakes rapidly mix the two different velocity fluids and shorten the potential core length. Inner

trip ring tends to speed up the air of the circular nozzle like an orifice and that is the reason for the bulging of graph at lower x/d value, which is increased with velocity ratio.

For outer trip ring excited co-axial jets the potential core is in 3d to 4d for different velocity ratio. Moreover, for different velocity ratio the rate of decrease of speed along with the centerline is almost the same. This may indicate that outer trip ring excited co-axial jets acts more like a single jet rather than co-axial jets. And with the increase of velocity ratio it helps very little to mix up the fluid. This behavior is depicted in the fig 5.4.4.

In figure 5.4.5 to 5.4.7 the effect of different types of excitation for the same velocity ratio is shown. For velocity ratio 0.25 the unexcited jet has a core length of 6d and that of for outer trip ring excitation is 4d and inner trip ring excitation is 2d. The inner trip ring also decrease the centerline velocity of the central jet at a very fast rate. For 0.50 velocity ratio there is a clear indication that inner trip ring tends to accelerate the fluid at lower x/d value while external trip ring decelerates it. For higher velocity ratio this effect is increased initially for excited jets. However, for inner and outer trip ring excited co-axial jets the decrease of change of velocity occurs in the same manner.

5.5 Centerline Temperature

The centerline mean temperature of non-isothermal jet flows is one of the most important parameters that reveal different important aspects of the thermal field of non-isothermal jets like thermal core length, diffusion mixing amongst the fluid streams etc. In the current investigation the centerline temperature of the jet is expressed as:

$$\theta_c = \frac{T_c - T_2}{T_1 - T_2}$$

Where, θ_c = Non-dimensional temperature variable.

T_c = Centerline temperature (K).

T_1 = Mean temperature of the central/ inner jet (K).

T_2 = Mean temperature of annular jet/ surroundings (K).

The effect of temperature ratio (T_2/T_1) on the centerline temperature profile of a non-isothermal co-axial jet is shown in figures 5.5.1, 5.5.2 and 5.5.3. This is observed that the centerline temperature remains constant up to some distance from the nozzle exit and then starts to decrease monotonically in the downstream direction. This region with undiminished centerline temperature is the called the thermal potential core of non-isothermal jets. However, as the jet proceeds in the downstream direction, thermal diffusion from the hot jet as well as mixing with the surrounding ambient fluid causes the thermal potential core to contract gradually as the shear layer does to the dynamical potential core. The bulk mixing in the developed zone of the non-isothermal single jet makes the centerline temperature to decrease monotonically behind the thermal potential core. For both of the temperature ratios (T_2/T_1 = 0.974 and 0.925) thermal potential core is found to be of length 4d. From these figures it is also observed that, the centerline temperature of non-isothermal single jet decreases more rapidly at lower temperature ratio. The fluctuation of temperature is found to be more prominent at its lower range than that in the higher one. It indicates that the instability of temperature is more at lower value of temperature ratio.

The effect of internal trip ring excitation method on the centerline temperature decay of non-isothermal single jet is shown in figures 5.5.4 and 5.5.5 for two different values of temperature ratios. In both the cases, the length of thermal potential core for inner trip ring excitation is lower. At temperature ratio of 0.925 the length of thermal potential core is found to be 3d and 2d for unexcited and inner trip ring excited jets respectively at temperature ratio of 0.925. And for temperature ratio of 0.974 it is 4d and 2d respectively. All the centerline temperature profile for temperature ratio 0.974 decreases in a stepped manner. This is due to the fact that the temperature indicator can not show fraction numbers. That's why the non-dimensional temperature variable has a low resolution, which creates this specific shape in the graphs.

Figures 5.5.6 to 5.5.11 illustrate a comparative study of the centerline temperature profile between different excited co-axial jets. In these figures, it is evident that at lower velocity ratio unexcited and outer trip ring excited co-axial jet centerline temperature follows the same path. With the increase of velocity ratio the difference of centerline temperature profile between unexcited and outer trip ring excited jet is also decreasing. Moreover, in

the entire cases inner trip ring excited co-axial jet has the shortest thermal potential core and the rate of change of temperature is also greater than other two cases i.e. without excitation and outer trip ring excitation.

Figures 5.5.12 to 5.5.23 show a closer look at the effect of the velocity ratio for a co-axial jet. For inner trip ring excited jets at temperature ratio of 0.925 and 0.974 with the increase of the velocity ratio the temperature profile tends to decrease slowly. However, the difference is so small that it can be inferred that velocity ratio has a very small effect on temperature profile of inner trip ring excited co-axial jets. Figure 5.5.24 indicates the comparison between different velocity ratios for inner trip ring excited co-axial jets. As we see there excited jet with zero velocity ratios i.e. single jet has more prominent temperature gradient than the others. The length of the thermal potential core is more or less insensitive to the velocity ratio. But beyond the thermal potential core the centerline temperature is found to decrease faster at lower velocity ratios. This may be due to rapid mixing of the fluid streams at lower velocity ratios of co-axial jets in the developed zone. However, for outer trip ring excited co-axial jets temperature decrease faster at higher velocity ratios. This may be due to the strong wake created by the outer ring at higher velocity, which mix the fluids better at higher velocity ratio.

Chapter 6

Conclusions and Recommendations

6.1 Conclusions:

Experimental investigations of thermally stratified co-axial jets have been performed to study the effect of velocity and temperature ratios and flow excitation by inner and outer trip rings. Determination of the dynamical velocity field and the thermal field of co-axial jets together with their mutual dependency are the main issue to be considered. Part of the result of the current study can be linked to that of Hasan [49] to make concluding remarks on some important flow phenomena of co-axial jet flow field. From the measurement and subsequent analysis of data and curves the following conclusions may be drawn.

1. In trip ring excited co-axial jets a negative pressure zone is created due to formation of wake and reverse flow in the place between the central and annular jets. The place of the wake depends on the thickness of the trip ring and the type of the ring i.e. outer or inner.
2. The width of the thermal potential core is decreased in non-isothermal co-axial jets than the single jet. However, the width is not dependent on the velocity ratio. For different velocity ratio the width is almost the same.
3. The inner trip ring excited single jet has a much shorter thermal potential core than the unexcited one.
4. The outer trip ring excited co-axial jets and unexcited co-axial jets have almost the same thermal potential core length for lower velocity ratio.
5. Temperature gradient is more prominent in unexcited non-isothermal co-axial jets than the excited ones.
6. Co-axial jets have longer potential core than that of the single jet. Irrespective of the velocity ratio, it is same (6d) for all unexcited co-axial jet.
7. Centerline velocity decays faster for lower velocity ratio and vice versa.
8. Inner trip ring is most efficient in mixing co-axial jets. The lengths of both dynamic and thermal potential core are shorter then that of outer trip ring excited or unexcited co-axial jets. In the case of dynamic potential core it is less than 3d.

9. For outer trip ring excited co-axial jets the length of the potential core is in between 3d to 4d.
10. Velocity ratio has a very little effect on centerline velocity decay in outer trip ring excited co-axial jets.
11. In non-isothermal jets, the centerline temperature decay takes place more quickly at lower temperature ratio that at higher one.
12. Outer trip ring has a very little effect on centerline temperature decay in lower velocity ratio, but at higher velocity ratio its effect is found to be noticeable.

6.2 Recommendations:

The present study is a preliminary work on trip ring excited non-isothermal co-axial jets. The research can be modified and extended in a diversified way. The following suggestions can be made for future work on this topic:

I. Same measurement can be done with more sensitive temperature system for higher values of temperature ratio (T_2/T_1) in the far field of jets.
II. Static pressure distribution can be obtained for the same configuration.
III. To perceive the flow structure of jet flow field more clearly, some important parameters like longitudinal turbulence intensity, transverse turbulence intensity, turbulence shear stress can be measured. Constant temperature anemometer or LASER Doppler anemometer may be used for this purpose.
IV. Flow visualization technique can be used to have a vivid picture of the mixing zone of co-axial jets.
V. All the above measurements can be made under controlled upstream acoustic excitation.

Figures

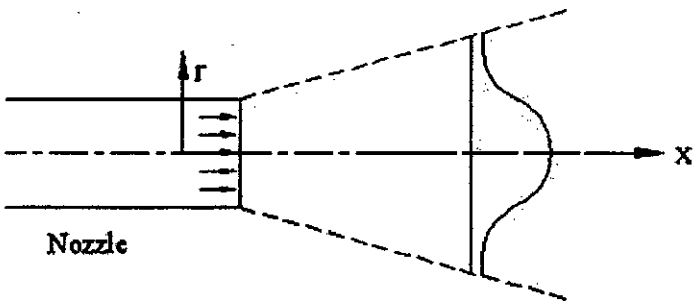

Figure 1.2.1 Free Jet

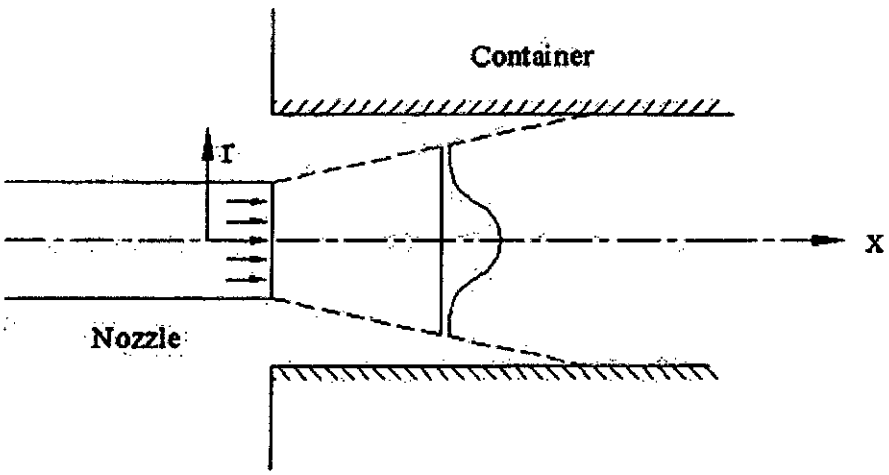

Figure 1.2.2 Confined or Bounded Jet

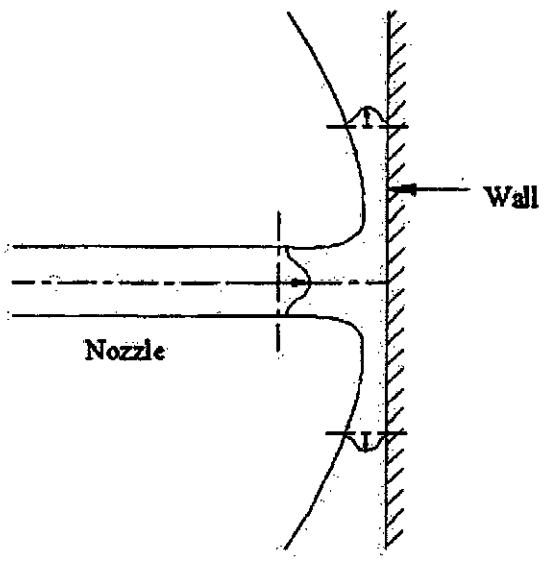

Figure 1.2.3 Wall Jet

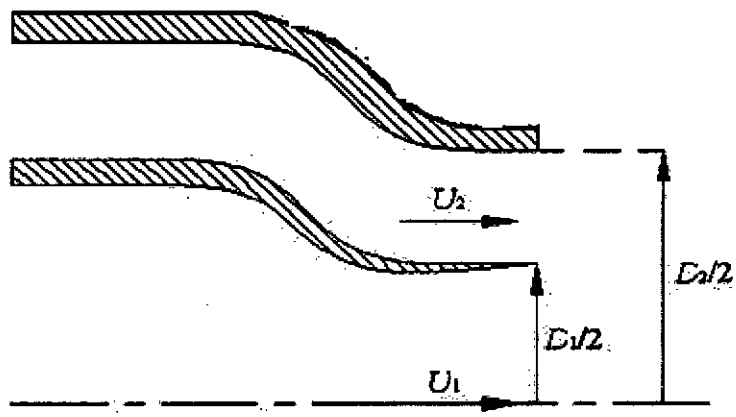

Figure 1.2.4 Co-axial Jet Configuration

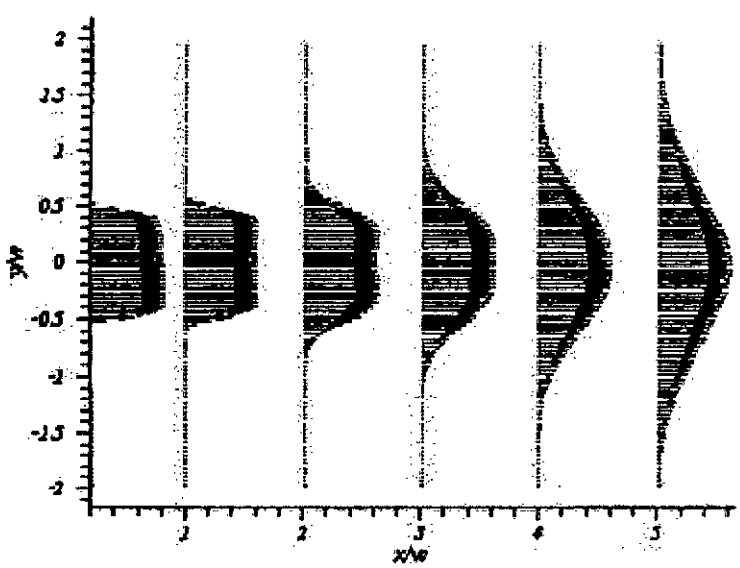

Figure 1.3.1 Velocity field distribution of a circular jet

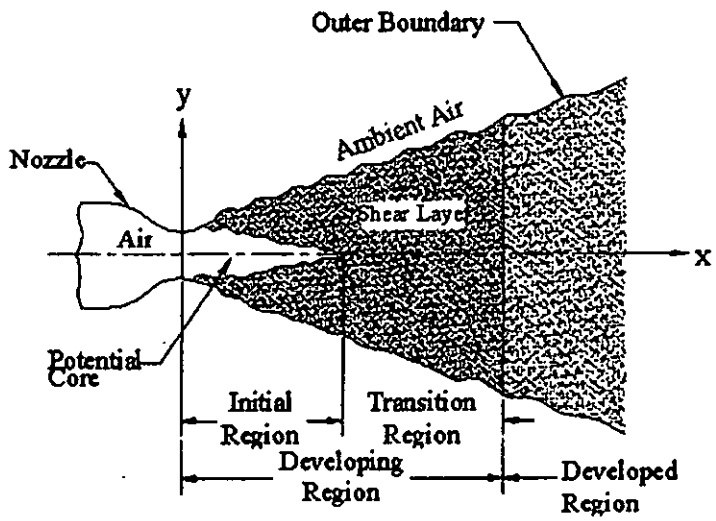

Figure1.4.1 Flow regions of a free jet

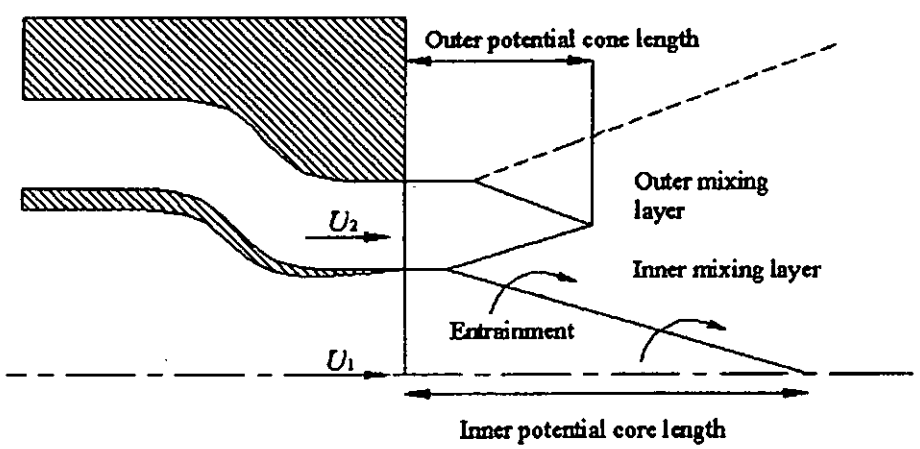

Figure1.5.1 Schematic Diagram of the Mixing Layers in the Near Field of Co-axial Free Jets.

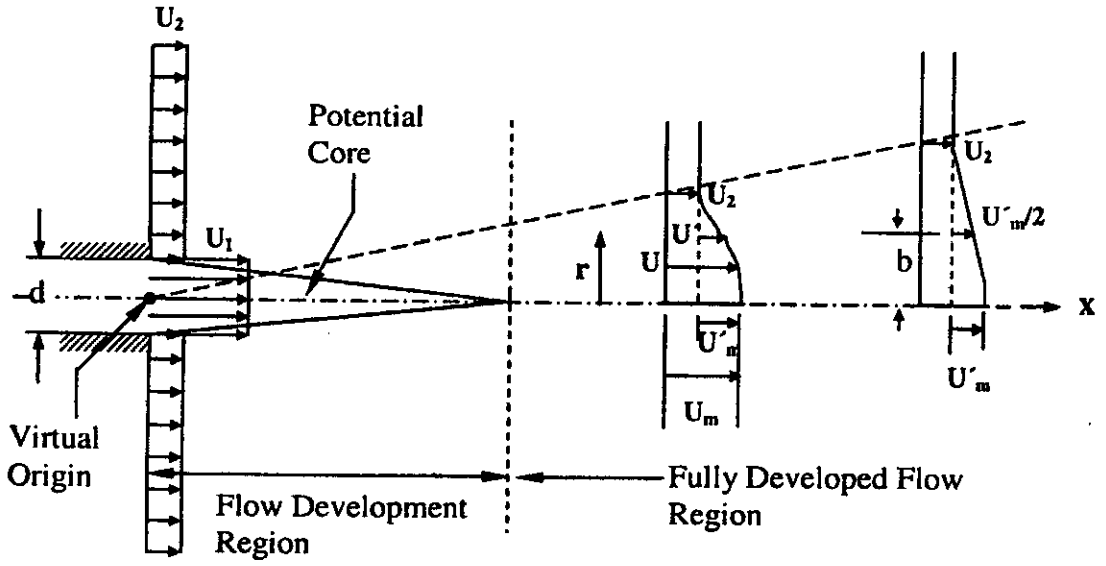

Figure 3.1.1: Co-axial Jet Flow Configuration

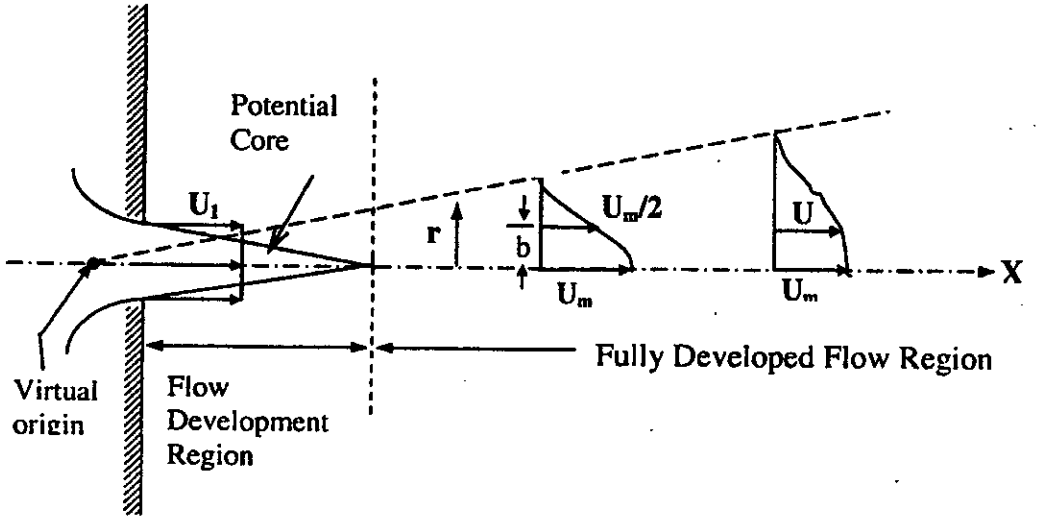

Figure 3.1.2: Circular Jet Flow Configuration

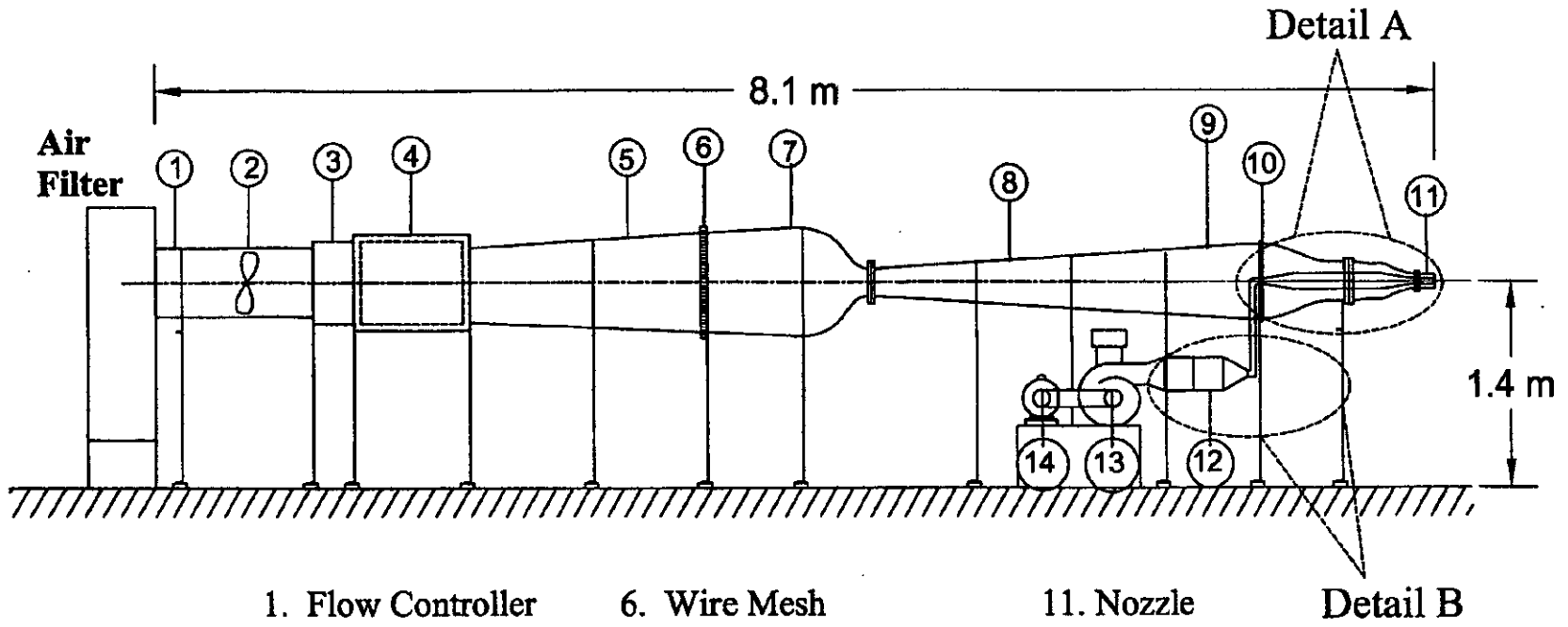

1. Flow Controller
2. Fan
3. Vibration isolator
4. Silencer
5. 1st Diffuser
6. Wire Mesh
7. 1st Settling Chamber
8. 2nd Diffuser
9. 2nd Settling Chamber
10. Wire Mesh
11. Nozzle
12. Heater
13. Blower
14. Motor

Figure 4.1.1: Schematic diagram of the jet flow facility

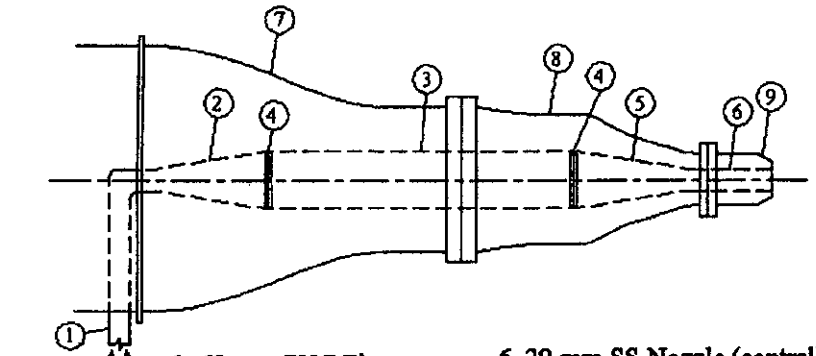

Detailed – A

Figure 4.1.2: Enlagred View of Co-axial Flow System

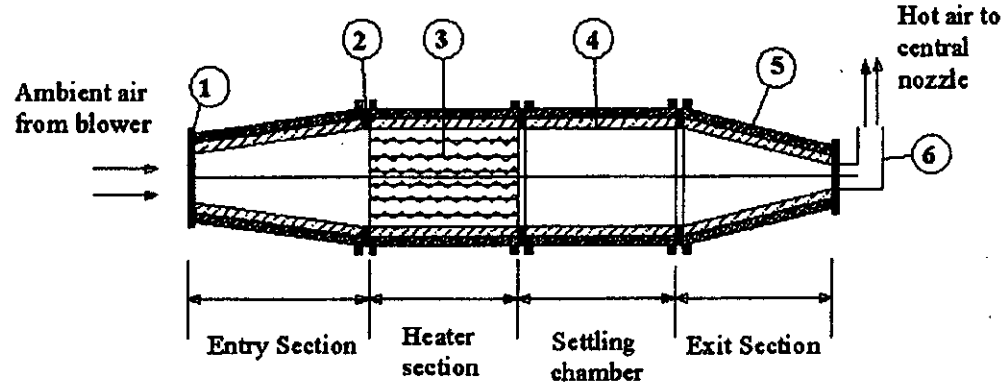

Detailed – B

Figure 4.1.3: Enlarged View of Air Heating System

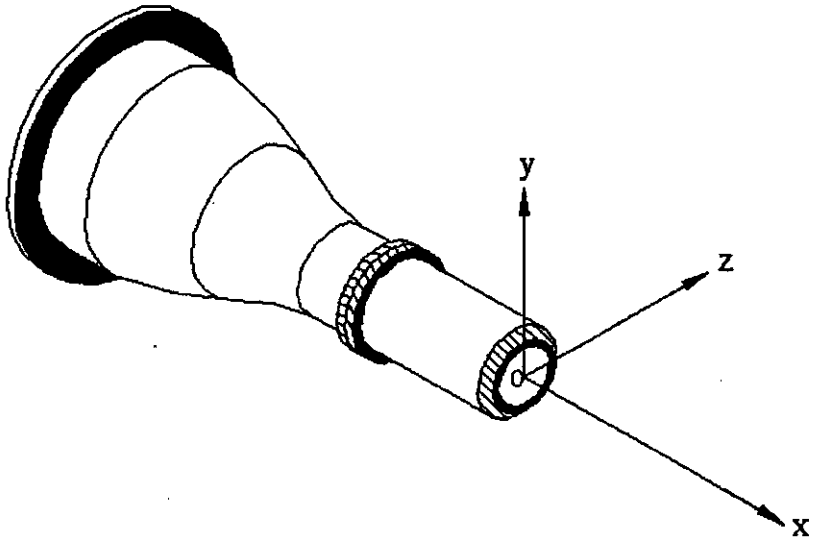

Figure 4.2.1: Co-ordinate System of Nozzle

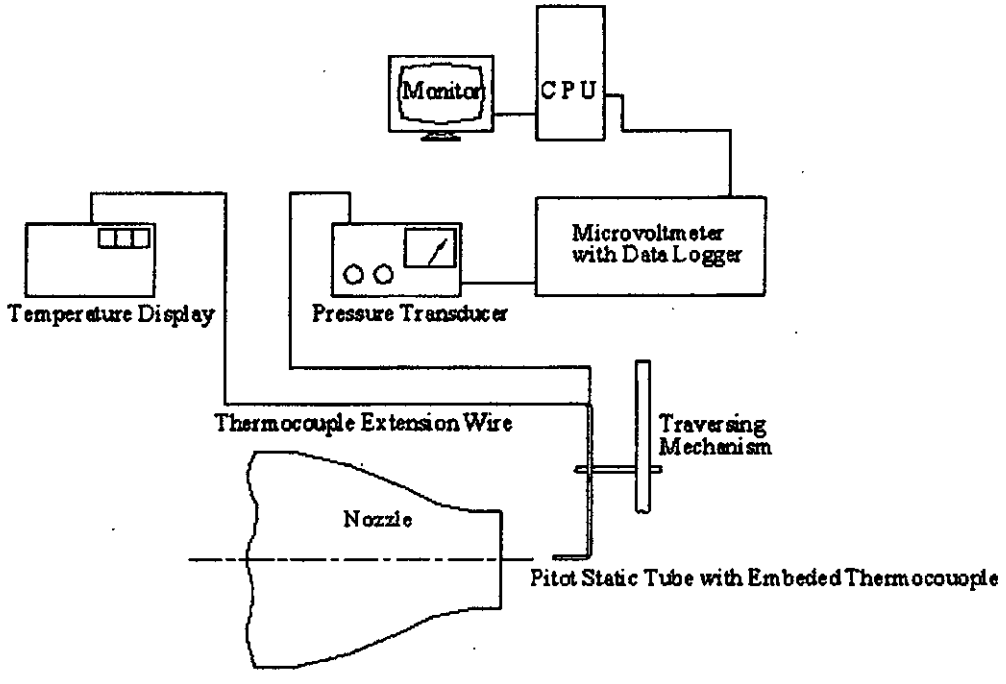

Figure 4.4.1 Schematic Diagram for Measuring Mean Velocity and Temperature

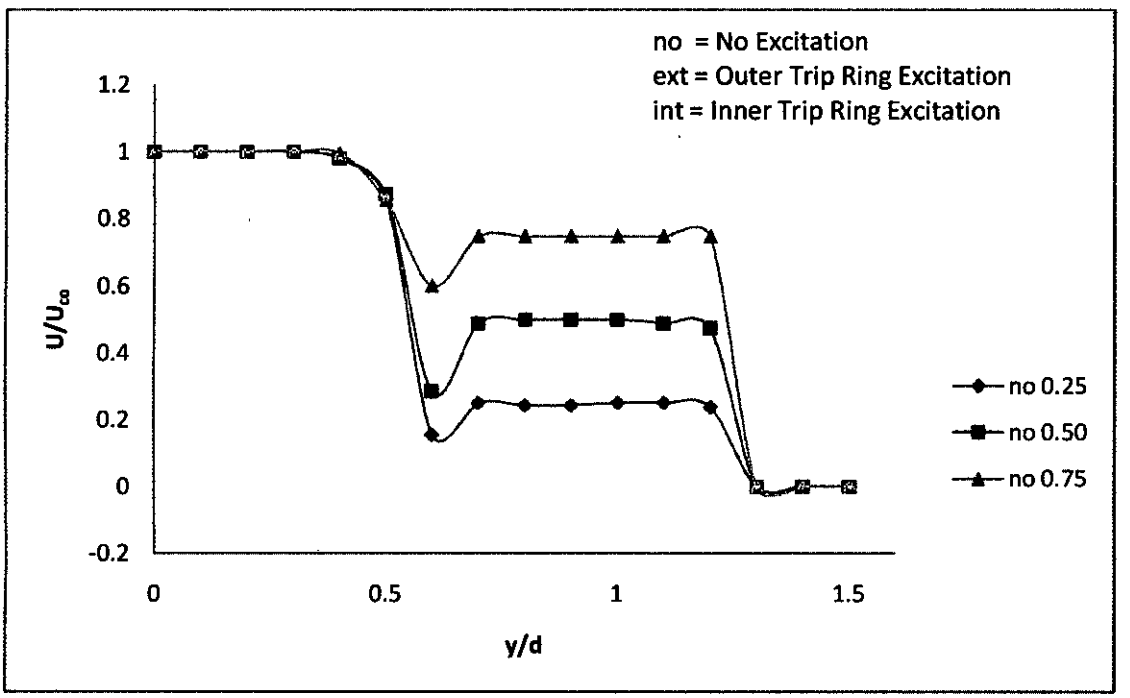

Fig 5.2.1: Non-dimensional exit velocity profiles of co-axial jet (A_2/A_1= 3.57, Re= 3.72x10^4) without any excitation at different velocity ratio

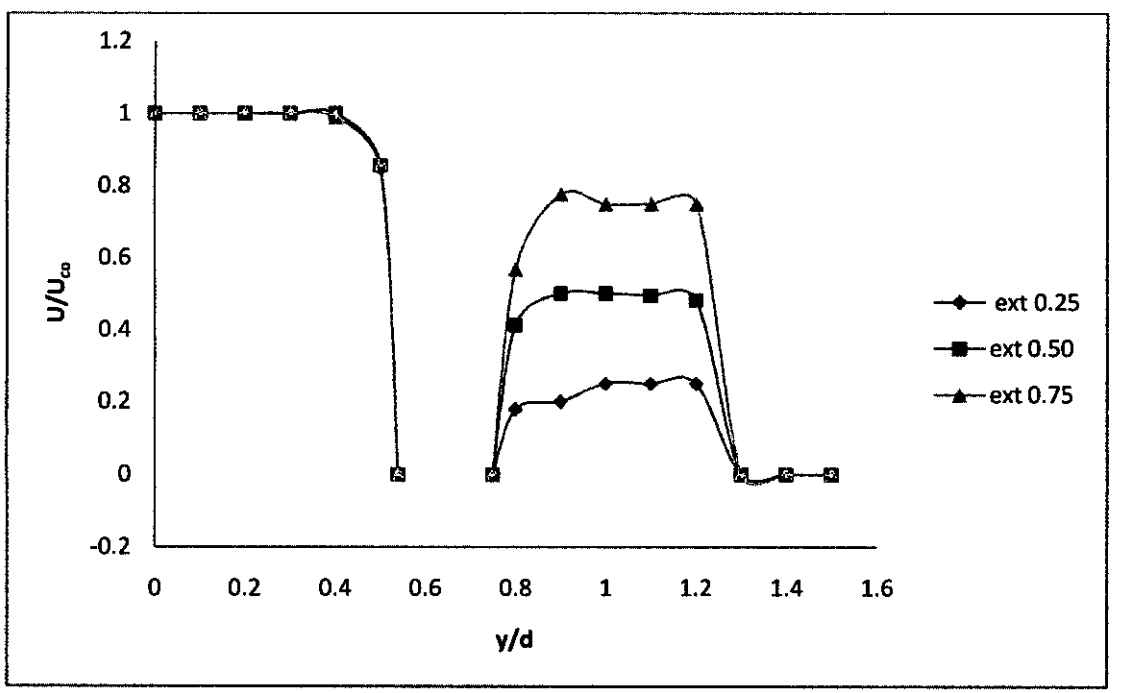

Fig 5.2.2: Non-dimensional exit velocity profiles of co-axial jet (Re= 3.72x10^4) with outer trip ring excitation at different velocity ratio

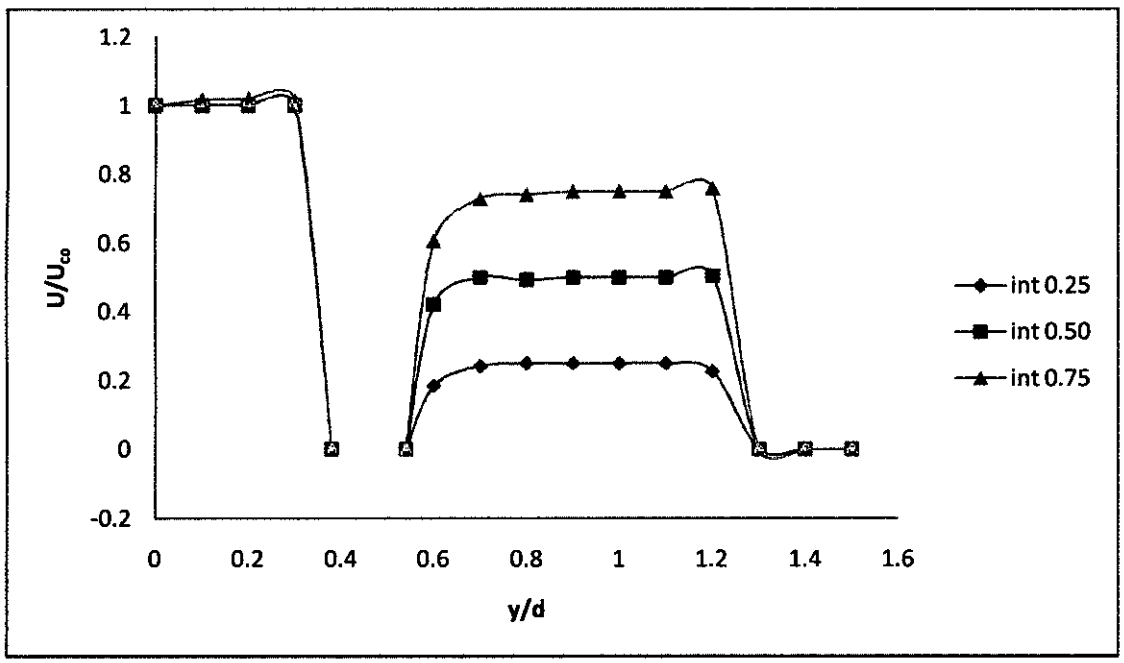

Fig 5.2.3: Non-dimensional exit velocity profiles of co-axial jets (Re= $3.72x10^4$) with inner trip ring excitation at different velocity ratio

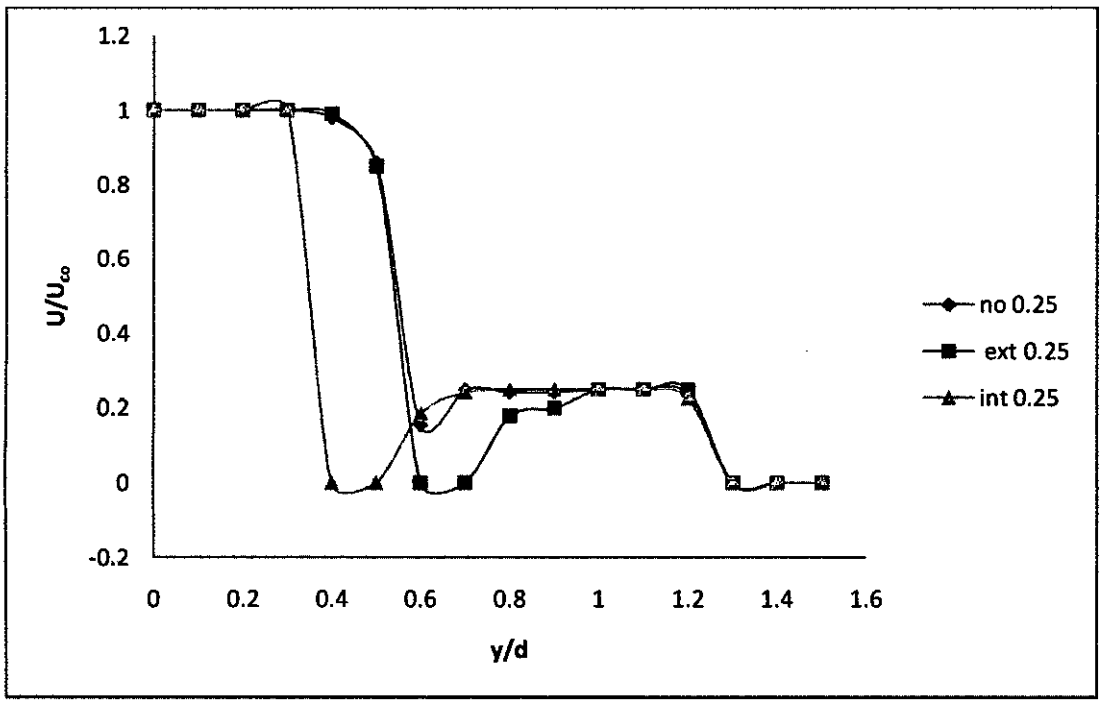

Fig 5.2.4: Non-dimensional exit velocity profiles of co-axial jet (Re= $3.72x10^4$) at velocity ratio of 0.25 with different excitation method

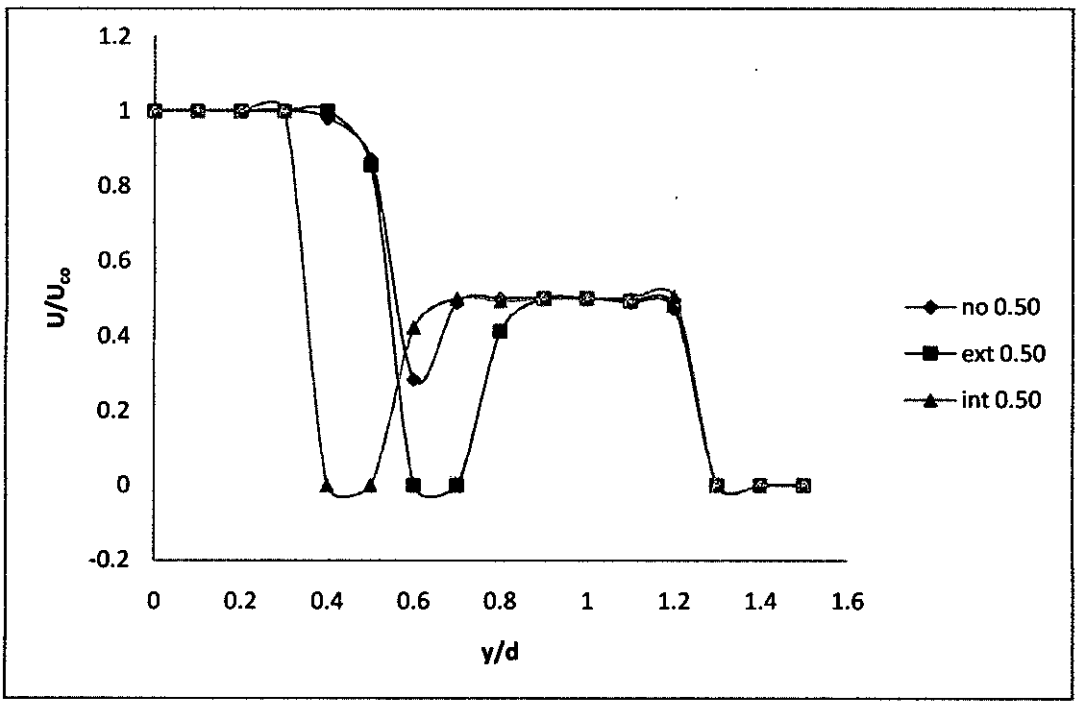

Fig 5.2.5: Non-dimensional exit velocity profiles of co-axial jet (Re= $3.72x10^4$) at velocity ratio of 0.50 with different excitation method

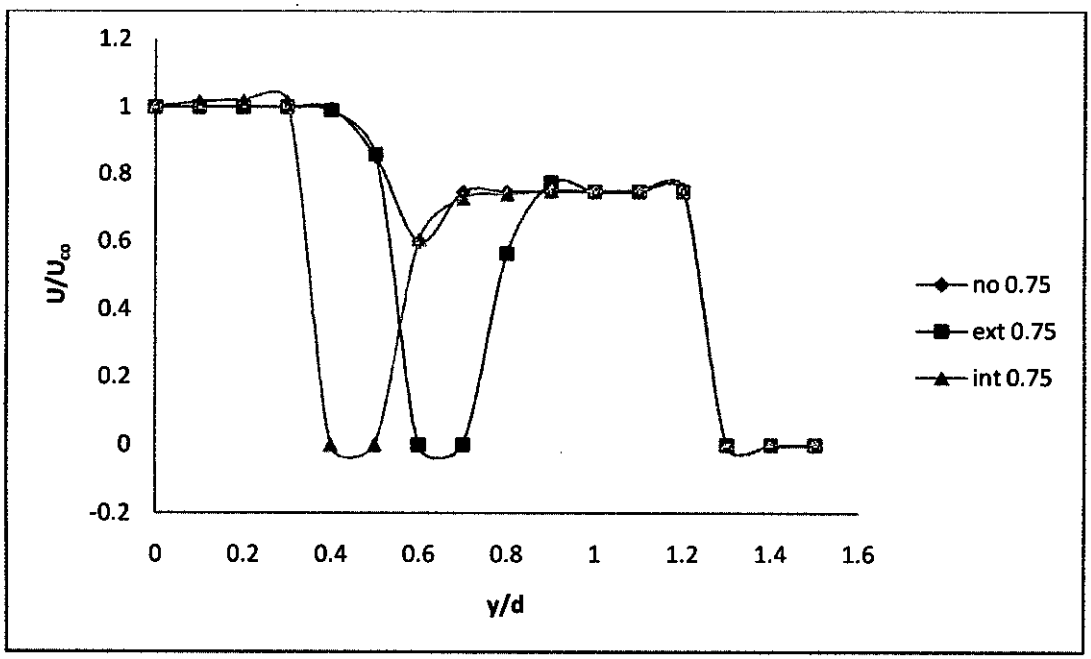

Fig 5.2.6: Non-dimensional exit velocity profiles of co-axial jet (Re= $3.72x10^4$) at velocity ratio of 0.75 with different excitation method

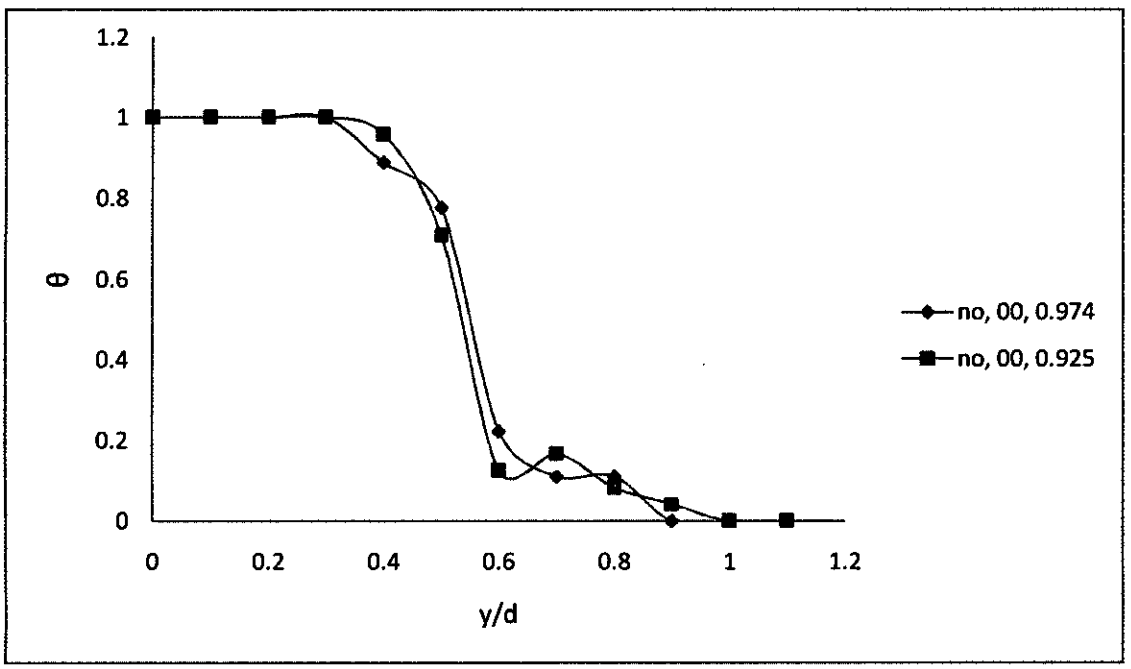

Fig 5.3.1: Non-dimensional exit temperature profiles of single jet (Re= $3.72x10^4$) with different temperature ratio

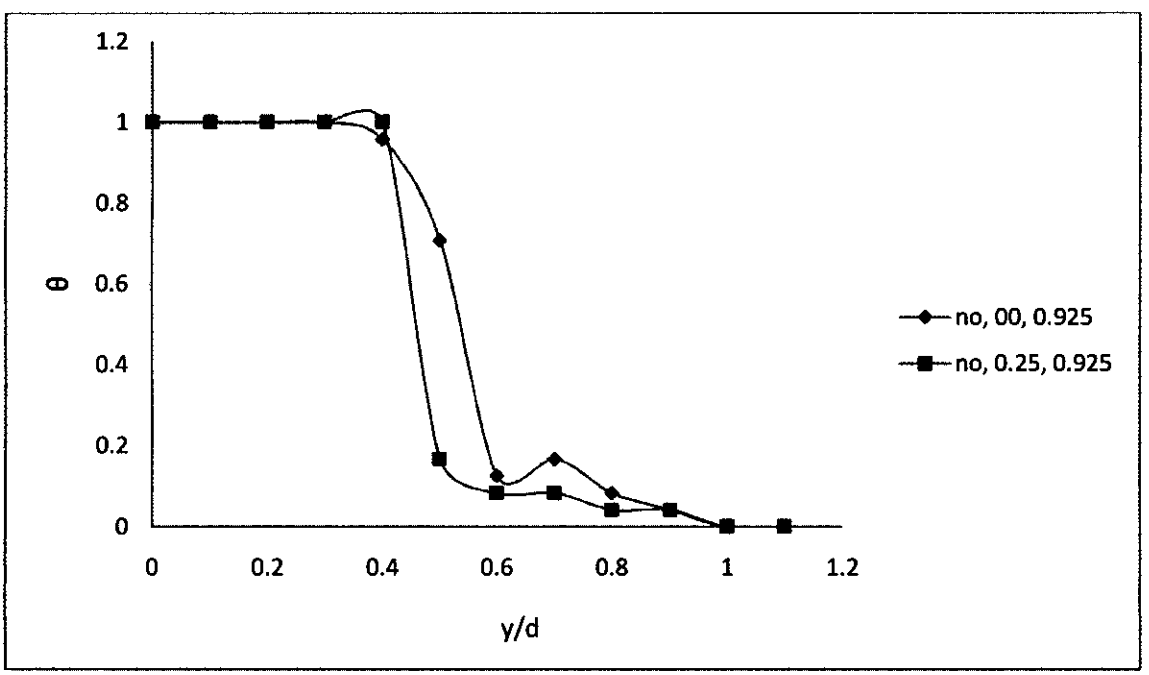

Fig 5.3.2: Comparison of non-dimensional exit temperature profiles of co-axial jet (U_2/U_1=0.25, Re= $3.72x10^4$) at temperature ratio of 0.925 with single jet

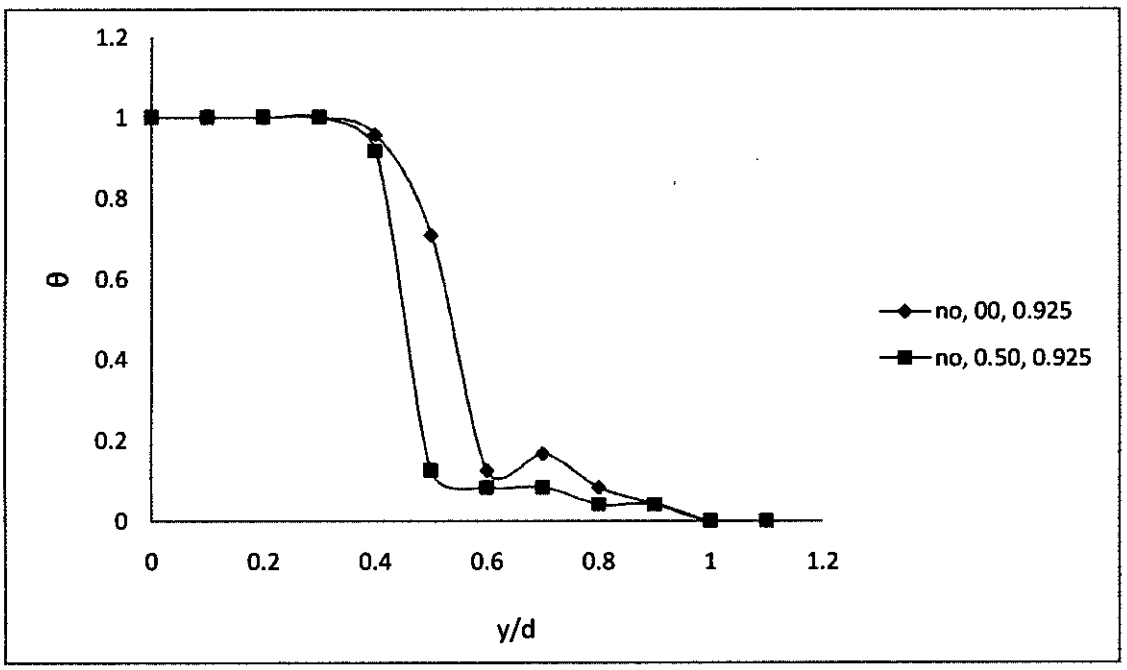

Fig 5.3.3: Comparison of non-dimensional exit temperature profiles of co-axial jet (U_2/U_1=0.50, Re= 3.72x10^4) at temperature ratio of 0.925 with single jet

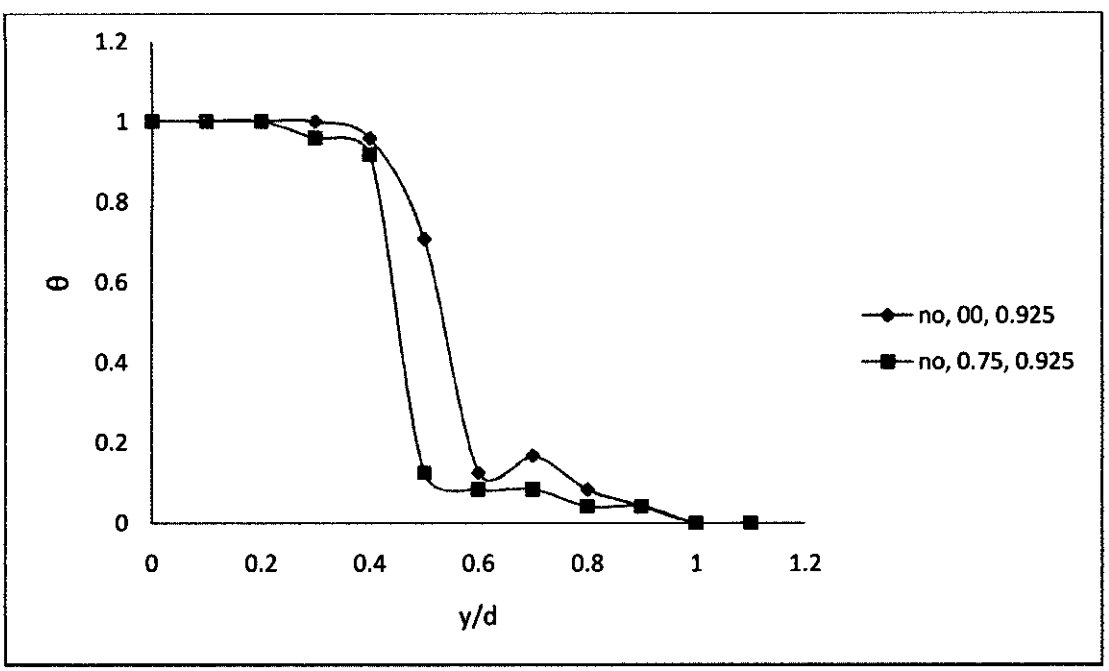

Fig 5.3.4: Comparison of non-dimensional exit temperature profiles of co-axial jet (U_2/U_1=0.75, Re= 3.72x10^4) at temperature ratio of 0.925 with single jet

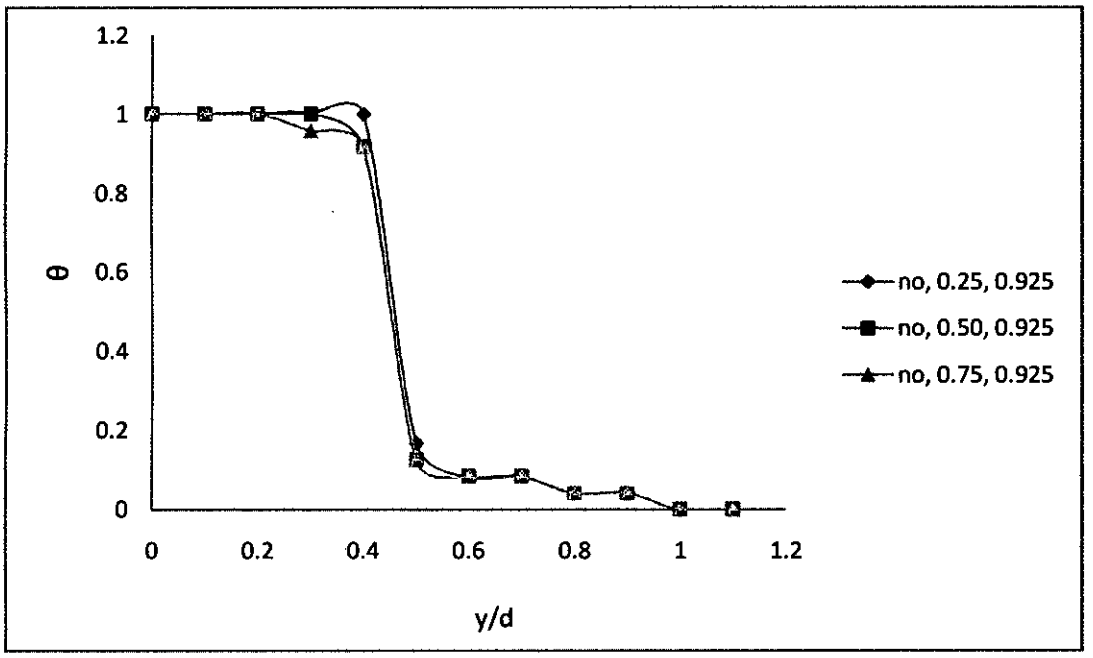

Fig 5.3.5: Non-dimensional exit temperature profiles of co-axial jet (Re= $3.72x10^4$) at temperature ratio of 0.925 with different velocity ratio

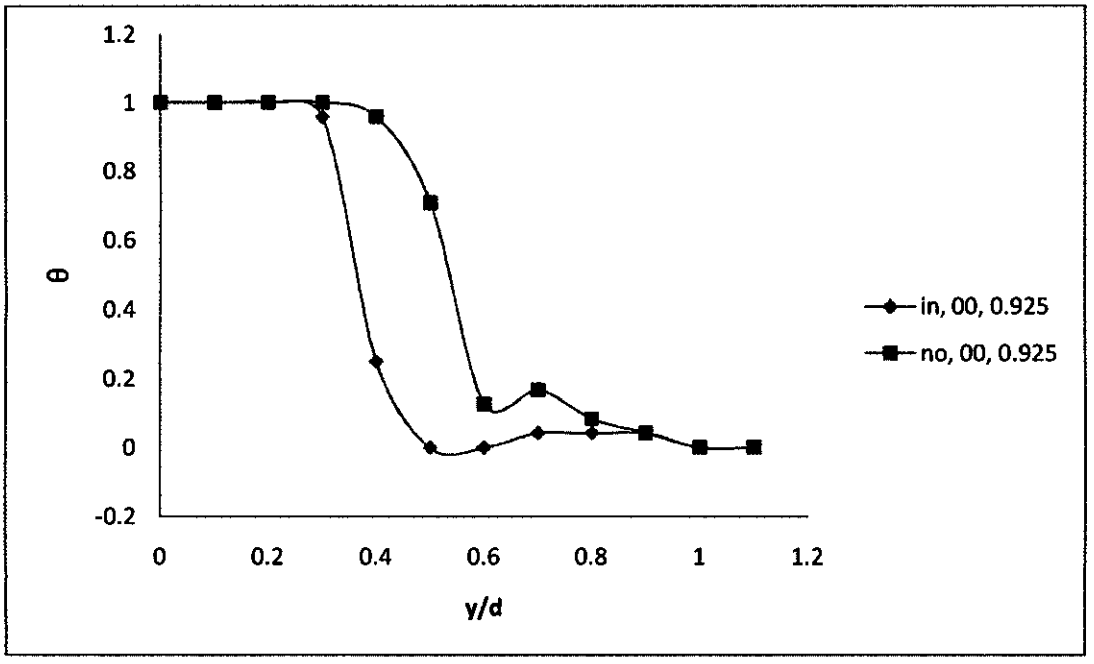

Fig 5.3.6: Comparison of non-dimensional exit temperature profiles of inner ring excited single jet (Re= $3.72x10^4$) at temperature ratio of 0.925 with unexcited single jet

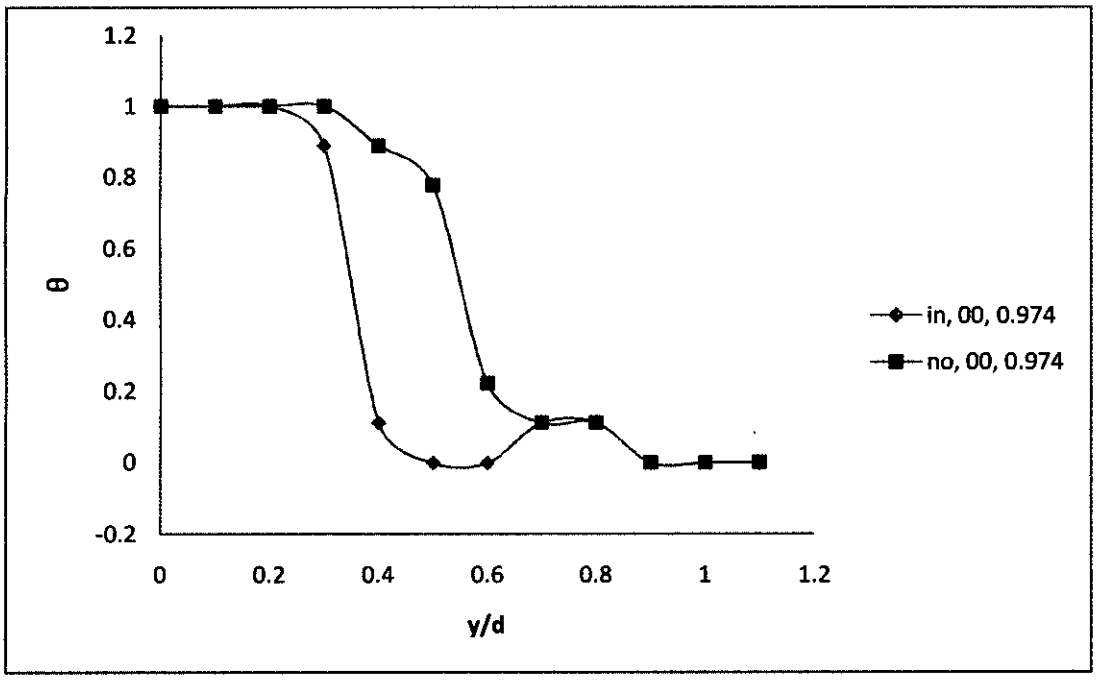

Fig 5.3.7: Comparison of non-dimensional exit temperature profiles of inner ring excited single jet (Re= $3.72x10^4$) at temperature ratio of 0.974 with unexcited single jet

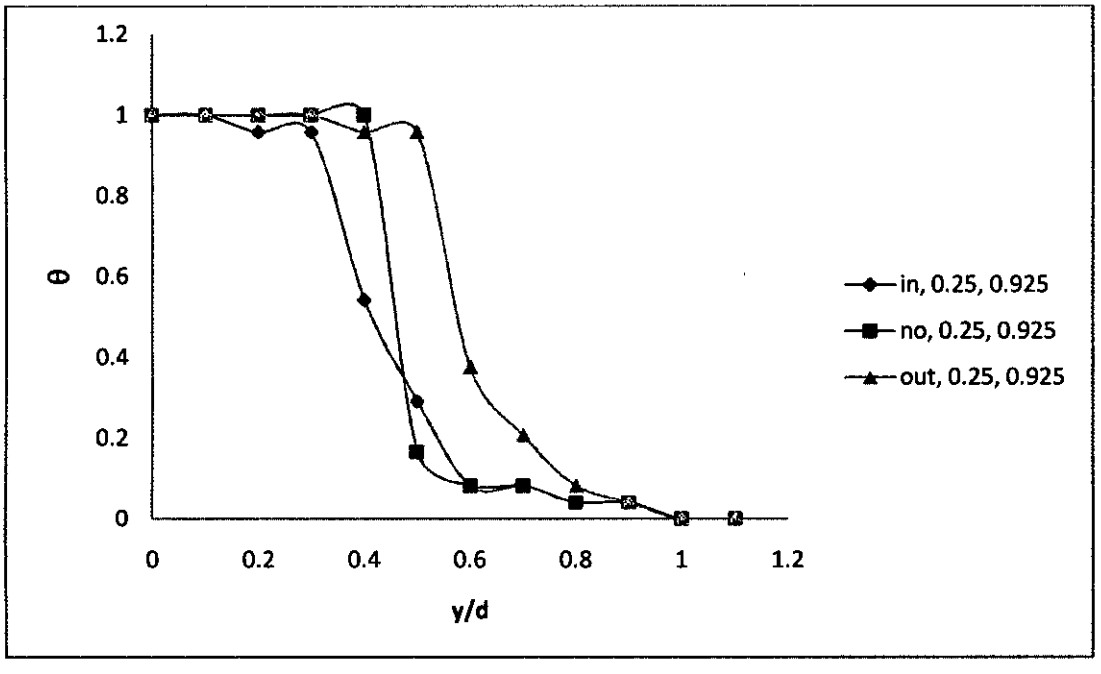

Fig 5.3.8: Non-dimensional exit temperature profiles of co-axial jet (Re= $3.72x10^4$) at temperature ratio of 0.925 and velocity ratio of 0.25 with different type of excitation

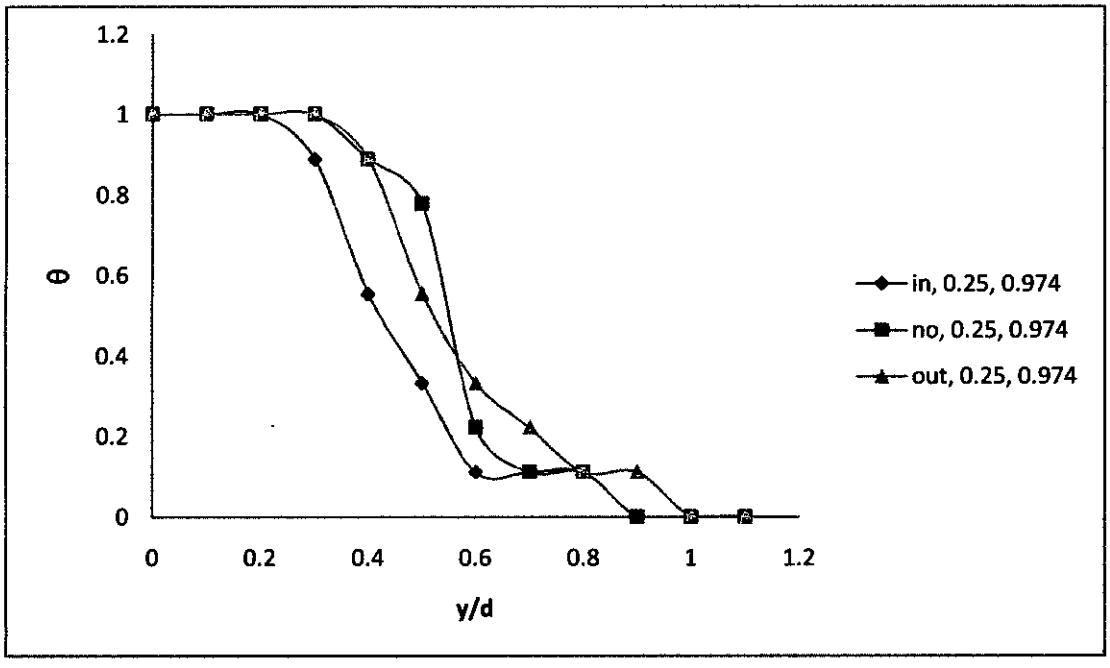

Fig 5.3.9: Non-dimensional exit temperature profiles of co-axial jet (Re= $3.72x10^4$) at temperature ratio of 0.974 and velocity ratio of 0.25 with different type of excitation

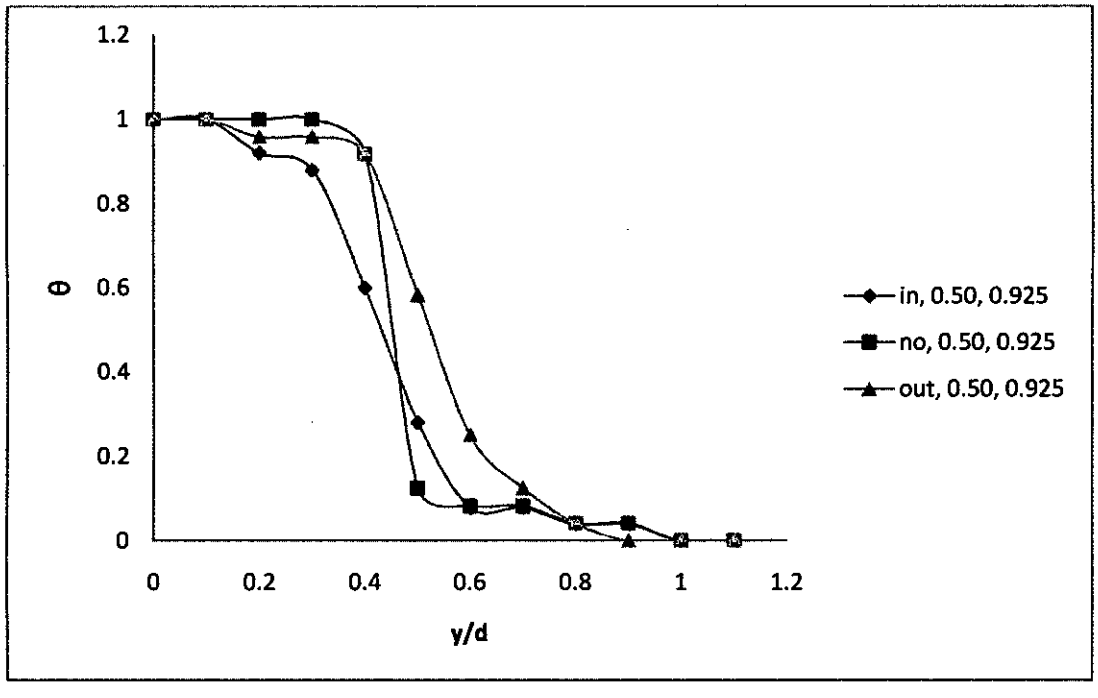

Fig 5.3.10: Non-dimensional exit temperature profiles of co-axial jet (Re= $3.72x10^4$) at temperature ratio of 0.925 and velocity ratio of 0.50 with different type of excitation

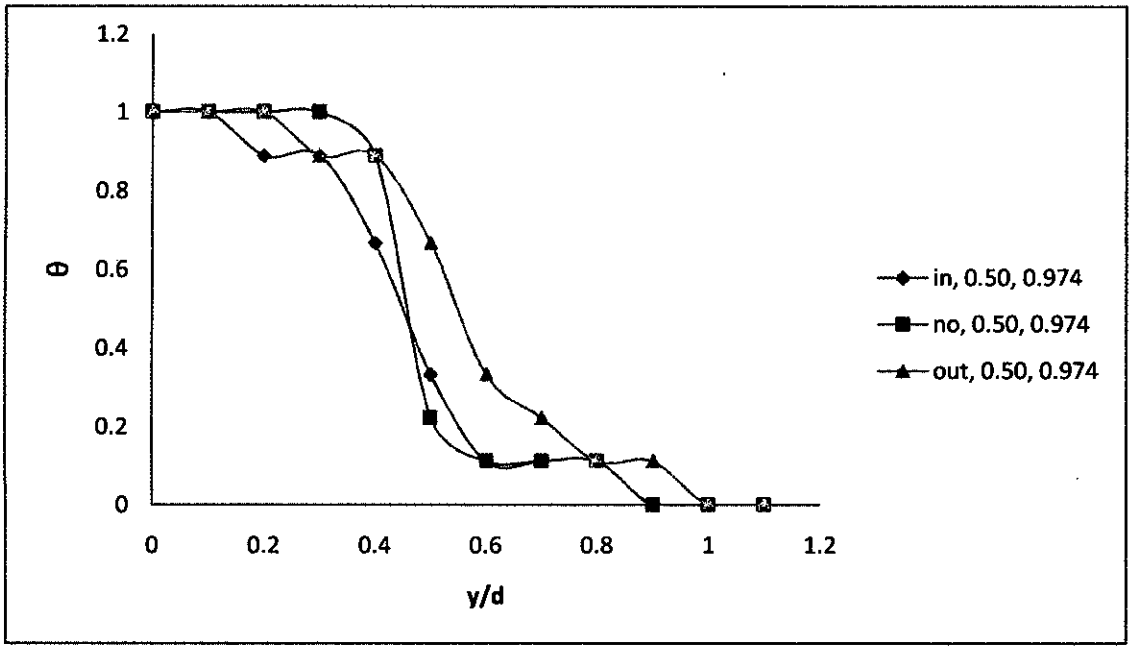

Fig 5.3.11: Non-dimensional exit temperature profiles of co-axial jet (Re= $3.72x10^4$) at temperature ratio of 0.974 and velocity ratio of 0.50 with different type of excitation

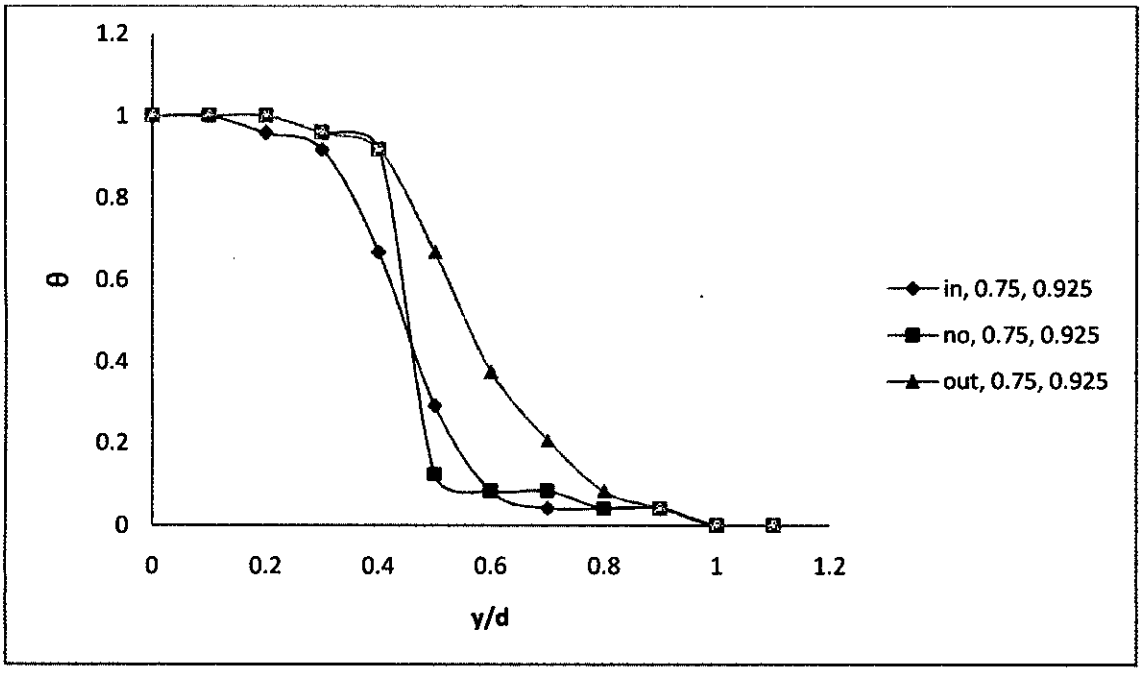

Fig 5.3.12: Non-dimensional exit temperature profiles of co-axial jet (Re= $3.72x10^4$) at temperature ratio of 0.925 and velocity ratio of 0.75 with different type of excitation

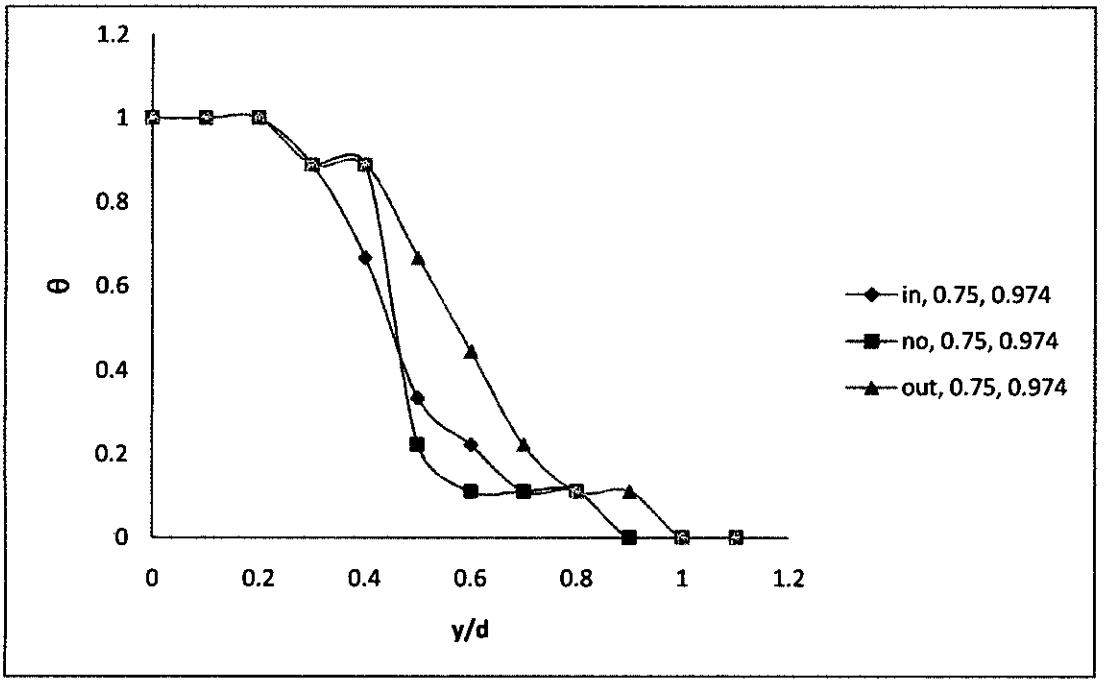

Fig 5.3.13: Non-dimensional exit temperature profiles of co-axial jet (Re= $3.72x10^4$) at temperature ratio of 0.974 and velocity ratio of 0.75 with different type of excitation

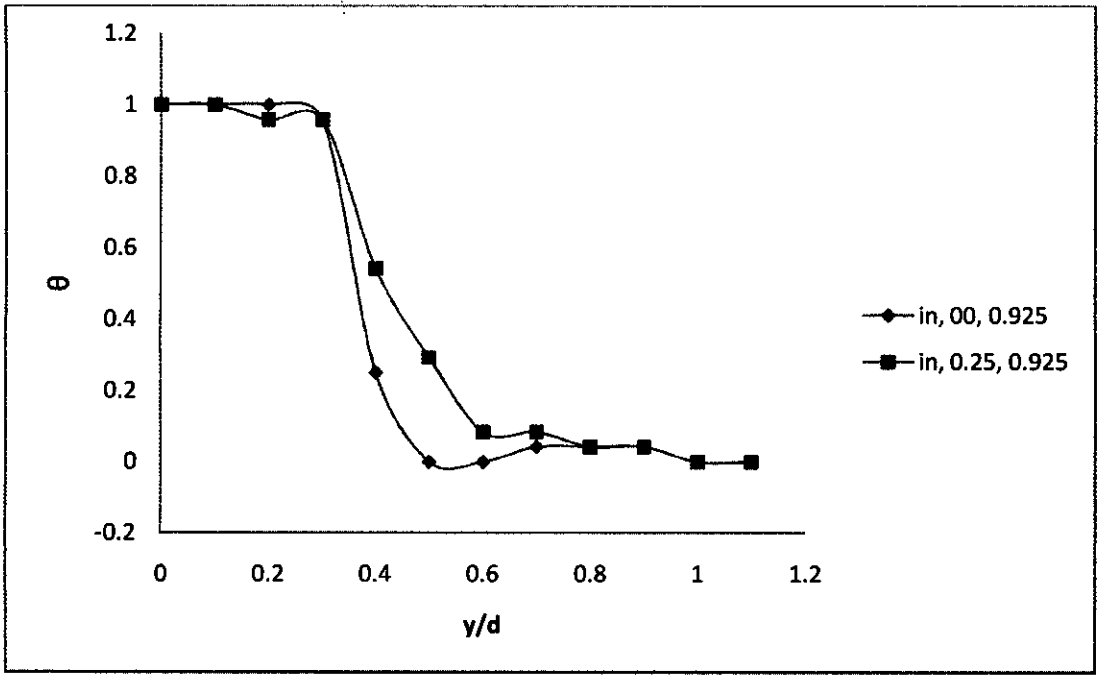

Fig 5.3.14: Comparison of non-dimensional exit temperature profiles of internal trip ring excited co-axial jets (U_2/U_1=0.25, Re= $3.72x10^4$) to internal trip ring excited single jet at temperature ratio of 0.925

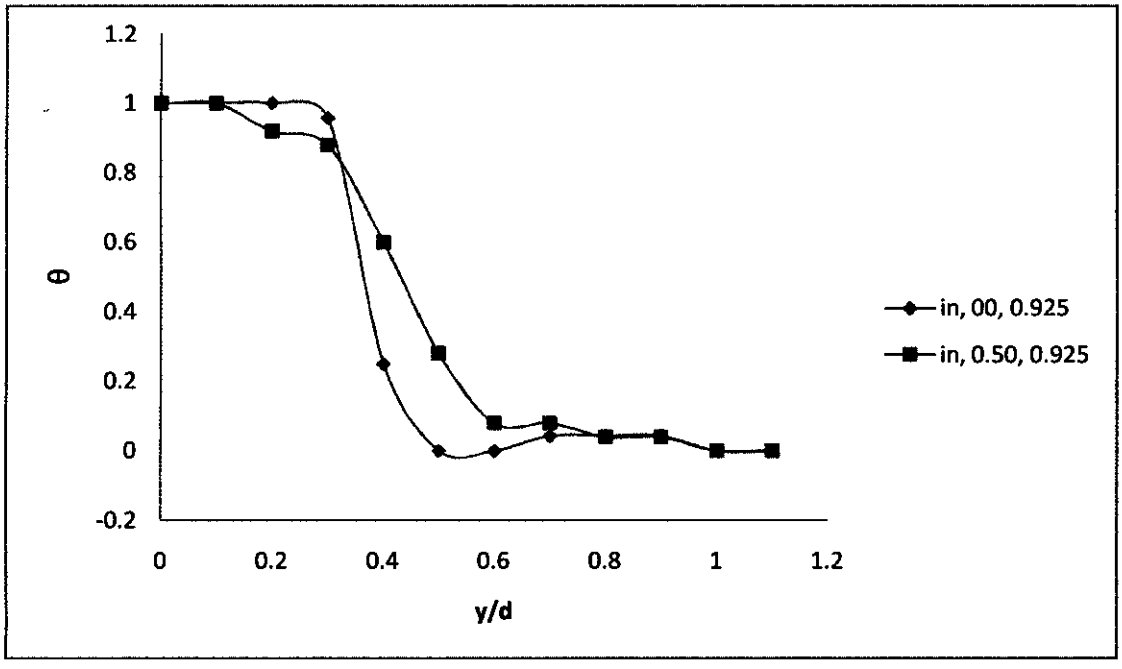

Fig 5.3.15: Comparison of non-dimensional exit temperature profiles of internal trip ring excited co-axial jets (U_2/U_1=0.50, Re= 3.72x10^4) to internal trip ring excited single jet at temperature ratio of 0.925

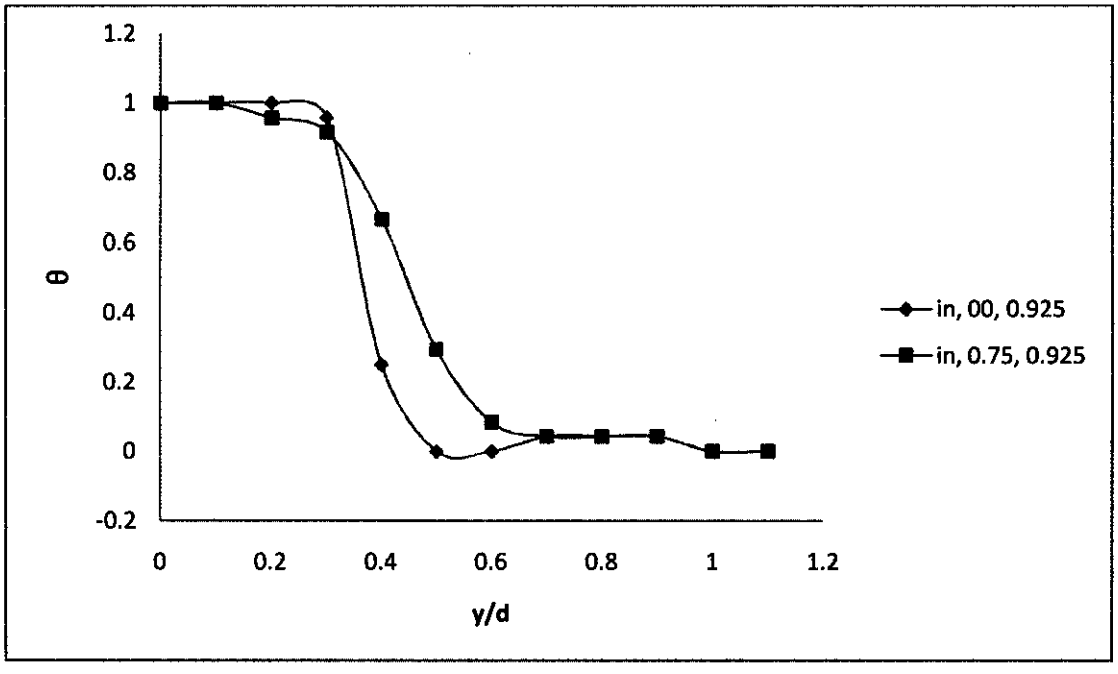

Fig 5.3.16: Comparison of non-dimensional exit temperature profiles of internal trip ring excited co-axial jets (U_2/U_1=0.75, Re= 3.72x10^4) to internal trip ring excited single jet at temperature ratio of 0.925

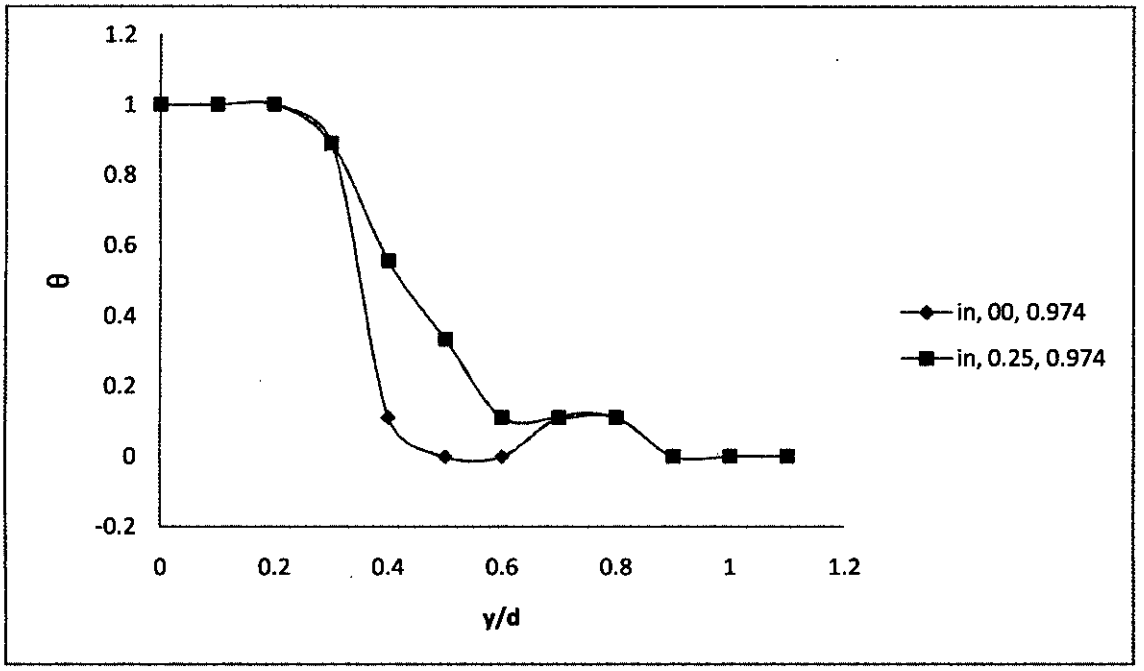

Fig 5.3.17: Comparison of non-dimensional exit temperature profiles of internal trip ring excited co-axial jets (U_2/U_1=0.25, Re= 3.72x10^4) to internal trip ring excited single jet at temperature ratio of 0.974

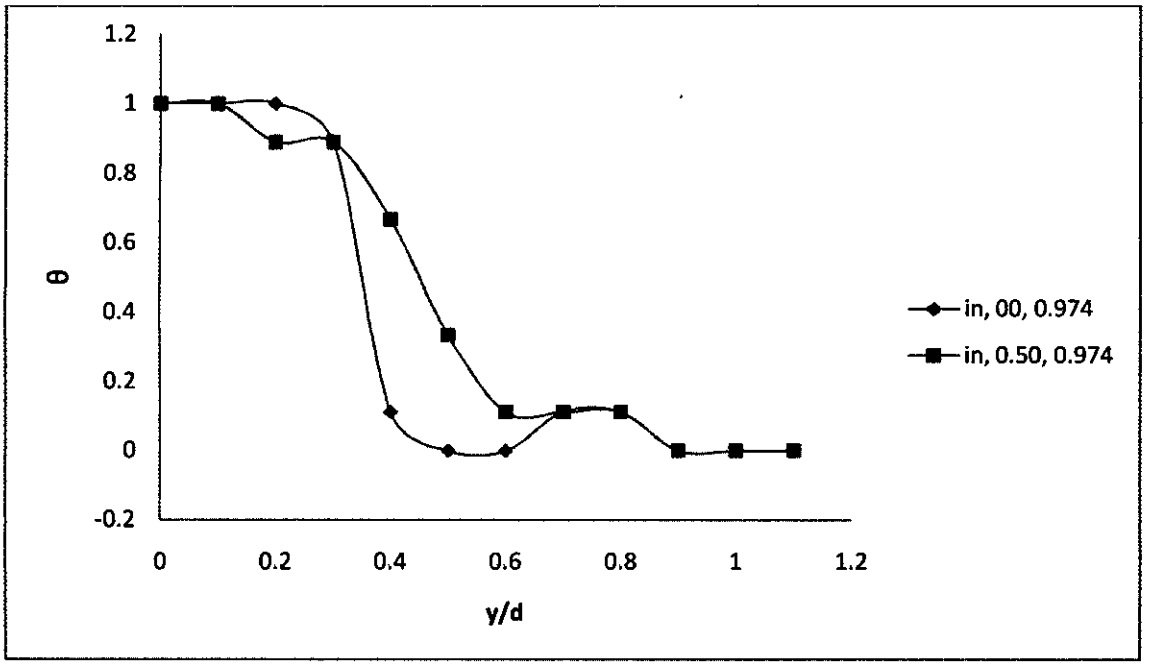

Fig 5.3.18: Comparison of non-dimensional exit temperature profiles of internal trip ring excited co-axial jets (U_2/U_1=0.50, Re= 3.72x10^4) to internal trip ring excited single jet at temperature ratio of 0.974

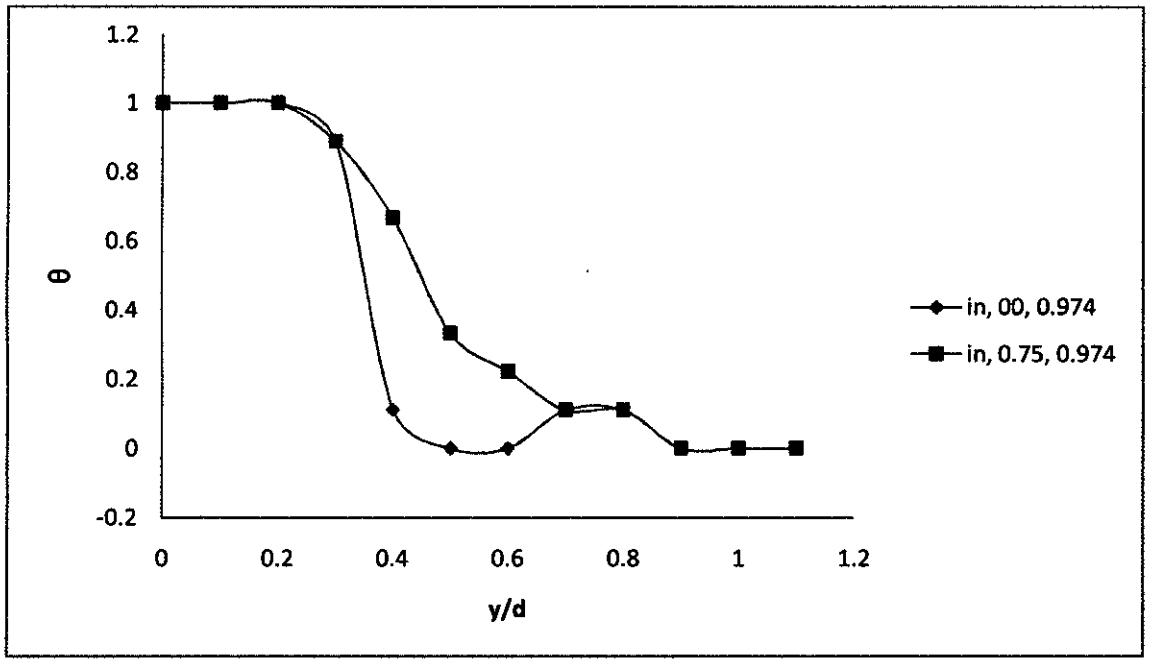

Fig 5.3.19: Comparison of non-dimensional exit temperature profiles of internal trip ring excited co-axial jets (U_2/U_1=0.75, Re= 3.72x10^4) to internal trip ring excited single jet at temperature ratio of 0.974

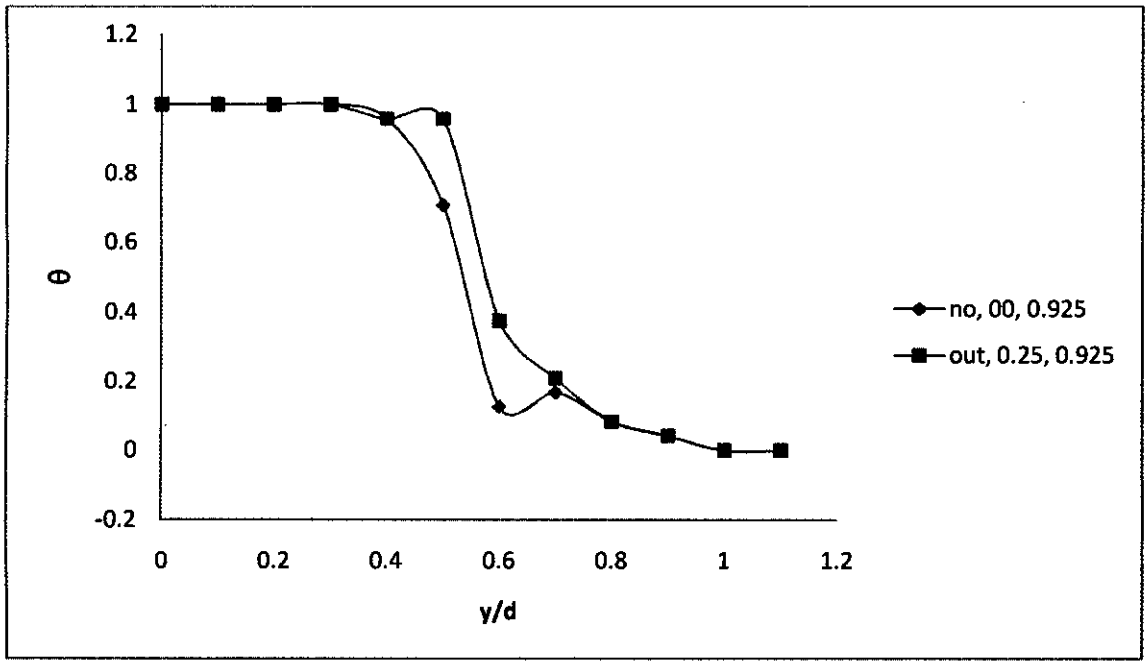

Fig 5.3.20: Non-dimensional exit temperature profiles of external trip ring excited co-axial jet (Re= 3.72x10^4) at temperature ratio of 0.925 with different velocity ratio

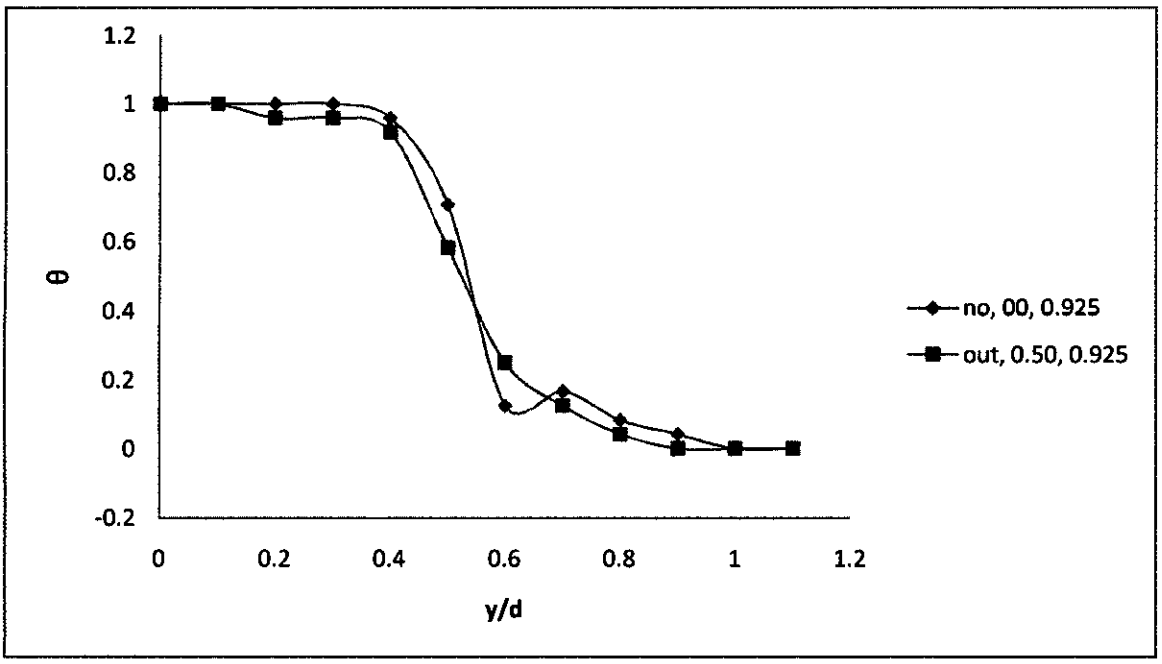

Fig 5.3.21: Non-dimensional exit temperature profiles of external trip ring excited co-axial jet (Re= 3.72×10^4) at temperature ratio of 0.925 with different velocity ratio

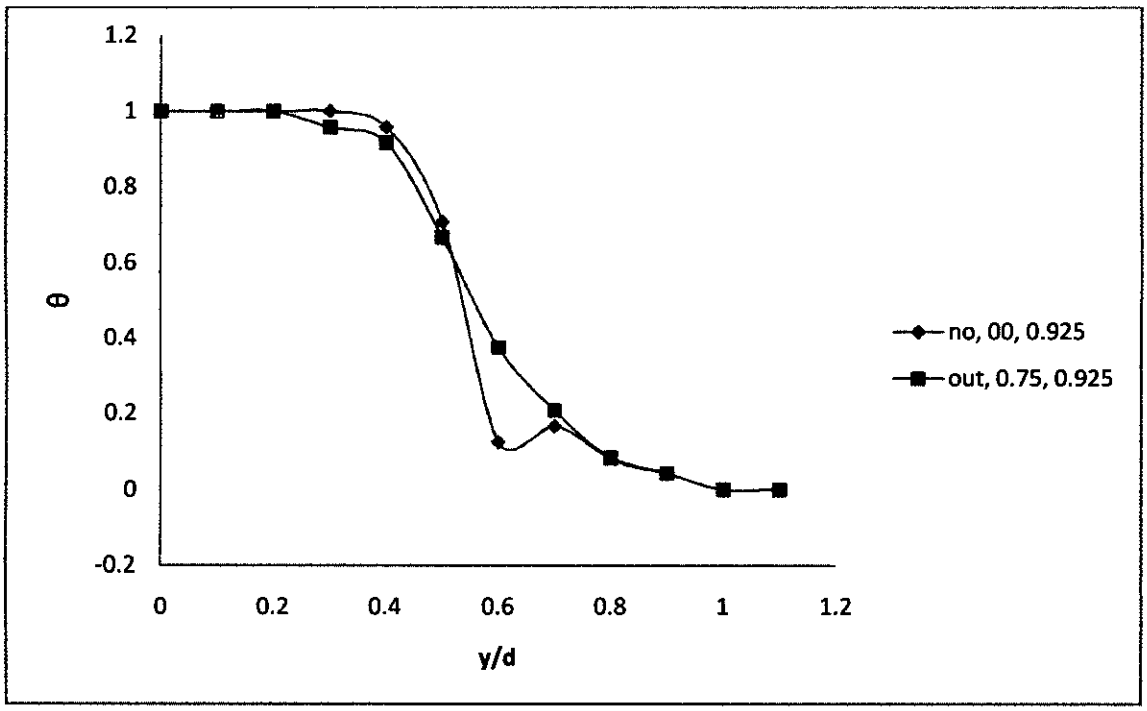

Fig 5.3.22: Non-dimensional exit temperature profiles of external trip ring excited co-axial jet (Re= 3.72×10^4) at temperature ratio of 0.925 with different velocity ratio

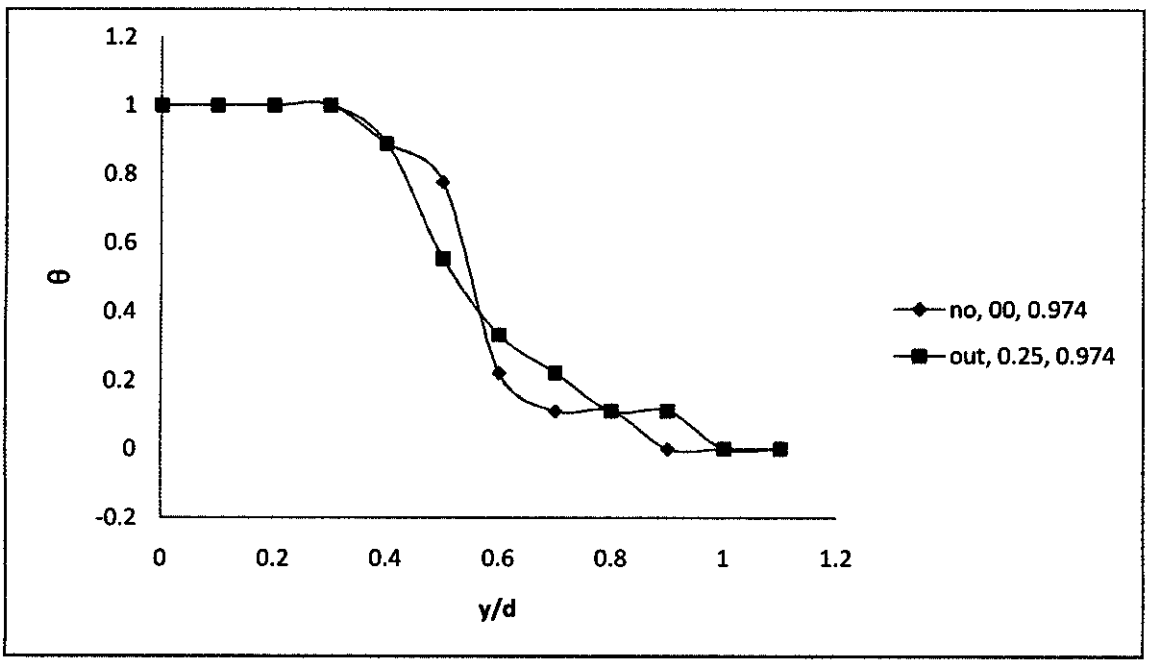

Fig 5.3.23: Non-dimensional exit temperature profiles of external trip ring excited co-axial jet (Re= $3.72x10^4$) at temperature ratio of 0.974 with different velocity ratio

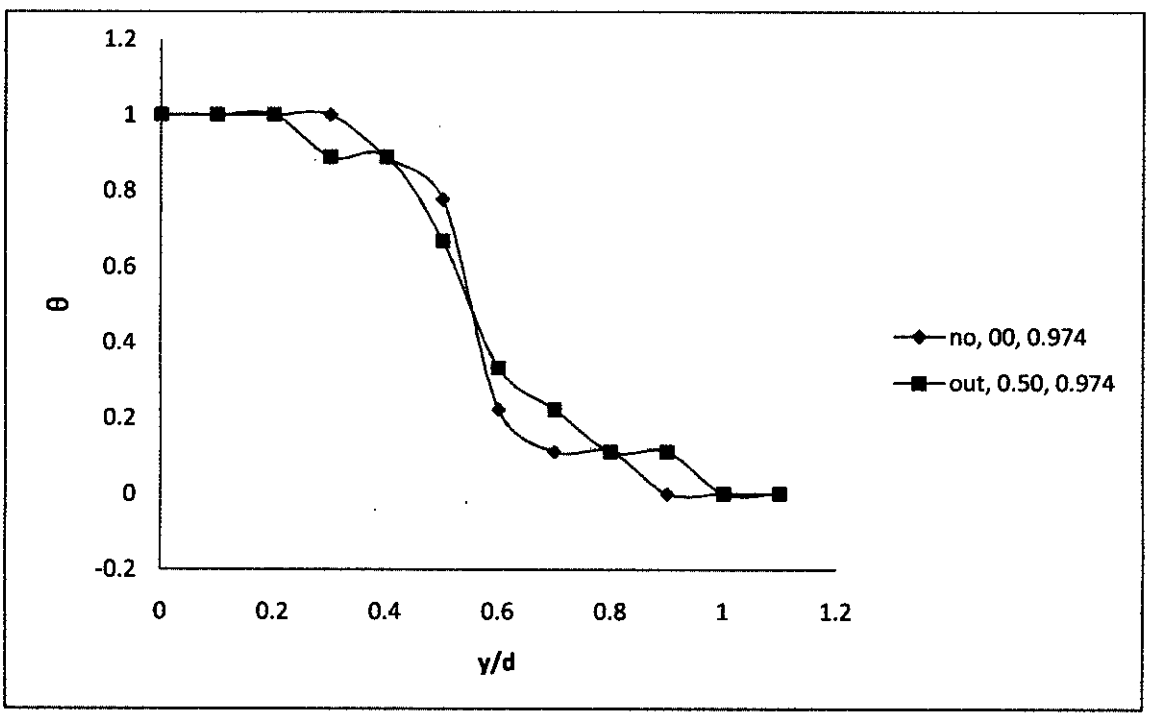

Fig 5.3.24: Non-dimensional exit temperature profiles of external trip ring excited co-axial jet (Re= $3.72x10^4$) at temperature ratio of 0.974 with different velocity ratio

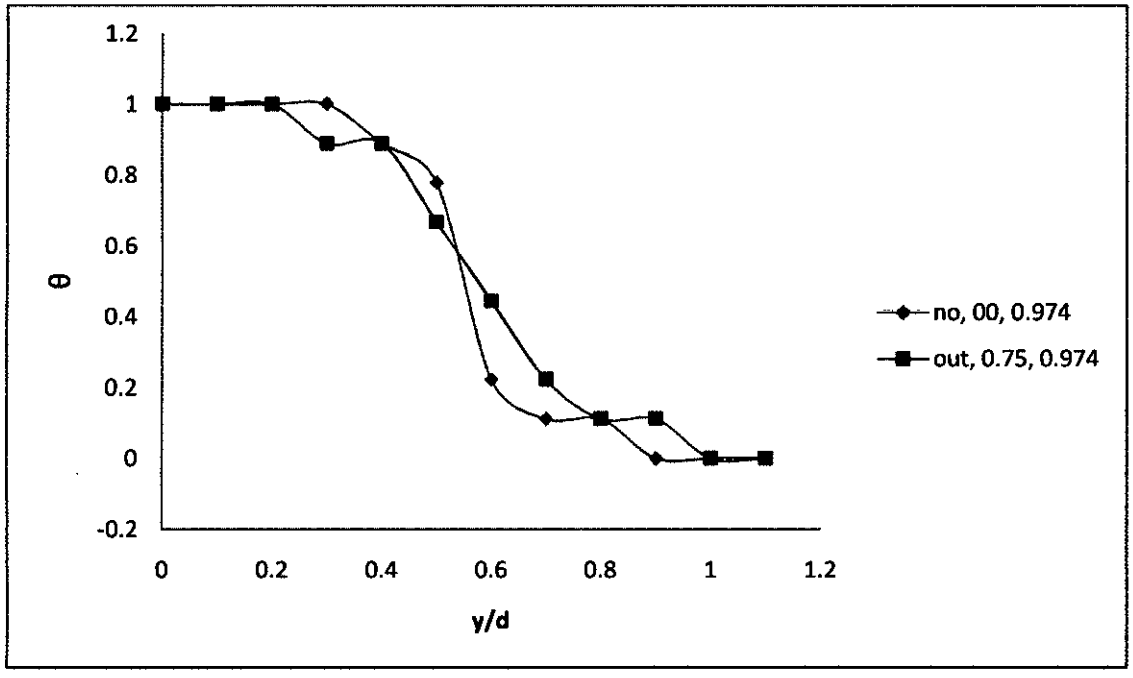

Fig 5.3.25: Non-dimensional exit temperature profiles of external trip ring excited co-axial jet (Re= $3.72x10^4$) at temperature ratio of 0.974 with different velocity

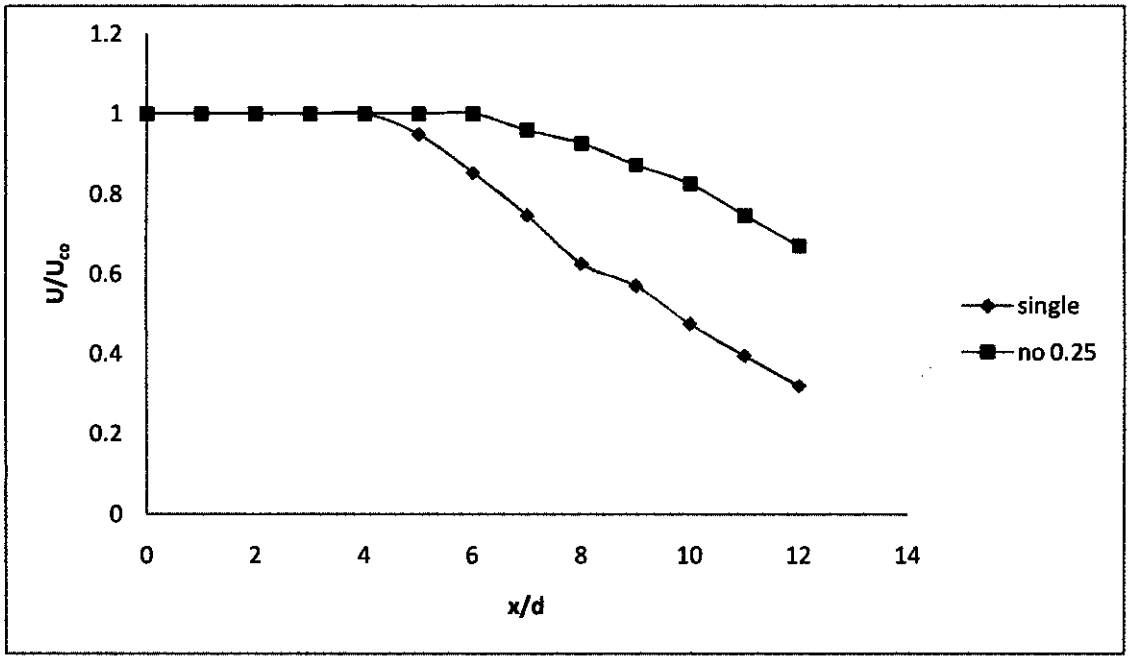

Fig 5.4.1: Non-dimensional centerline velocity profiles of single jet and co-axial jet at velocity ratio of 0.25

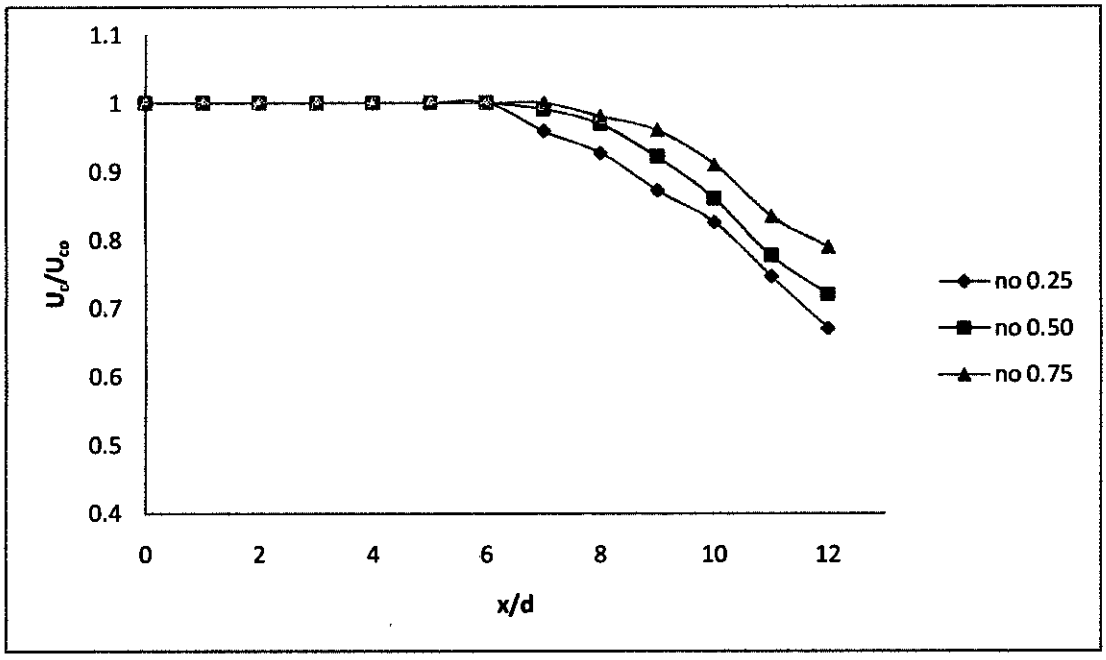

Fig 5.4.2: Non-dimensional centerline velocity profiles of co-axial jet without any excitation at different velocity ratio

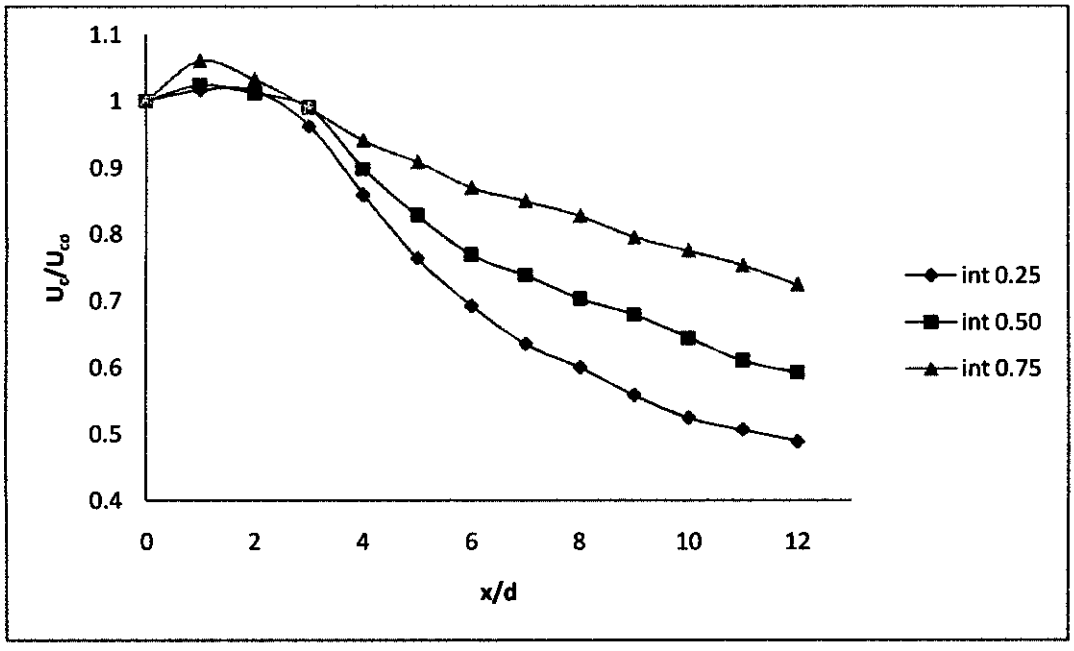

Fig 5.4.3: Non-dimensional centerline velocity profiles of co-axial jet with internal trip ring excitation at different velocity ratio

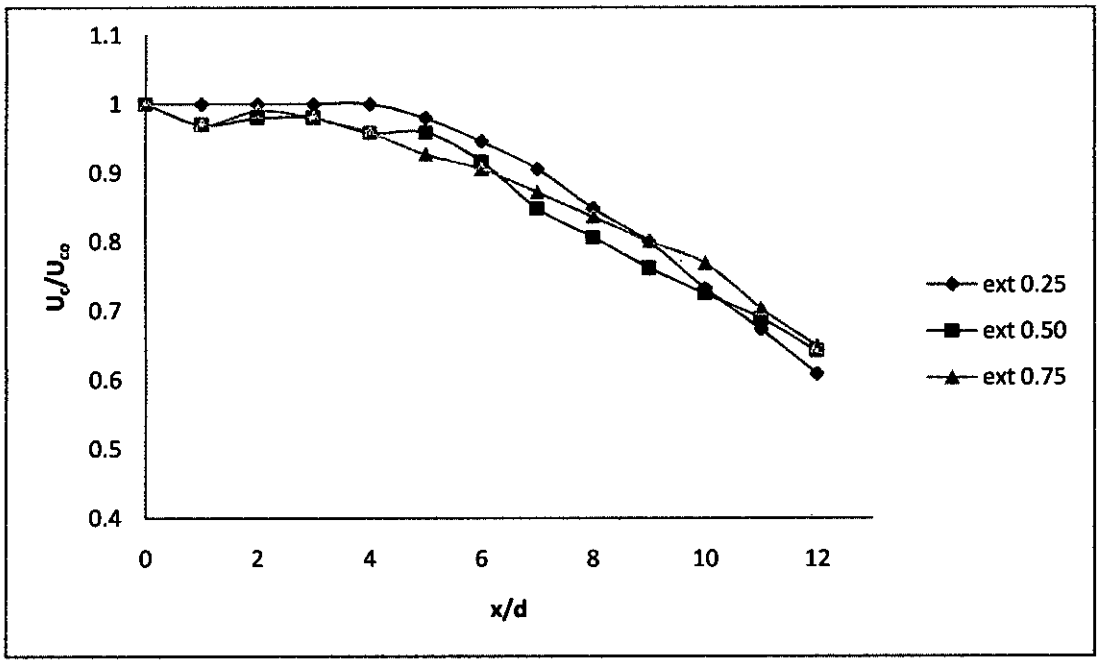

Fig 5.4.4: Non-dimensional centerline velocity profiles of co-axial jet with external trip ring excitation at different velocity ratio

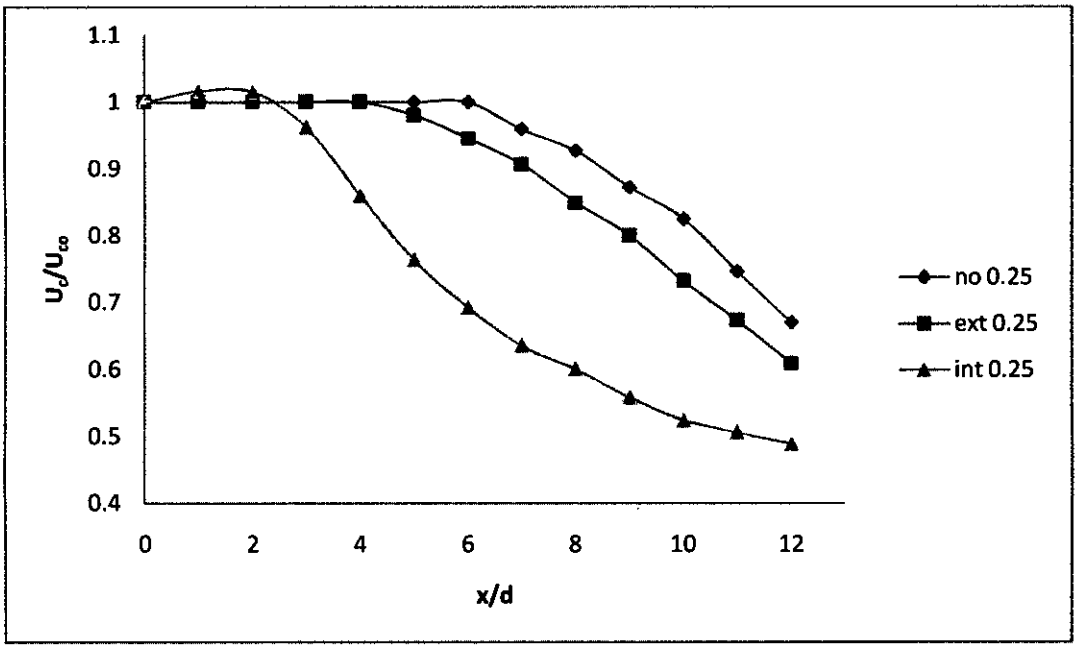

Fig 5.4.5: Non-dimensional centerline velocity profiles of co-axial jet with a velocity ratio of 0.25 at different excitation method

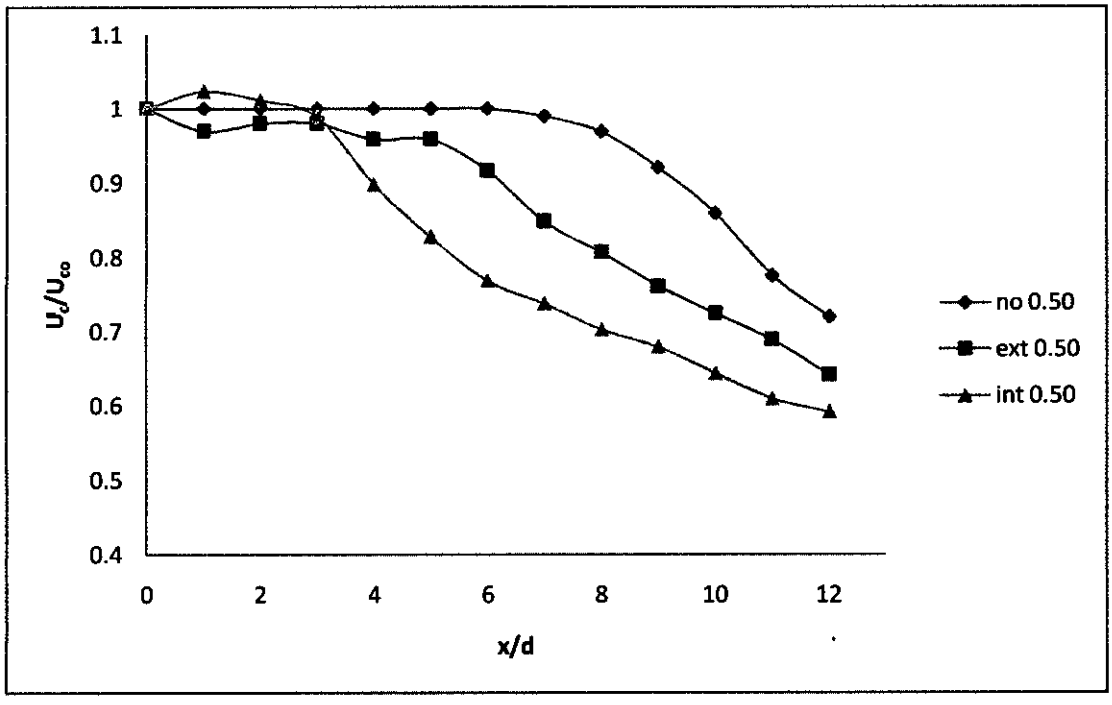

Fig 5.4.6: Non-dimensional centerline velocity profiles of co-axial jet with a velocity ratio of 0.50 at different excitation method

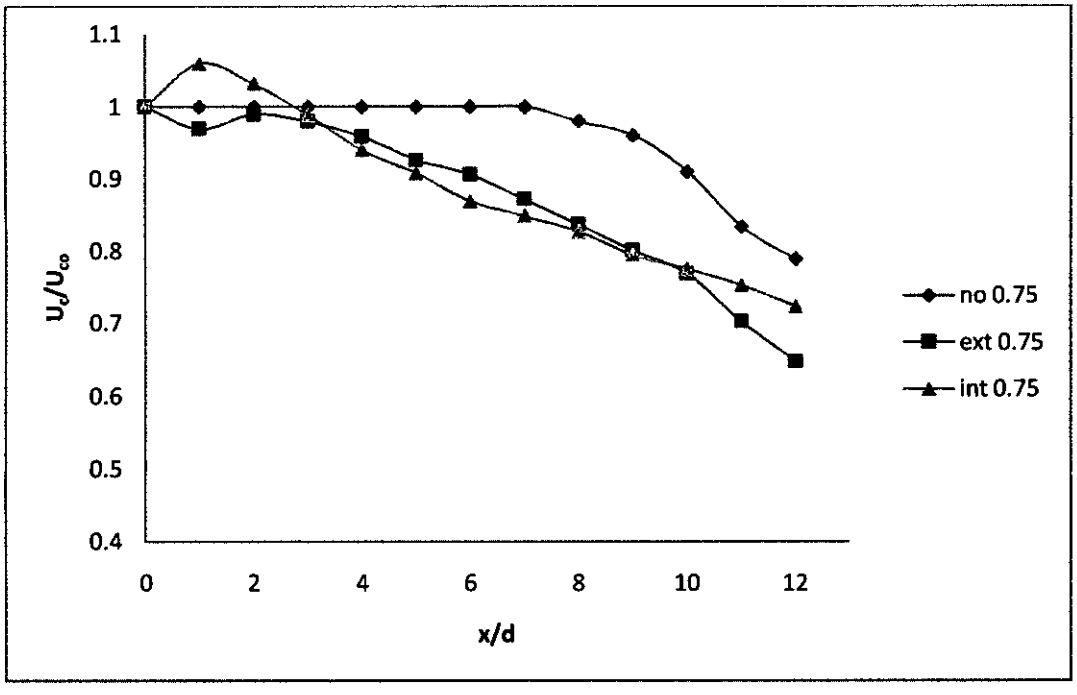

Fig 5.4.7: Non-dimensional centerline velocity profiles of co-axial jet with a velocity ratio of 0.75 at different excitation method

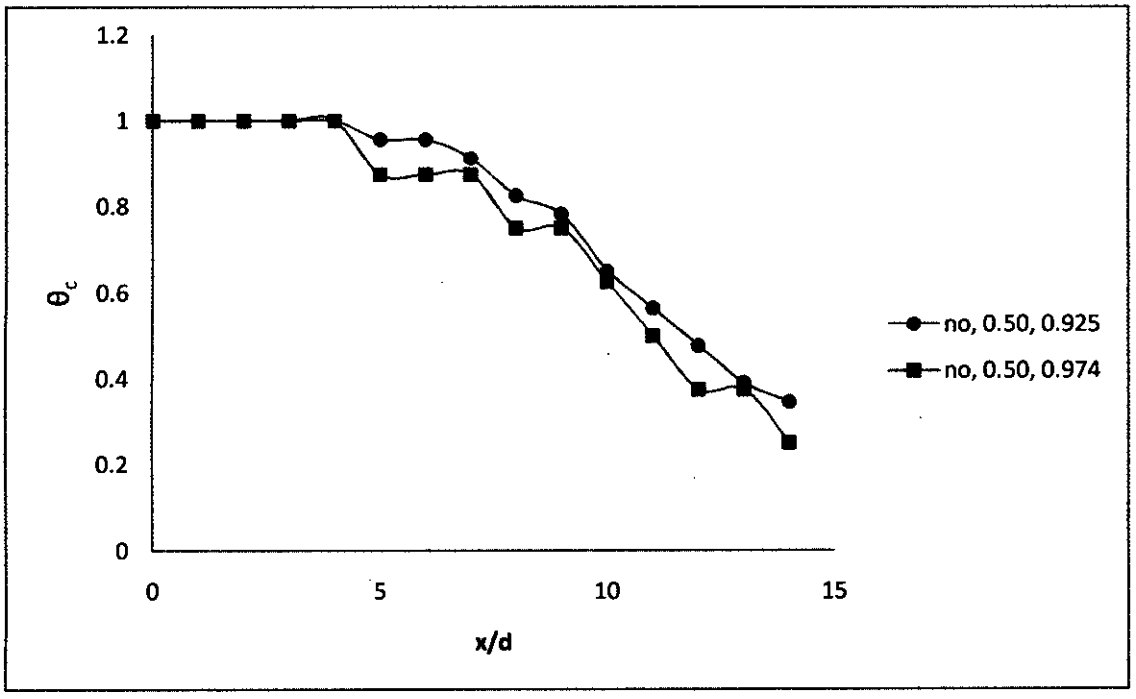

Figure 5.5.1: centerline temperature profile of unexcited co-axial jet at velocity ratio of 0.5 at different temperature ratio

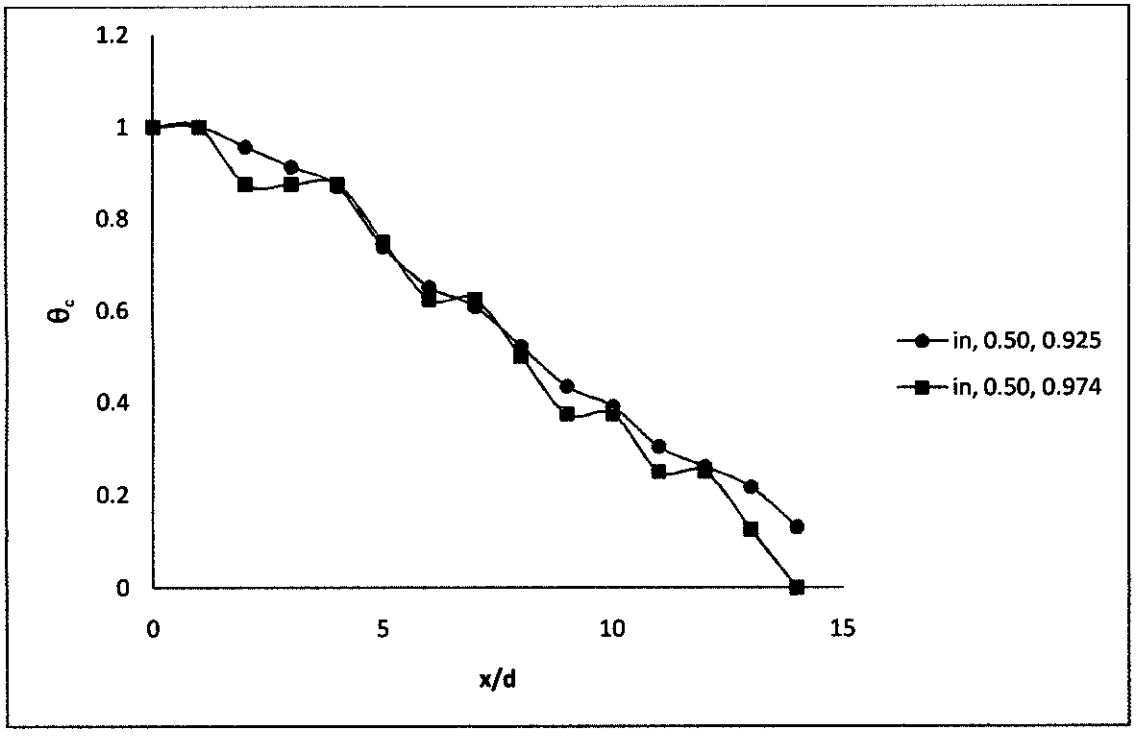

Figure 5.5.2: centerline temperature profile of internal trip ring excited co-axial jet at velocity ratio of 0.5 at different temperature ratio

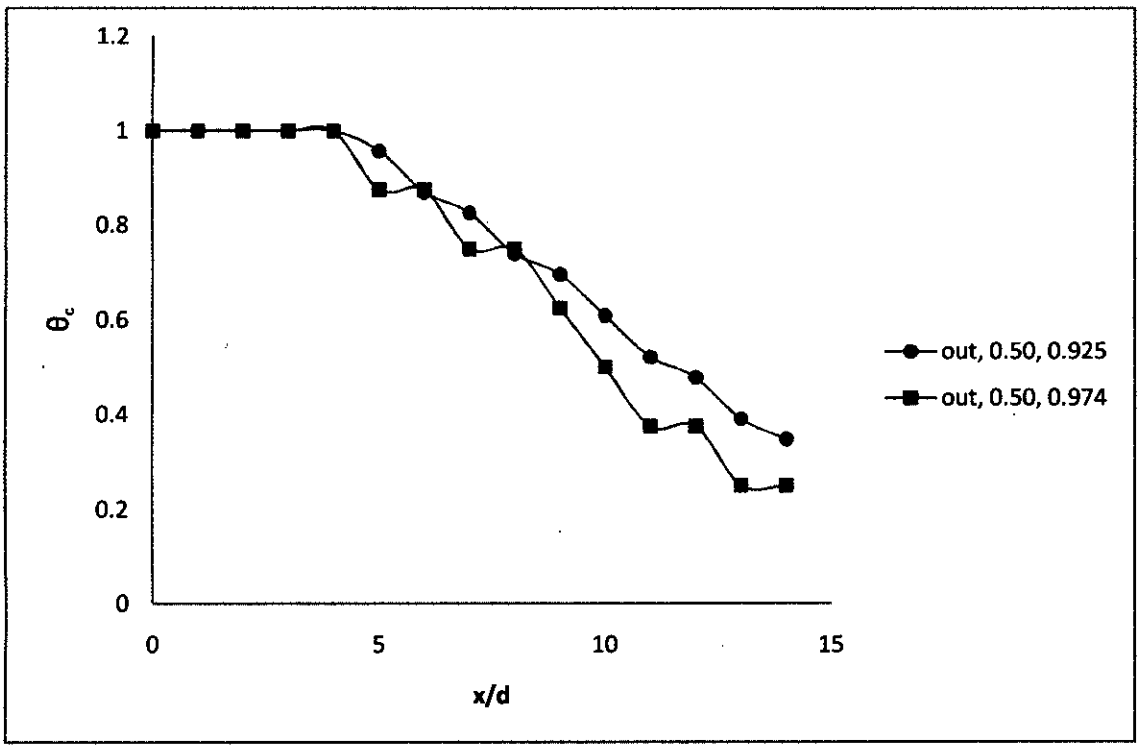

Figure 5.5.3: centerline temperature profile of external trip ring excited co-axial jet at velocity ratio of 0.5 at different temperature ratio

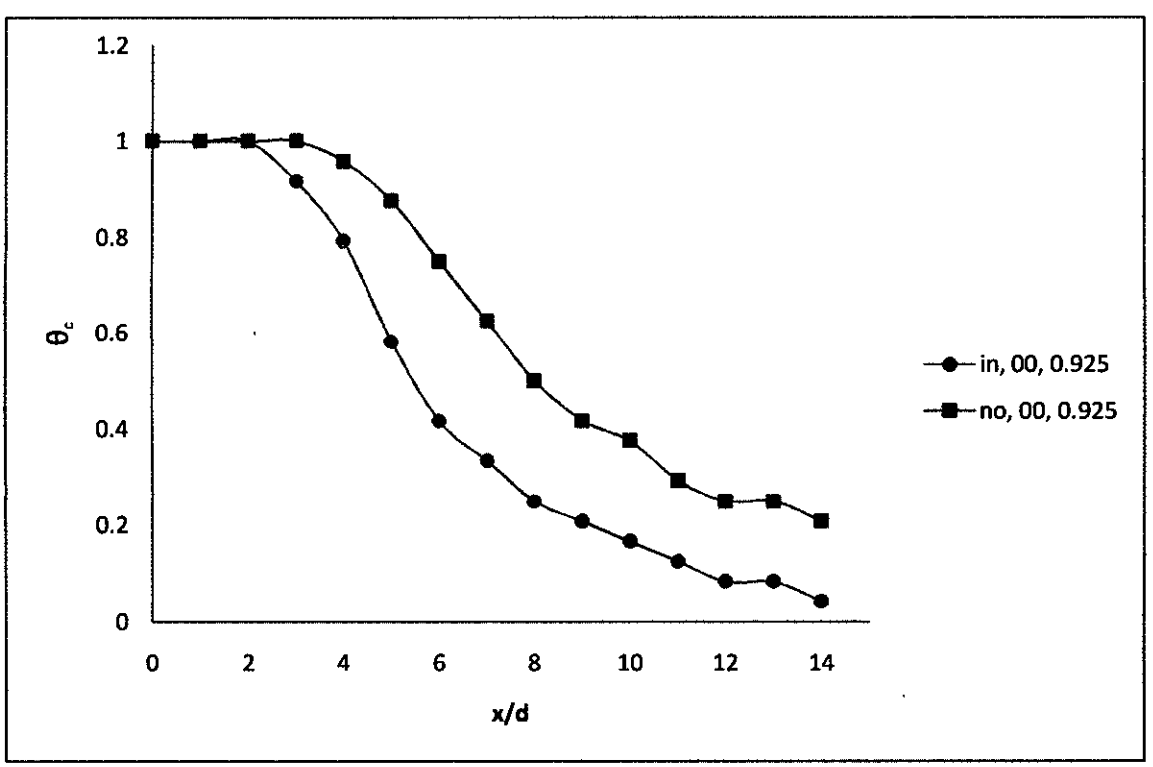

Figure 5.5.4: centerline temperature profile of co-axial jets at velocity ratio of 0.0 and temperature ratio of 0.925 with different type of excitation

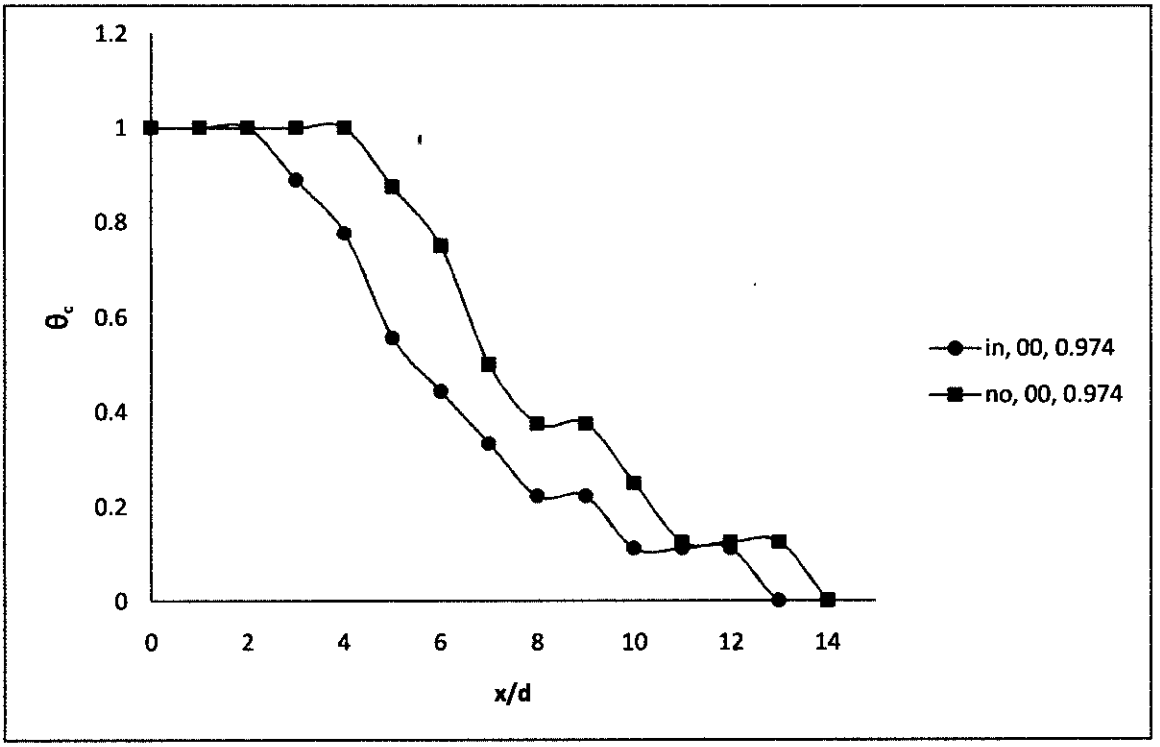

Figure 5.5.5: centerline temperature profile of co-axial jets at velocity ratio of 0.0 and temperature ratio of 0.974 with different type of excitation

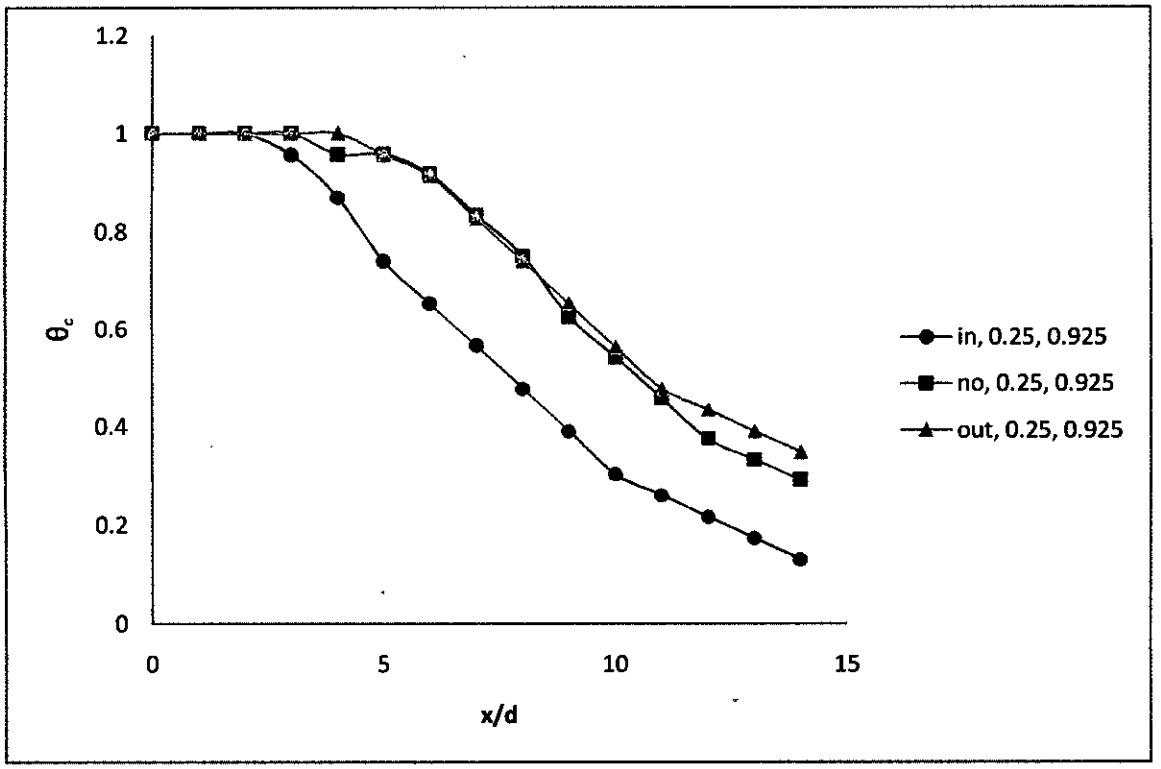

Figure 5.5.6: centerline temperature profile of co-axial jets at velocity ratio of 0.25 and temperature ratio of 0.925 with different type of excitation

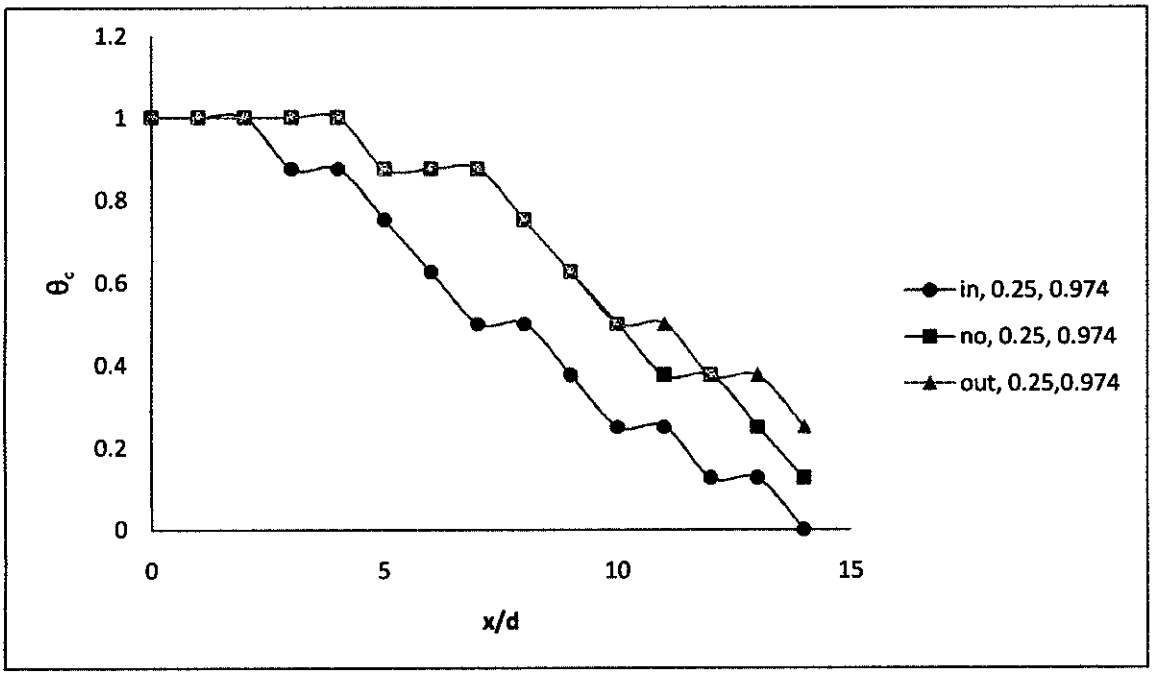

Figure 5.5.7: centerline temperature profile of co-axial jets at velocity ratio of 0.25 and temperature ratio of 0.974 with different type of excitation

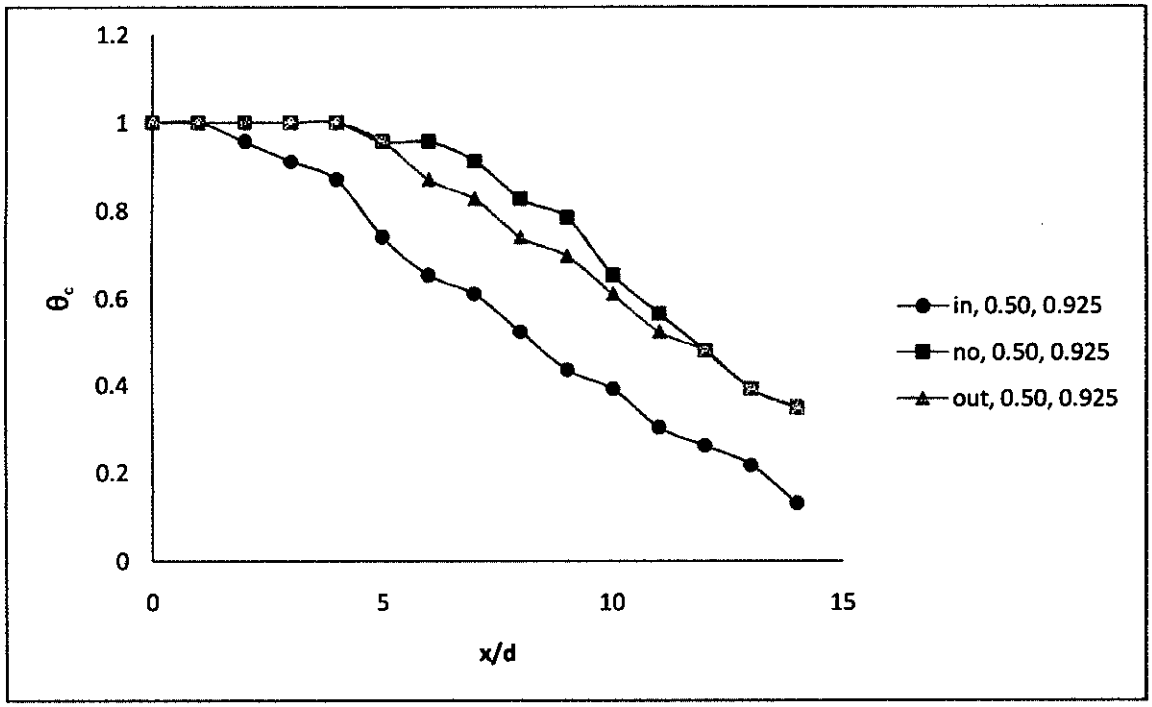

Figure 5.5.8: centerline temperature profile of co-axial jets at velocity ratio of 0.50 and temperature ratio of 0.925 with different type of excitation

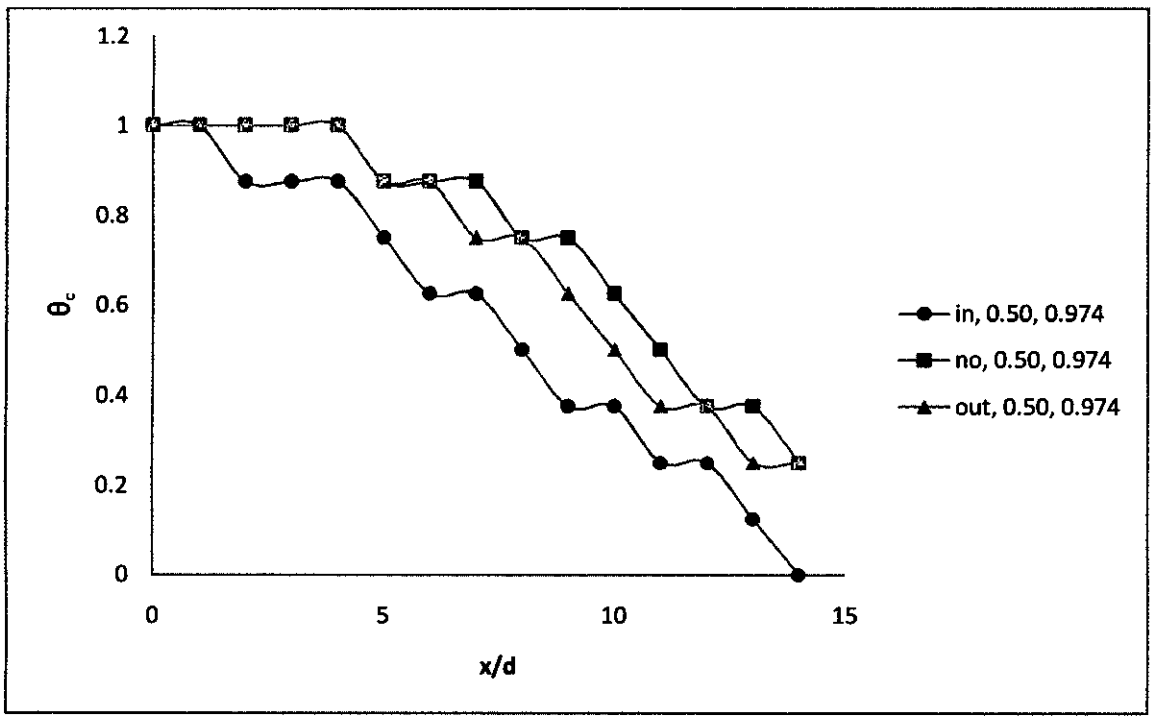

Figure 5.5.9: centerline temperature profile of co-axial jets at velocity ratio of 0.50 and temperature ratio of 0.974 with different type of excitation

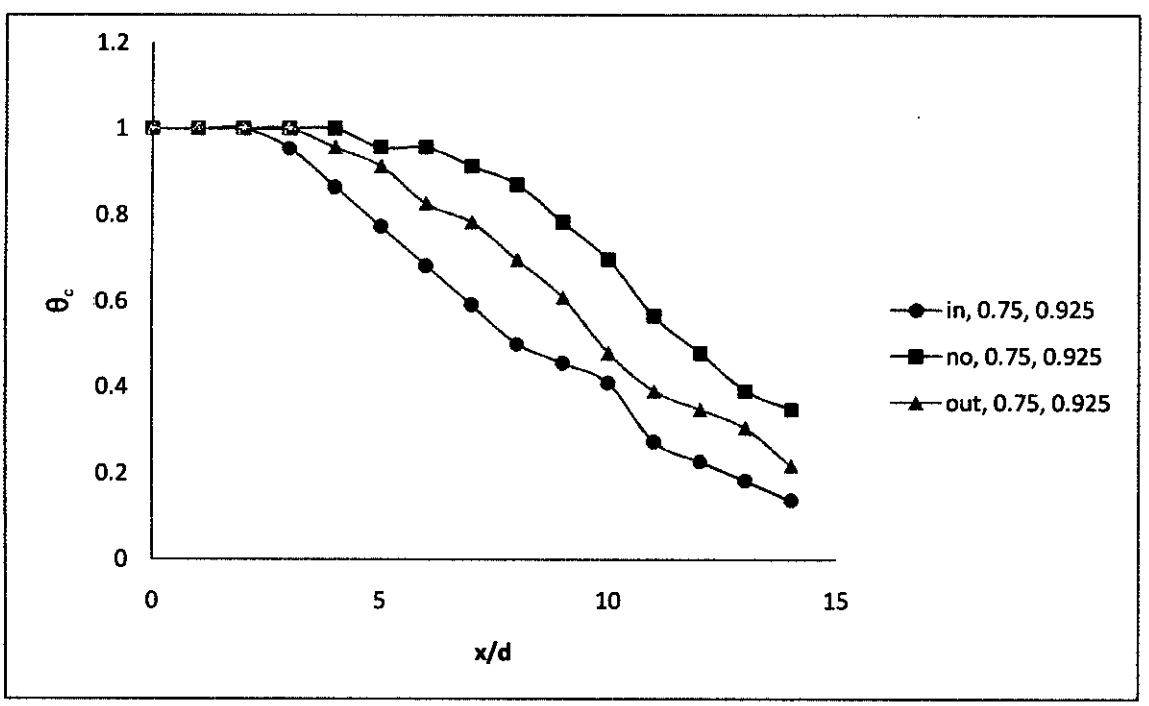

Figure 5.5.10: centerline temperature profile of co-axial jets at velocity ratio of 0.75 and temperature ratio of 0.925 with different type of excitation

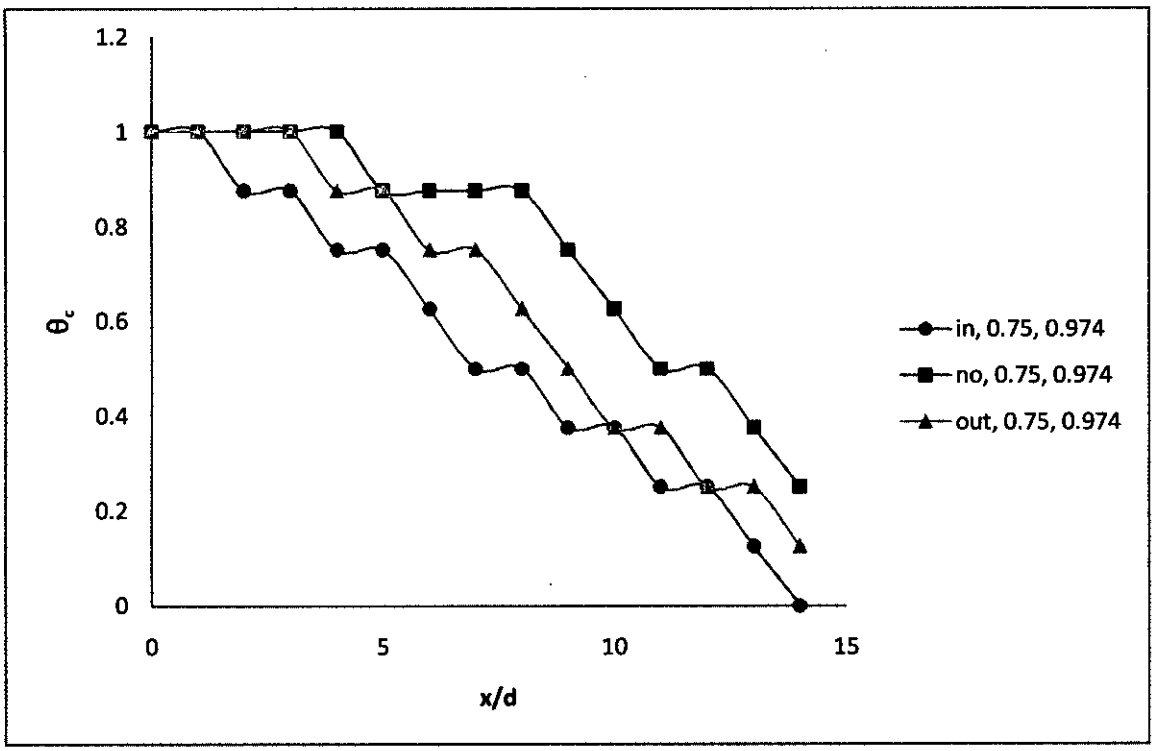

Figure 5.5.11: centerline temperature profile of co-axial jets at velocity ratio of 0.75 and temperature ratio of 0.974 with different type of excitation

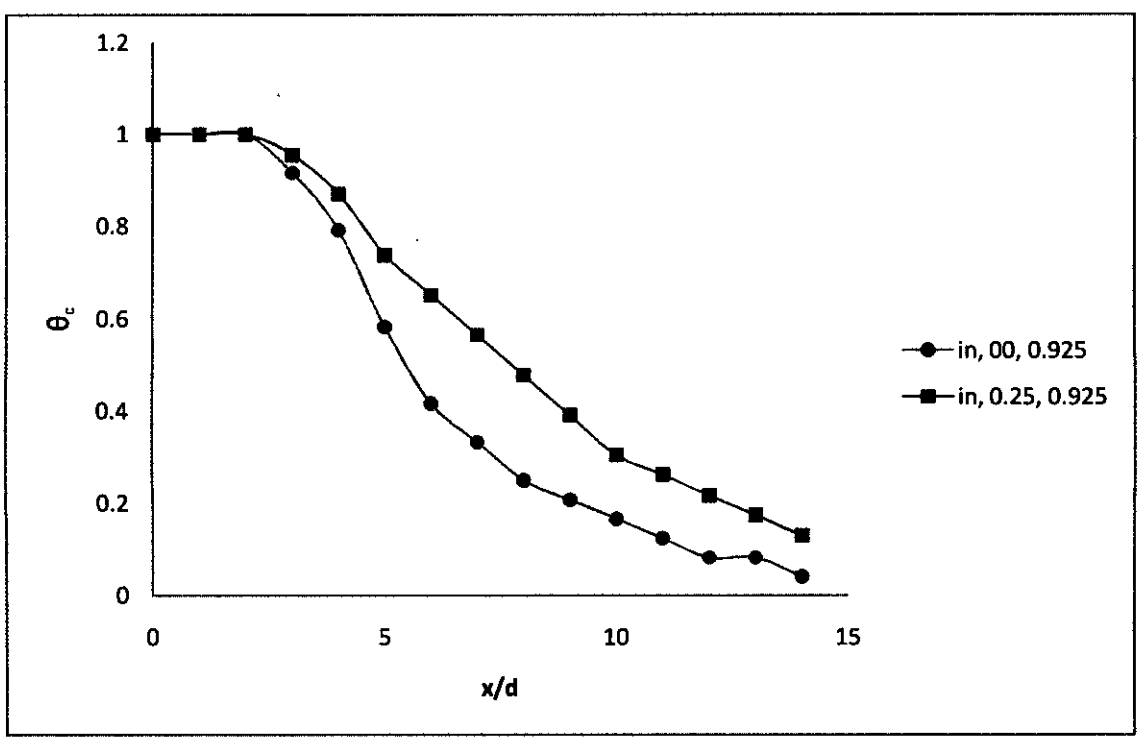

Figure 5.5.12: Comparison of the centerline temperature profile of internal trip ring excited co-axial jets of velocity ratio of 0.25 and 0.00 at temperature ratio of 0.925

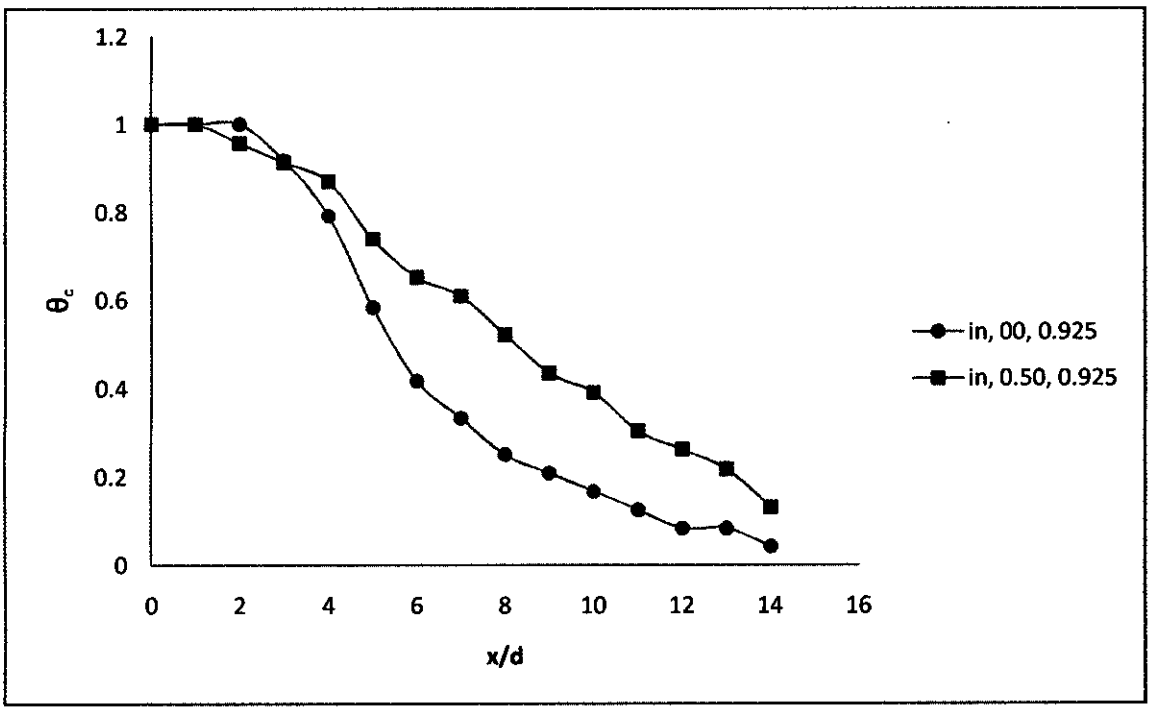

Figure 5.5.13: Comparison of the centerline temperature profile of internal trip ring excited co-axial jets of velocity ratio of 0.50 and 0.00 at temperature ratio of 0.925

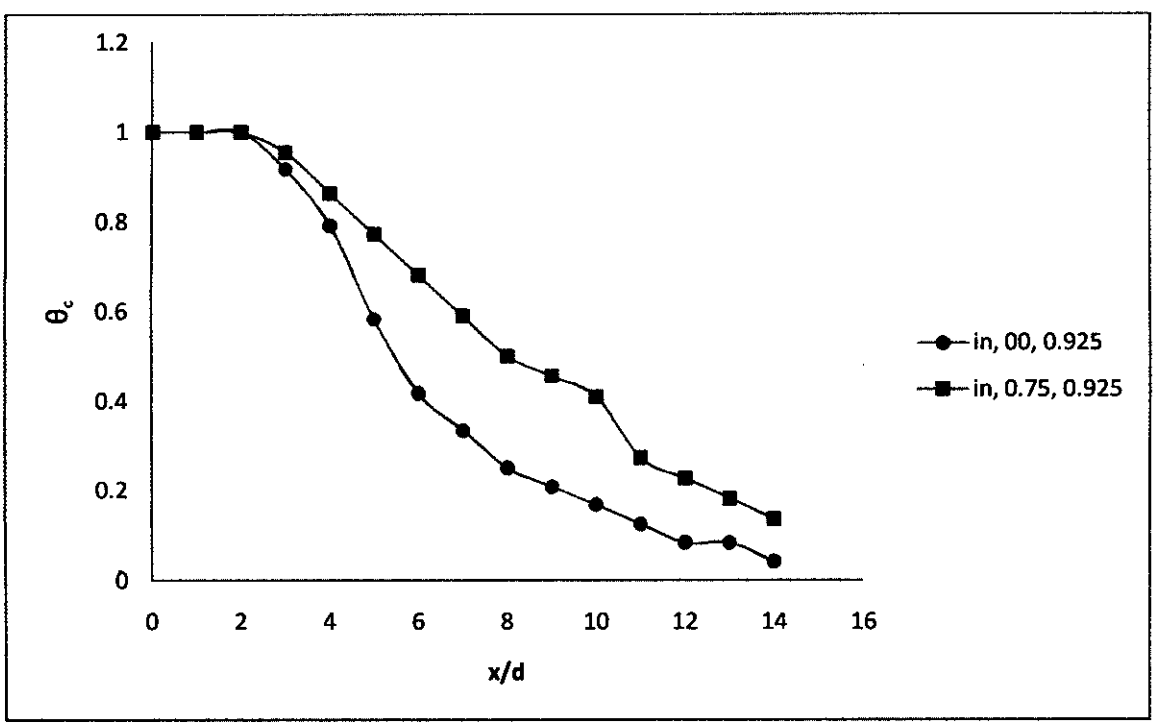

Figure 5.5.14: Comparison of the centerline temperature profile of internal trip ring excited co-axial jets of velocity ratio of 0.75 and 0.00 at temperature ratio of 0.925

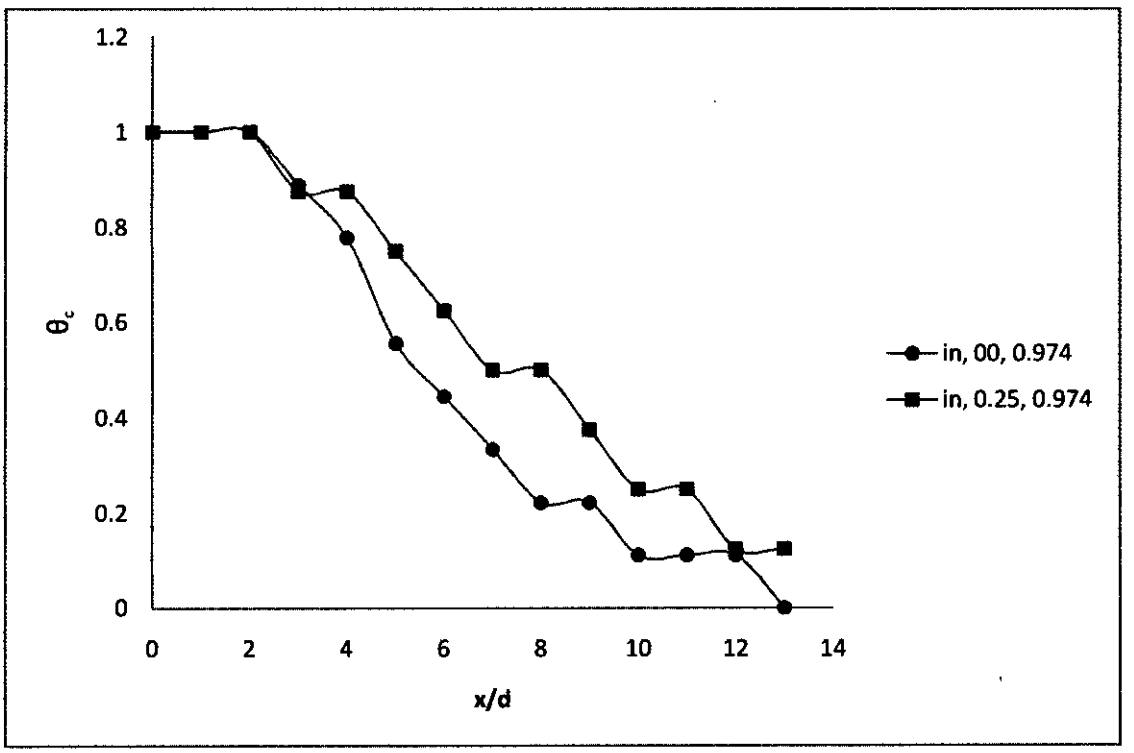

Figure 5.5.15: Comparison of the centerline temperature profile of internal trip ring excited co-axial jets of velocity ratio of 0.25 and 0.00 at temperature ratio of 0.974

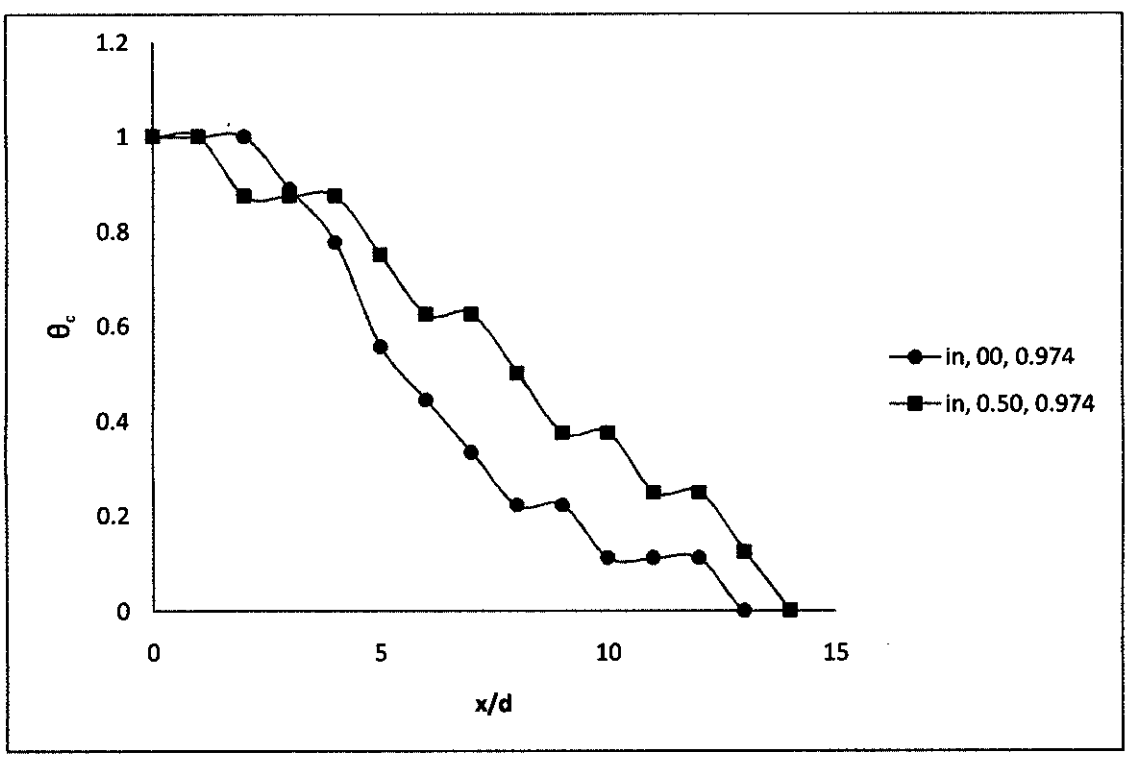

Figure 5.5.16: Comparison of the centerline temperature profile of internal trip ring excited co-axial jets of velocity ratio of 0.50 and 0.00 at temperature ratio of 0.974

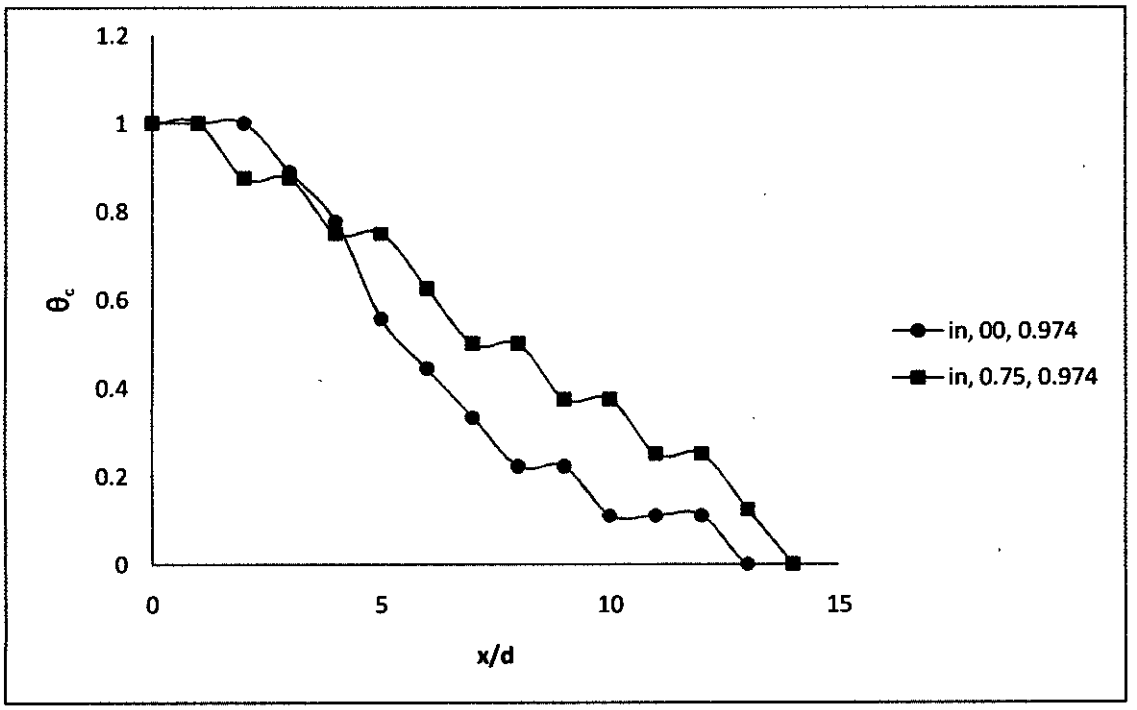

Figure 5.5.17: Comparison of the centerline temperature profile of internal trip ring excited co-axial jets of velocity ratio of 0.75 and 0.00 at temperature ratio of 0.974

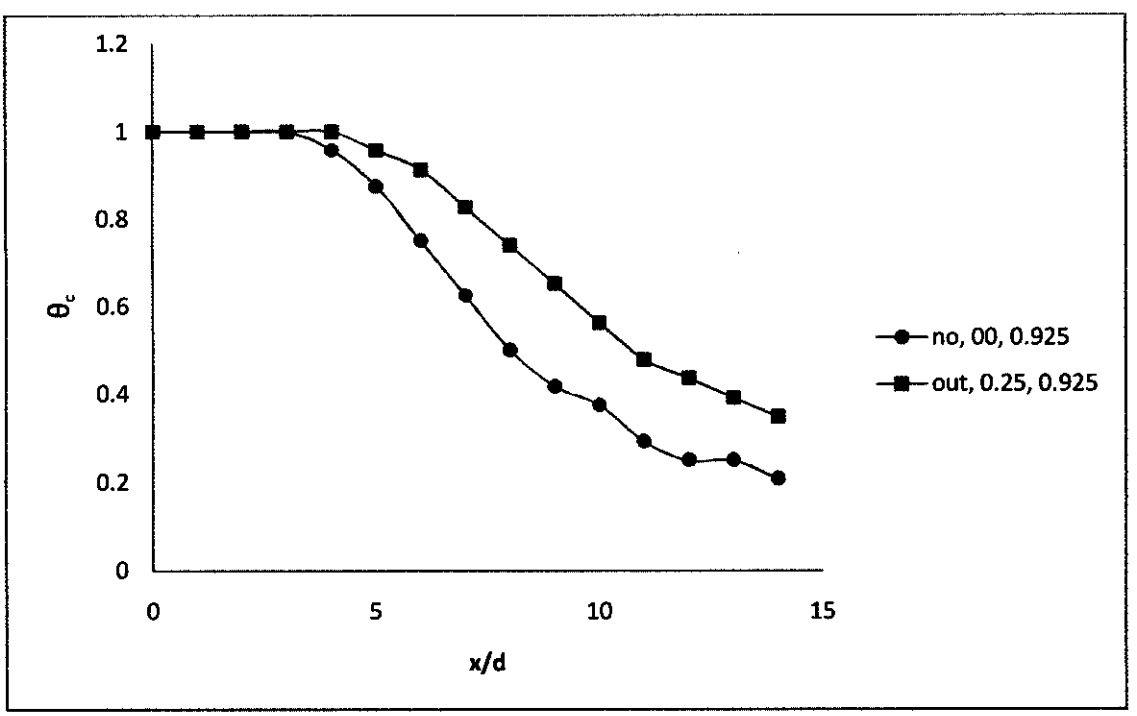

Figure 5.5.18: centerline temperature profile of external trip ring excited co-axial jets at temperature ratio of 0.925 with different velocity ratio

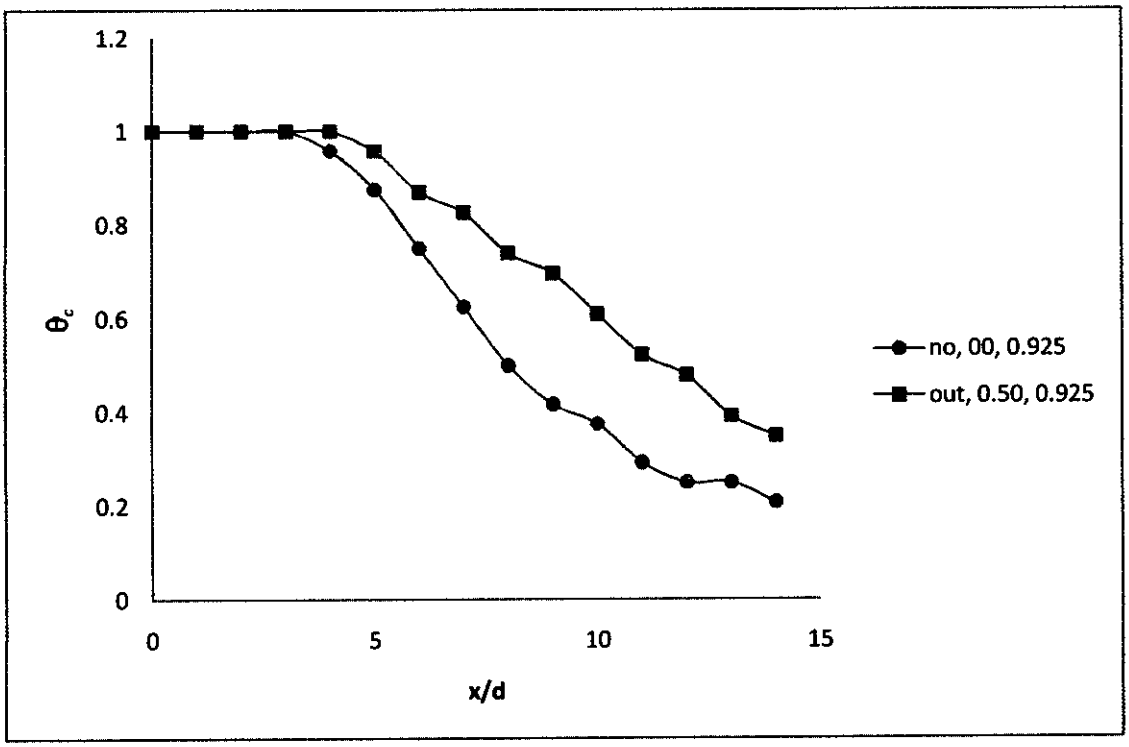

Figure 5.5.19: centerline temperature profile of external trip ring excited co-axial jets at temperature ratio of 0.925 with different velocity ratio

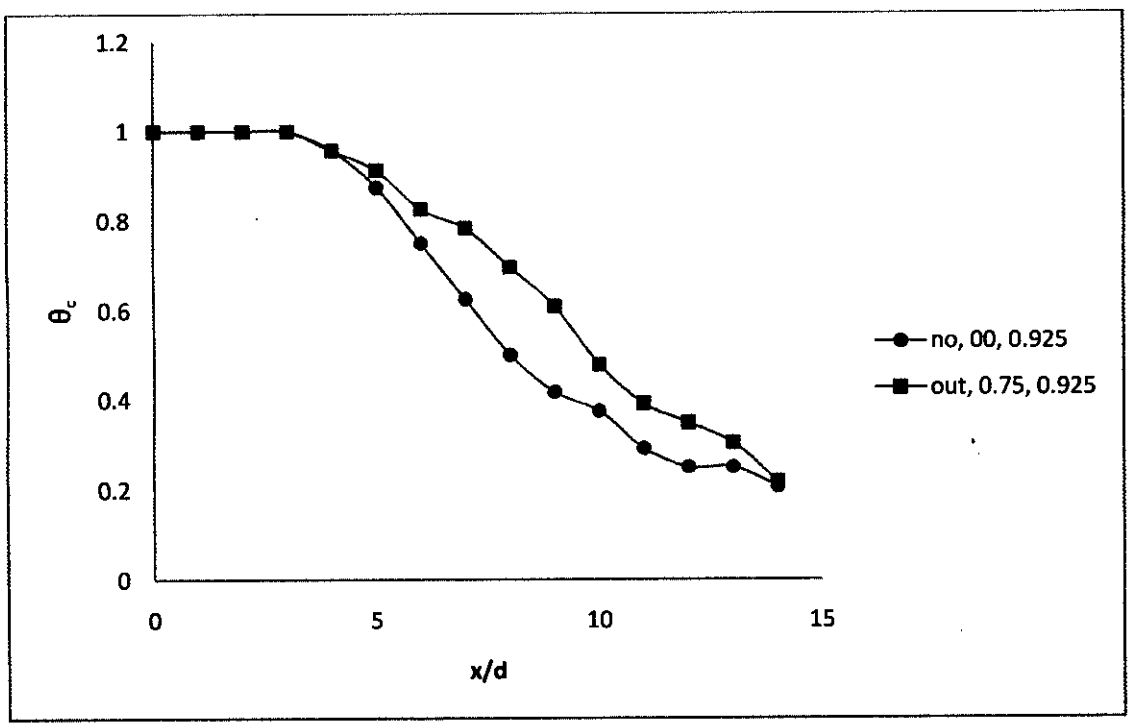

Figure 5.5.20: centerline temperature profile of external trip ring excited co-axial jets at temperature ratio of 0.925 with different velocity ratio

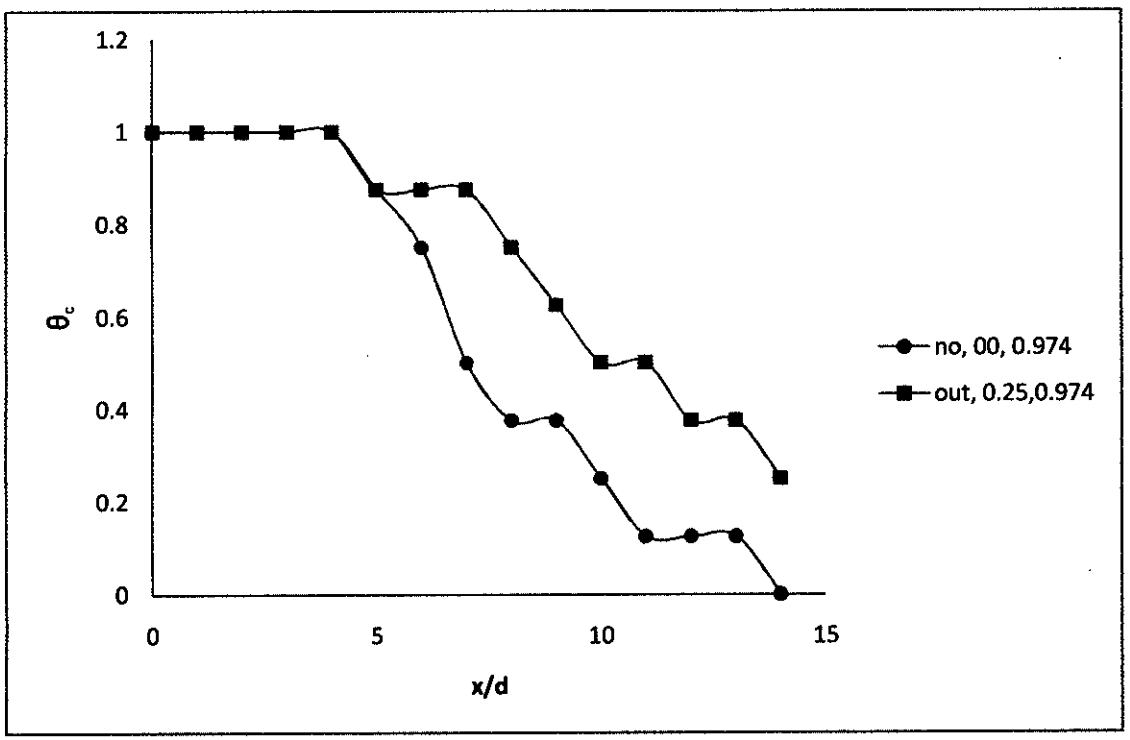

Figure 5.5.21: centerline temperature profile of external trip ring excited co-axial jets at temperature ratio of 0.974 with different velocity ratio

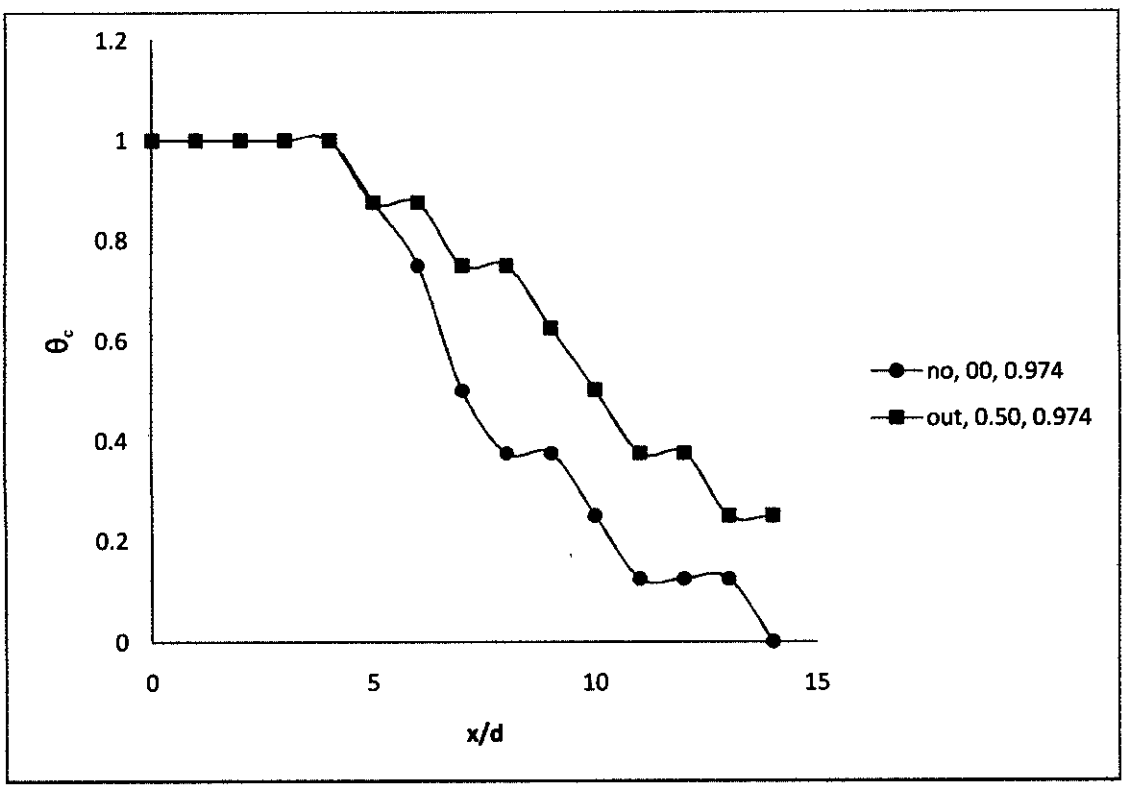

Figure 5.5.22: centerline temperature profile of external trip ring excited co-axial jets at temperature ratio of 0.974 with different velocity ratio

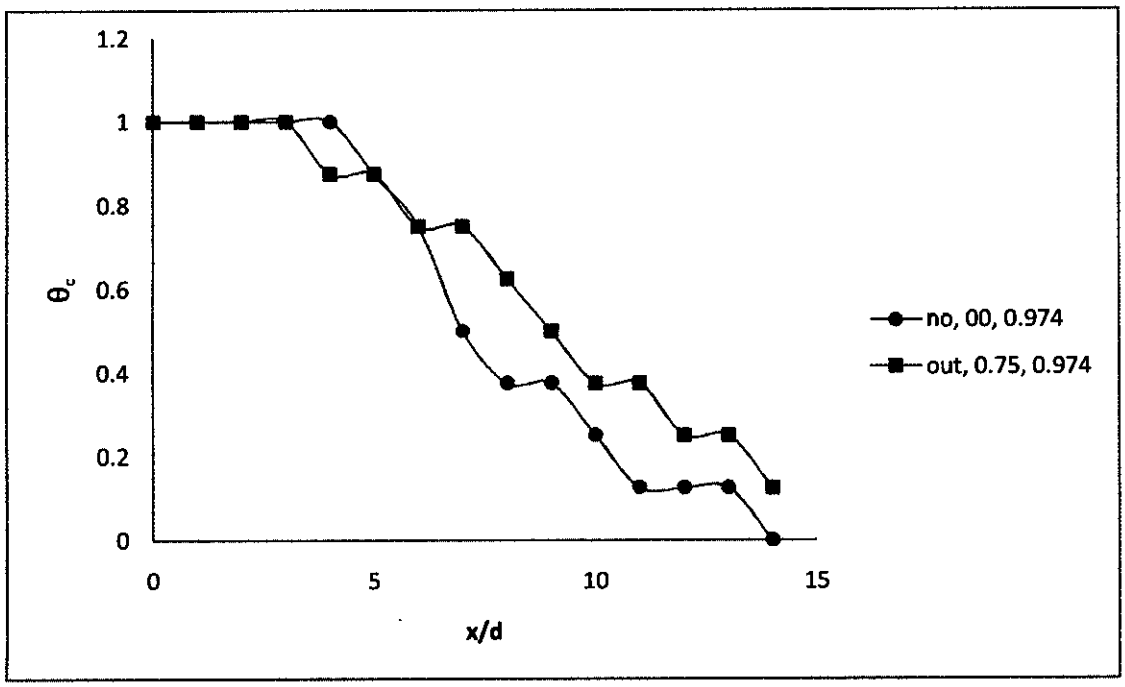

Figure 5.5.23: centerline temperature profile of external trip ring excited co-axial jets at temperature ratio of 0.974 with different velocity ratio

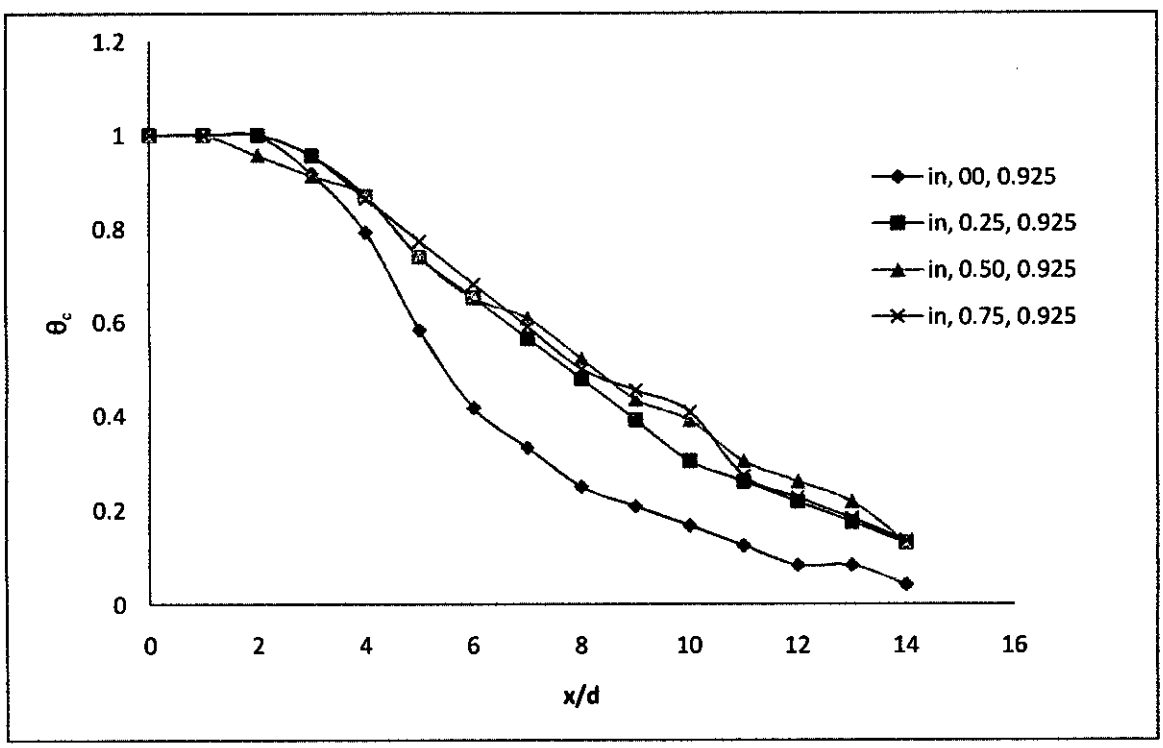

Figure 5.5.24: Comparison of non-dimensional centerline temperature profile for different velocity ratio of inner trip ring excited co-axial jets at temperature ratio of 0.925

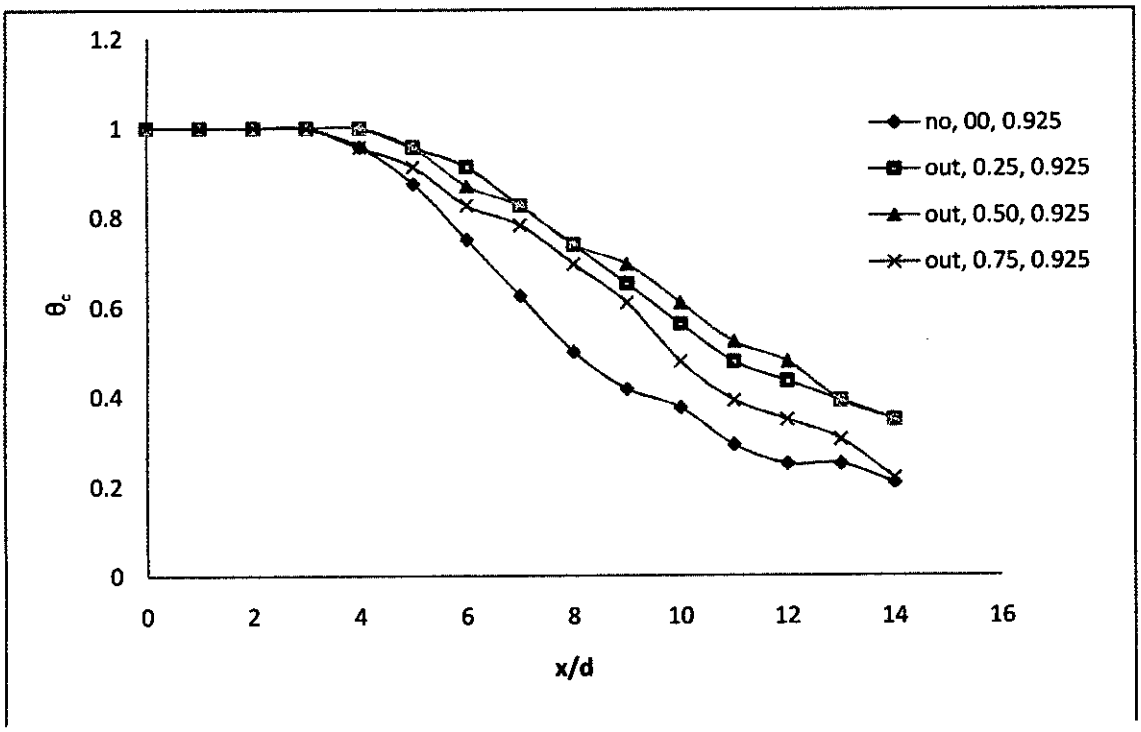

Figure 5.5.25: Comparison of non-dimensional centerline temperature profile for different velocity ratio of outer trip ring excited co-axial jets at temperature ratio of 0.925

References

1. Ahmed, R. A. and Sharma, A. D., "Effect of Velocity Ratio on the Turbulent Mixing of Confined Co-axial Jet", Experimental Thermal and Fluid Science, Vol. 22, Issue 1-2, pp. 19-33, August 2000.
2. Alpinieri, Louis J., "Turbulent Mixing of Co-axial Jets", AIAA Journal, Vol. 2, No. 9, pp. 1560-1567, 1967.
3. Antonia, R. A. and Bilger, R. W., "An Experimental Investigation of an Axisymmetric Jet in a Co-flowing Air Stream", Journal of Fluid Mechanics, Vol. 61, part 4, pp. 805-822, 1973.
4. Au, H. and Ko, N. W. M., "Co-axial Jets of Different Mean Velocity Ratios; Part-2", Journal of Sound and Vibration, Vol. 116(3), pp. 427-443, 1987.
5. Begum, R., "Experimental Study of Co-axial Free Jets", M.Sc. Thesis, Mechanical Engineering Department, BUET, Dhaka, 2004.
6. Billant, P., Chomaj, J. M. and Huerre, "Experimental Study of Vortex Breakdown in Swirling Jet", Journal of Fluid Mechanics, Vol. 376, pp. 183-219, 1998.
7. Bradbury, L. J. S., "The Spread of a Turbulent Plane Jet into a Parallel Moving Air-Stream", Journal of Fluid Mechanics, Vol. 27, pp. 381-394, 1967.
8. Bradshaw, P., "The Effect of Initial Conditions on the Development of a Free Shear Layer", Journal of Fluid Mechanics, Vol. 26, pp. 225-236, 1966.
9. Breyer, D. W. and Pankhurst, R. C., "Pressure Probe Methods for Determining Wind Speed and Flow Direction", National Physical Laboratory, 1971.
10. Buresti, G., Talamelli, A. and Patenga P., "Experimental Characterization of the Velocity Field of a Co-axial Jet Configuration", Experimental Thermal and Fluid Science, Vol. 9, Issue 2, pp. 135-146, August 1994.
11. Champagne, F. H., and Wygnanski, I. J., "An Experimental Study of co-axial Trubulent Jet", International Journal of Heat and Mass Transfer, Vol. 14, pp. 1445-1464, 1971.

12. Chigier, N. A. and Beer, J. M., "The Flow Region near the Nozzle in Double Concentric Jets", Journal of Basic Engineering, pp. 797-804, 1964.
13. Choi, D. W., Gessner, F. B. and Oates, G. C., "Measurements of Confined Co-axial Jet Mixing with Pressure Gradient", Journal of Fluid Engineering, Vol. 108, pp. 39-46, 1986.
14. Chowdhury, R. T., "Experimental Study of Swirling Co-axial Jets", M.Sc. Thesis, Mechanical Engineering Department, BUET, Dhaka, 2004.
15. Elbanna, H. and Sabbagh, J. A., "Interactions of Two Non-equal Plane Parallel Jets", AIAA Journal, Vol. 25, No. 1, pp. 12-13, 1987.
16. Farve-Marinet, M. and Schettini, E. B. C., "The Density Field of Co-axial Jets with Large Velocity Ratio and Large Density Difference", International Journal of Heat and Mass Transfer, Vol. 44, Issue 10, pp. 1913-1924, May 2001.
17. Frostall, W. and Shapiro, A. H., "Momentum and Mass Transfer in Co-axial Gas Jets", Trans. ASME Vol. 73, pp. 219, 1951.
18. Gamma, B. A., "Study of the Effect of Excitation on A Circular Air Jet", M.Sc. Thesis, Mechanical Engineering Department, BUET, Dhaka, 1993.
19. Georgiou, G., "Annular Liquid Jets at High Reynolds Number", International Journal for Numerical Methods in Fluids, Vol. 42, pp. 117-130, 2003.
20. Hibara, H., "Swirling Jet along a Solid Surface", Hiroshima University, Hiroshima, Japan.
21. Hossain, M. M., "Experimental Study of the flow in Circular Swirling Jets", Ph.D. Thesis, Mechanical Engineering Department, BUET, Dhaka, 2003.
22. Husain, A. K. M. F. and Zedan, M. F., "Effect of Initial Condition on the Axisymmetric Free Shear Layer; Effect of the Initial Fluctuation Level", Physics of Fluids, Vol. 21, pp. 1475, 1978.
23. Islam, A., "Flow Characteristics in the Near Field of A Circular Splined Jet", M.Sc. Thesis, Mechanical Engineering Department, BUET, Dhaka, 1995.

24. Islam, T., "Flow Characteristics of Unexcited and Excited Circular Wedge Shaped Jets", Ph.D. Thesis, Mechanical Engineering Department, BUET, Dhaka, 1995.

25. Kline, S. J. and McClintock, F. A., "Describing Uncertainties in Single Sample Experiments", Mechanical Engineering, p-3, 1953.

26. Ko, N. W. M. and Chan, W. T., "Similarity in the Initial Region of Annular Jets: Three Configurations", Journal of Fluid Mechanics, Vol. 84, Part-4,pp. 641-656, 1978.

27. Ko, N. W. M. and Chan, W. T., "The Inner Regions of Annular Jets", Journal of Fluid Mechanics, Vol. 95, Part-4, pp. 549-584, 1979.

28. Ko, N. W. M. and Davis, P. O. A. L., "The Near Field within the Potential Core of Subsonic Cold Jets", Journal of Fluid Mechanics, Vol. 50, pp. 49-78, 1971.

29. Kriaa W., Adberrazak K., Mhiri H., Palec Le. G. and Bournot, P. "A numerical study of non-isothermal turbulent co-axial jets", Journal of Heat and Mass Transfer, Springer-Verlag 2007.

30. Lenzo, C. S., and Dalal, T. N., "Center-Line Velocity Decay in Co-axial Free Jets", Journal of Applied Mechanics, Transaction of ASME, pp. 514-516, June 1975.

31. Lighthill, M. J., "Jet Noise", AIAA Journal, Vol. 1, No. 7, pp. 1507-1517, 1963.

32. Lima, M. M. C. L and Palma, J. M. L. M., "Mixing in Co-axial Confined Jets of Large Velocity Ratio", [Internet]

33. Morton, B. R., "Co-axial Turbulent Jets", International Journal of Heat and Mass Transfer, Vol. 5, pp. 955-965, 1962.

34. Murakami, Erina and Papamoschou, Dimitri, "Mean Flow Development in Dual Stream Compressible Jets", AIAA Journal, Vol. 40, No. 2, pp. 1131-1138, 2002.

35. Obot Y. Nalma, Trabold A. Thomas, Graska L. Michael and Gandhl Faroukh, "Velocity and Temperature Fields in Turbulent Jets Issuing from

Sharp-Edged Inlet Round Nozzle", Ind. Eng. Chem. Fundam., Vol. 25, no. 3, 1986.

36. Rajaratnam, N., "Turbulent Jets", Elsevier Scientific Publications Company, Amsterdam-Oxford-Newyork, 1976.
37. Rehab, H., Villermaux, E. and Hopfinger, E. J., "Flow Regimes of Large Velocity Ratio CO-axial Jet", Journal of Fluid Mechanics, Vol. 345, pp. 357-381, 1997.
38. Saffir. A. A., "The velocity and temperature field of rectangular jets" , Int. Journal of Heat and Mass Transfer, Vol. 19, pp. 1289-1297, 1976.
39. Selim, M. A., "Flow Structure of the Circular Wedge Shaped Jets", M.Sc. Thesis. Mechanical Engineering Department, BUET, Dhaka, 1988.
40. Squire, H. B. and Troucher, J., "Round Jet in a General Stream", Aeronautical Research Council, London, 1944.
41. Tagila, C. D., Blum, L., Gass, T., Ventikes, Y. and Poullkakas, D., "Numerical and Experimental Investigation of an Annular Jet Flow with Large Blockage", Journal of Fluids Engineering, Vol. 126, pp. 375-384, 2004.
42. Thaser, L. W. and Binder, R. C., "A practical Application of Uncertainty Calculation to Measured Data", Transaction of ASME, pp. 373-376, 1957.
43. Villermaux, E., and Rehab, H., "Mixing in co-axial jet", Journal of Fluid Mechanics, Vol. 425, pp. 161-185, 2000.
44. Warda, H. A., Kasab, S. Z. and Elshobagy, K. A., "An Experimental Investigation of the Near-filed Region of a Free Turbulent Co-axial Free jet Using LDA", Flow Measurement and Instrumentation, Vol. 10 Issue 1, pp. 15-16, March 1999.
45. Wicker, R. B. and Eaton, J. K., "Near Field of a Co-axial Jet with and without Axial Excitation", AIAA Journal, Vol. 32, No. 3, pp. 542-546, 1994.
46. Williams, T. J., Ali, M. R. M. H. and Anderson, J. S., "Noise and Flow Characteristics of Co-axial Jets", Journal of Mechanical Engineering Science, Vol. 11, No. 2, pp. 133-142, 1962.

47. Wygnanski, I. and Fiedler, H. E., "Some Measurements in the Self-Preserving Jet", Journal of Fluid Mechanics, Vol. 38, pp. 577-612, 1969.

48. Yue, W., "Air Jets in Ventilation Application", [Source: The Internet]

49. Hasan, Mohammad Nasim, "Experimental Study of Flow Characteristics in the Near Field of a Thermally Stratified Co-axial Free Jet" M.Sc. Thesis, Mechanical Engineering Department, BUET, Dhaka, 2008.